

# THE INSTITUTE OF MEDICAL SCIENCES

AT THE  
PRESBYTERIAN MEDICAL CENTER  
SAN FRANCISCO

GPO PRICE \$ \_\_\_\_\_

CSFTI PRICE(S) \$ \_\_\_\_\_

Hard copy (HC) \_\_\_\_\_

Microfiche (MF) \_\_\_\_\_

ff 653 July 65

FINAL REPORT  
ON  
INVESTIGATION OF THE FEASIBILITY  
OF  
AN EXTERNAL BIOSENSOR  
FOR  
CONTINUOUS DETERMINATION OF BLOOD OXYGENATION  
(AND CONCOMITANT HEART RATE AND RESPIRATORY RATE)  
BASED UPON OPTICAL BACKSCATTER  
FOR USE IN  
SPACECRAFT AND AIRCRAFT

FACILITY FORM 502

N 68-36572

(ACCESSION NUMBER)

(THRU)

153

(PAGES)

(CODE)

CR-97318

(NASA CR OR TMX OR AD NUMBER)

(CATEGORY)

NATIONAL AERONAUTICS AND SPACE ADMINISTRATION  
CONTRACT NO. NAS 9-2937

THE LABORATORY OF TECHNICAL DEVELOPMENT

June 24, 1964 - November 1, 1965

# THE INSTITUTE OF MEDICAL SCIENCES

AT THE  
PRESBYTERIAN MEDICAL CENTER  
SAN FRANCISCO

FINAL REPORT  
ON  
INVESTIGATION OF THE FEASIBILITY  
OF  
AN EXTERNAL BIOSENSOR  
FOR  
CONTINUOUS DETERMINATION OF BLOOD OXYGENATION  
(AND CONCOMITANT HEART RATE AND RESPIRATORY RATE)  
BASED UPON OPTICAL BACKSCATTER  
FOR USE IN  
SPACECRAFT & AIRCRAFT

NATIONAL AERONAUTICS AND SPACE ADMINISTRATION  
CONTRACT NO. NAS 9-2937

**THE LABORATORY OF TECHNICAL DEVELOPMENT**

June 24, 1964 - November 1, 1965



## I OVERVIEW OF THE PROGRAM

This document is the Final Report on National Aeronautics and Space Administration Contract No. NAS 9-2937, "The Investigation and Development of an External Biosensor for the Continuous Determination of Blood Oxygenation and Concomitant Heart Rate and Respiratory Rate for Use in Spacecraft and Aircraft". The work reported was conducted during the period June 24, 1964 to November 1, 1965 at the Laboratory of Technical Development, Institute of Medical Sciences, Presbyterian Medical Center, San Francisco, California.

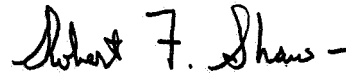
This study program was designed to explore the feasibility of developing an accurate and reliable external biosensor based upon the principle of optical backscatter. The objective of the program was detailed in the contract statement of work as follows:

"Objective: The range of blood-oxygen saturation compatible with normal physiologic performance of man is narrow and is not dependent upon physical activity or level of anxiety, nor does it vary from individual to individual. Since the maintenance of normal blood-oxygen saturation requires proper function of the life support system, respiratory system and cardiovascular system, this one measurement will monitor the integrated performance of the man-machine system most critical to sustaining life during space flight. Since an operational biosensor, capable of continuous blood-oxygen saturation measurements and capable of meeting all the operational requirements of space flight, does not exist, it is the intent of this Work Statement to define a feasibility study of such a biosensor, based upon the principle of optical backscatter."

### AUTHORIZATION

The work described in this report was performed in the Laboratory of Technical Development, Institute of Medical Sciences, Presbyterian Medical Center, San Francisco, during the period June 24, 1964 through November 1, 1965. The report was prepared by Dr. Robert F. Shaw and Mr. Wali M. Malik, with technical contributions by Mr. Frank Litz, Mr. Richard Weeks, Dr. Lawrence R. Adams, Mr. Roger Muldavin, Dr. Robert C. Eberhart and Mrs. Susanne Bock.

Approved by:

  
Robert F. Shaw, M.D.  
Laboratory Director



## TABLE OF CONTENTS

	Page
LIST OF FIGURES	iii
I OVERVIEW OF THE PROGRAM	1
II SPECTROPHOTOMETRIC STUDIES OF HEMOLYZED BLOOD	8
A. General	8
B. Theoretical Basis	10
C. Improvement in Anaerobic Sampling	15
D. Operational Oxygen Saturation Data	18
E. Experiments in Precision Limits	22
F. Effect of Oxygenating and Deoxygenating Gas Flow	27
G. Effect of Amount of Hemolyzing Agent	27
H. Chemical vs. Physical Deoxygenation	31
I. Summary	33
III SPECTROPHOTOMETRIC STUDIES OF WHOLE BLOOD	
A. General	34
B. Whole-Blood Transmission-Mode Studies	40
C. Whole-Blood Backscatter-Mode Studies	46
D. Conclusions	58
IV SPECTROPHOTOMETRIC STUDIES OF THE SKIN-TISSUE SYSTEM	
A. General	59
B. Studies on Transmittance of Excised Human Skin	60
1. Specimens	60
2. Apparatus	60
3. Procedure	60
4. Results	62
C. Microscopic and Photomicroscopic Visible and Infrared Fixed-Focus Studies of Intact Skin	65
1. Microscopic Studies	65
2. Infrared Photomicrographic Studies	65
D. Congruent Backscatter Spectrum of Living and Excised Skin	67
1. Backscatter Spectrum of Living Skin	67
2. Measurements of Excised Skin	69
3. Experimental Data	69
4. Experimental Results	72
5. Interpretation of Results	73
E. Photographic-Photometric Studies	74
1. General	74
2. Methods	74
3. Experimental Data	77
4. Experimental Results	80
5. Conclusions	81
F. Methods for Increasing Skin Blood Flow	83

	Page
V	EXPERIMENTAL BACKSCATTER-MODE EXTERNAL BIOSENSOR SYSTEM DEVELOPMENT AND PERFORMANCE
A.	General 85
B.	Skin-Tissue-Blood Simulator Cuvettes 86
C.	Experimental External Biosensor Systems 91
1.	General 91
2.	Chopped-Light Apparatus 93
3.	d.c.-Photomultiplier Apparatus 99
4.	Biosensor Transducers Configuration 99
D.	Experimental External Biosensor System Studies Utilizing a Congruent Optical Geometry 104
E.	Experimental External Biosensor System Studies Performed on the Skin-Tissue-Blood Simulator Cuvettes 108
F.	Experimental External Biosensor System Studies Performed Upon Experimental Animals 117
G.	Experimental External Biosensor System Studies Performed Upon Human Patients 125
H.	Experimental External Biosensor System Studies Performed Upon Human Volunteers 135
VI	CONCLUSIONS 136
	REFERENCES 140



### List of Figures

	Page
Figure FR-1. Spectrophotometric Studies of Hemolyzed Blood. Absorption spectra of oxyhemoglobin and reduced hemoglobin.	11
Figure FR-2. Spectrophotometric Studies of Hemolyzed Blood. Anaerobic sample capsule for obtaining whole-blood samples for oxygen saturation determination.	16
Figure FR-3. Spectrophotometric Studies of Hemolyzed Blood. Delivery of hemolyzed blood from anaerobic sample capsule to spectrophotometric cuvette.	17
Figure FR-4. Spectrophotometric Studies of Hemolyzed Blood. Experimentally-determined ratios O. D. 480/O. D. 506 for tank-oxygen oxygenated and tank-nitrogen deoxygenated hemolyzed-blood samples.	19
Figure FR-5. Spectrophotometric Studies of Hemolyzed Blood. Precision attained in experimentally-determined ratios O. D. 480/O. D. 506 for oxyhemoglobin, serial optical-density measurement vs. simultaneous optical-density measurement protocol.	23
Figure FR-6. Spectrophotometric Studies of Hemolyzed Blood. Precision attained in experimentally-determined ratios O. D. 480/O. D. 506 for hemoglobin, serial optical-density measurement protocol vs. simultaneous optical-density measurement protocol.	24
Figure FR-7. Spectrophotometric Studies of Hemolyzed Blood. Summary of precision attained in experimentally-determined ratios O. D. 480/O. D. 506 for Hb and HbO <sub>2</sub> , serial optical-density measurement protocol vs. simultaneous optical-density measurement protocol.	25
Figure FR-8. Spectrophotometric Studies of Hemolyzed Blood. Experimentally-determined effect on optical properties of heart-lung machine hemolyzed blood.	28

	Page
Figure FR-9. Spectrophotometric Studies of Hemolyzed Blood. Experimentally-determined effect on optical properties of hemolyzed heart-lung machine blood.	29
Figure FR-10. Spectrophotometric Studies of Hemolyzed Blood. Effect of the addition of excess hemolyzing agent on experimentally-determined ratios O. D. 480/O. D. 506 for oxyhemoglobin.	30
Figure FR-11. Spectrophotometric Studies of Hemolyzed Blood. Comparison of experimentally-determined ratios O. D. 480/O. D. 506 for physically vs. chemically deoxygenated hemoglobin.	32
Figure FR-12. Spectrophotometric Studies of Whole Blood. Performance of a commercial backscatter whole-blood oximeter measured against standard-of-reference determination of oxygen saturation.	36
Figure FR-13. Spectrophotometric Studies of Whole Blood. Hematocrit sensitivity of a commercial backscatter whole-blood oximeter.	37
Figure FR-14. Spectrophotometric Studies of Whole Blood. Transmission Mode: Oxygen Saturation vs. O. D. 805/ O. D. 660.	41
Figure FR-15. Spectrophotometric Studies of Whole Blood. Schematic diagram of the transmission cuvette oximetric apparatus.	42
Figure FR-16. Spectrophotometric Studies of Whole Blood. Transmission Mode: Percent Oxygen Saturation vs. O. D. 805/O. D. 660.	43
Figure FR-17. Spectrophotometric Studies of Whole Blood. Transmission Mode: Negative Slope of Optical Density vs. Oxygen Saturation.	45
Figure FR-18. Spectrophotometric Studies of Whole Blood. Backscatter Mode: Schematic diagram of congruent optical system in pump-oxygenator flowthrough cuvette apparatus.	47



	Page
Figure FR-19. Spectrophotometric Studies of Whole Blood. Backscatter Mode: Schematic diagram of pump-oxygenator flowthrough cuvette system.	48
Figure FR-20. Spectrophotometric Studies of Whole Blood. Backscatter Mode: Pump-oxygenator, cuvette and flow circuit.	49
Figure FR-21. Spectrophotometric Studies of Whole Blood. Backscatter Mode: Detail of pump-oxygenator flowthrough cuvette apparatus showing cooled lamp housing and equipment for measuring the intensity of light backscattered from whole blood.	50
Figure FR-22. Spectrophotometric Studies of Whole Blood. Backscatter Mode: Detail of pump-oxygenator flowthrough cuvette apparatus showing whole-blood cuvette for backscatter measurements.	51
Figure FR-23. Spectrophotometric Studies of Whole Blood. Backscatter Mode: Detail of pump-oxygenator flowthrough cuvette apparatus showing anaerobic sample capsules, removable, for reference oxygen saturation measurement on hemolyzed blood samples.	52
Figure FR-24. Spectrophotometric Studies of Whole Blood. Backscatter Mode: Percent oxygen saturation vs. backscattered light intensity ratio for various hematocrits.	54
Figure FR-25. Spectrophotometric Studies of Whole Blood. Backscatter Mode: Hematocrit vs. backscattered light intensity ratio at 100% oxygen saturation.	55
Figure FR-26. Spectrophotometric Studies of Whole Blood. Backscatter Mode: Hematocrit vs. $I_{625}$ at 100% oxygen saturation.	56
Figure FR-27. Spectrophotometric Studies of the Skin-Tissue System: Geometry for Transmittance Measurements on Excised Skin.	61

	Page
Figure FR-41. Experimental External Biosensor Systems: Diagram of Annular Lucite Transducer (ALT).	100
Figure FR-42. Experimental External Biosensor Systems: Diagram of Multiple Bundle Annular Transducer (MBAT).	101
Figure FR-43. Experimental External Biosensor System Studies Utilizing a Congruent Optical Geometry.	106
Figure FR-44. Experimental External Biosensor System Studies on Skin-Tissue-Blood Simulator Cuvette Systems. Annular lucite transducer (ALT)/photomultiplier biosensor system transfer functions obtained on STBS-II using ALT transducers of various dimensions.	109
Figure FR-45. Experimental External Biosensor System Studies on Skin-Tissue-Blood Simulator Cuvette Systems. Annular lucite transducer (ALT)/photomultiplier biosensor systems transfer functions obtained on STBS-III using ALT transducers of various dimensions.	111
Figure FR-46. Experimental External Biosensor System Studies on Skin-Tissue-Blood Simulator Cuvette Systems. Effect of hematocrit on transfer functions obtained on STBS-III using annular lucite transducer ALT # 2 (Figure FR-45)/photomultiplier biosensor system.	112
Figure FR-47. Experimental External Biosensor System Studies on Skin-Tissue-Blood Simulator Cuvette Systems. Contiguous field transducer (CFT)/chopped light apparatus (CLA) biosensor system transfer functions obtained on STBS-III.	113
Figure FR-48. Experimental External Biosensor System Studies on Skin-Tissue-Blood Simulator Cuvette Systems. Multiple bundle annular transducer (MBAT)/photomultiplier biosensor system transfer function obtained on STBS-III, compared with ALT transducer of approximately same dimensions.	115
Figure FR-49. Experimental External Biosensor System Studies Conducted on Experimental Animals. Annular lucite transducer (ALT)/photomultiplier biosensor system transfer functions obtained on experimental animals breathing controlled O <sub>2</sub> /N <sub>2</sub> mixtures.	116



	Page
Figure FR-50. Experimental External Biosensor System Studies Conducted on Experimental Animals. Annular lucite transducer (ALT)/photomultiplier biosensor system transfer functions obtained at three locations on a Chester White pig breathing controlled O <sub>2</sub> /N <sub>2</sub> mixtures.	118
Figure FR-51. Experimental External Biosensor System Studies Conducted on Experimental Animals. Comparison of contiguous field transducer (CFT)/chopped light apparatus (CLA) and annular lucite transducer (ALT)/photomultiplier biosensor systems. Transfer functions obtained on a Chester White pig breathing controlled O <sub>2</sub> /N <sub>2</sub> mixtures.	119
Figure FR-52. Experimental External Biosensor System Studies Conducted on Experimental Animals. Multiple bundle annular transducer (MBAT)/photomultiplier biosensor system transfer functions obtained on 8/10/65 on the forehead of a Chester White pig breathing controlled O <sub>2</sub> /N <sub>2</sub> mixtures.	120
Figure FR-53. Experimental External Biosensor System Studies Conducted on Experimental Animals. Multiple bundle annular transducer (MBAT)/photomultiplier and contiguous field transducer (CFT)/chopped light apparatus (CLA) biosensor systems' transfer functions obtained several weeks after data presented in Figure FR-52 on a Chester White pig under normal and erythemized skin conditions breathing controlled O <sub>2</sub> /N <sub>2</sub> mixtures.	121
Figure FR-54. Experimental External Biosensor System Studies Performed on a Multi-Channel Recorder for Data Acquisition in Human and Animal Studies.	127
Figure FR-55. Experimental External Biosensor System Studies Conducted on Patients during Open-Heart Surgery. Contiguous field transducer (CFT)/chopped light apparatus (CLA) biosensor system transfer function obtained on G.M., white, Female, Age 63, during open-heart surgery.	129

Figure FR-56.	Experimental External Biosensor System Studies Conducted on Patients during Open-Heart Surgery. Multiple bundle annular transducer (MBAT)/photomultiplier biosensor system transfer functions obtained on three patients.	Page. 131
Figure FR-57.	Experimental External Biosensor System Studies Conducted on Patients during Open-Heart Surgery. Multiple bundle annular transducer (MBAT)/photomultiplier biosensor system transfer functions obtained on eight patients.	132
Figure FR-58.	Experimental External Biosensor System Studies Conducted on Patients during Open-Heart Surgery. Multiple bundle annular transducer (MBAT)/photomultiplier biosensor system transfer functions for eight patients shown in Figure FR-57, showing effect on transfer functions of a theoretical algebraic data-correlation factor.	134

## I OVERVIEW OF THE PROGRAM

This document is the Final Report on National Aeronautics and Space Administration Contract No. NAS 9-2937, "The Investigation and Development of an External Biosensor for the Continuous Determination of Blood Oxygenation and Concomitant Heart Rate and Respiratory Rate for Use in Spacecraft and Aircraft". The work reported was conducted during the period June 24, 1964 to November 1, 1965 at the Laboratory of Technical Development, Institute of Medical Sciences, Presbyterian Medical Center, San Francisco, California.

This study program was designed to explore the feasibility of developing an accurate and reliable external biosensor based upon the principle of optical backscatter. The objective of the program was detailed in the contract statement of work as follows:

"Objective: The range of blood-oxygen saturation compatible with normal physiologic performance of man is narrow and is not dependent upon physical activity or level of anxiety, nor does it vary from individual to individual. Since the maintenance of normal blood-oxygen saturation requires proper function of the life support system, respiratory system and cardiovascular system, this one measurement will monitor the integrated performance of the man-machine system most critical to sustaining life during space flight. Since an operational biosensor, capable of continuous blood-oxygen saturation measurements and capable of meeting all the operational requirements of space flight, does not exist, it is the intent of this Work Statement to define a feasibility study of such a biosensor, based upon the principle of optical backscatter."

The feasibility study program was motivated not only by the pressing need for a reliable, operational external biosensor for measuring blood oxygen saturation and the current unavailability of suitable operational instrumentation, but by preliminary data and theoretical considerations which suggested that the implementation of a backscatter mode of operation might overcome difficulties encountered by previous instrumentation based upon transmission techniques.

As outlined in the Proposal, a backscatter mode of operation held promise of the advantages of greater flexibility and comfort in the anatomic site of location of the biosensor, and constancy of geometric relationship between light source and photodetector, independent of individual variations in the anatomy of the subjects.

Further, while conventional transmission-mode instrumentation attempted to implement a transfer function relating blood oxygen saturation to the ratio of the logarithms of the ratios of the incident to transmitted light intensities of the system, i.e., Beer's Law:

$$\text{O.S.} = K_1 \frac{\text{Log} \frac{I_{\lambda_s \text{ incident}}}{I_{\lambda_s \text{ transmitted}}}}{\text{Log} \frac{I_{\lambda_i \text{ incident}}}{I_{\lambda_i \text{ transmitted}}}} + K_2, \quad \text{Eq. 1}$$

where  $\lambda_s$  is a signal wavelength (at which the extinction coefficients for oxygenated and reduced hemoglobin differ appreciably), and

$\lambda_i$  is an isosbestic wavelength (at which the extinction coefficients for oxygenated and reduced hemoglobin are identical)

the backscatter mode of operation gave promise of approximating a linear relationship between oxygen saturation and backscattered light intensities, i.e.,



$$O.S. = K_1 \cdot \frac{I_{\lambda_s} \text{ backscattered}}{I_{\lambda_i} \text{ backscattered}} + K_2$$

Eq. 2

where the ratio  $\frac{I_{\lambda_i}}{I_{\lambda_s}}$  of the light source is held constant.

As noted in the program Proposal, instrumentation to electronically process linear Equation 2 is far simpler than the instrumentation required to process the logarithmic relationships of Equation 1. In addition, the successful realization of an external biosensor system performing in accordance with Equation 2 would have other outstanding features making it particularly suitable for use by active personnel, as noted below.

Variations in the physical coupling of external biosensor transducers to the skin cause variations in the optical coupling between the light source and the skin and the photodetectors. These variations in light coupling tend to be proportionate at the various wavelengths of interest, i.e., they are neutral density changes. Consequently, the behaviour of the transmittance and backscatter transfer functions (Equations 1 and 2 above) with regard to neutral density changes, becomes important in the practical realization of operational external biosensors for use on active personnel.

It can be seen by inspection that Equation 2 is independent of any neutral density changes that might occur in optical coupling between the light source, the skin and the photodetector, while Equation 1 is sensitive to such neutral density changes. Since variation in pressure, position or motion of the transducer with respect to the subject will effectively change optical coupling and produce neutral density changes at the various wavelengths, it is clear that a biosensor system implementing Equation 2 should have the outstanding advantage over transmission devices of freedom from motion artifact and be uniquely appropriate for operational

use with active duty personnel where motion inevitably occurs.

\* \* \* \* \*

During the sixteen months and eight days of this contract, the program objective quoted above was pursued in accordance with the contract Statement of Work.

At the outset of the program, in addition to evaluation, procurement and calibration of required instrumentation, an investigation of hemolyzed-blood spectrophotometry was undertaken to institute an intra-laboratory oxygen-saturation standard-of-reference methodology of the highest order of accuracy (Section II). This phase of the program resulted in a substantial advance in the state of the art of laboratory blood oxygen saturation measurement.

During the first nine months of the program, simultaneous studies were conducted (1) of the spectrophotometric properties of whole-blood samples of varying film depths and various hematocrits (Section III), (2) of the spectrophotometric properties of bloodless skin and tissue samples of various pigmentation and various anatomic sites, and (3) of the spectrophotometric properties of human subjects of various pigmentation at various skin sites, various skin temperatures and various skin-blood flows (Section IV). It was anticipated that the results of these separate and parallel studies would be brought together to establish the basic design criteria for the various experimental external biosensor systems.

These studies lead to the design and fabrication of both chopped light and d.c. experimental biosensor systems in which light wavelength centering frequency, spectral bandwidth and sensor disk configurations were adjustable variables

(Section V). These systems were extensively applied to simulated skin-tissue-blood systems, to experimental animals, to open-heart surgery patients and to human volunteers in order to define the transfer functions relating backscattered light intensity to blood oxygen saturation (Section V).

Considerable data was acquired from simulated systems in which the oxygen saturation and hematocrit of whole-blood samples were alterable variables. Extensive data were acquired from experimental studies performed upon both Chester White pigs and human patients undergoing open-heart surgery. In these studies arterial oxygen saturation, skin site, skin blood flow, skin temperature, heart rate, respiratory rate, systemic blood pressure, systemic blood flow and systemic temperature were manipulable variables (Section V).

\* \* \* \* \*

Careful analysis of these data indicated that the principle of optical backscatter can be utilized for measuring oxygen saturation of whole-blood samples with a high degree of accuracy, reliability and convenience through the implementation of a congruent optical geometry in which the blood volume illuminated by the light source and the blood volume viewed by the photometric sensor are congruent. This implementation linearly related oxygen saturation to the transfer function of Equation 2, above:

$$\text{O.S.} = K_1 \cdot \frac{I_{\lambda_s} \text{ backscattered}}{I_{\lambda_i} \text{ backscattered}} + K_2$$

where the ratio  $\frac{I_{\lambda_i}}{I_{\lambda_s}}$  of the light source is held constant.

However, the congruent optical geometry proved to be

unsatisfactory in in-vivo studies upon human subjects because of the excessive levels of non-information-bearing photic energy returned from the skin surface and tissues which proved to be "noise", compared with the signal bearing photic energy returned from the blood contained within the skin.

The likelihood of an unacceptable signal-to-noise ratio for a congruent backscatter optical geometry had been anticipated in the original proposal, and transducer configurations in which the illuminated area and sensor observed areas were offset from each other rather than congruent were designed and investigated (such as the annular sensor illustrated in Figure 8 of the Proposal).

Experimental Biosensor Systems operation utilizing such transducers was extensively studied upon experimental animals, human patients and human volunteers. While the non-congruent optical geometry proved to have satisfactory sensitivity and signal-to-noise characteristics, data from these studies demonstrated a significant transmissive component to the spectrophotometric behavior of non-congruent backscatter-mode transducers. This transmissive component of realizable backscatter systems was manifest by two phenomena:

1. a relationship between oxygen saturation and light intensity measurements at a signal and an isosbestic wavelength that is between the relationships characterizing congruent backscatter systems and pure transmission mode systems,

$$O.S. = K_1 \cdot \text{Log} \frac{I_{\lambda_s} \text{ backscattered}}{I_{\lambda_i} \text{ backscattered}} + K_2 \quad \text{Eq. 3}$$

where the ratio  $\frac{I_{\lambda_i}}{I_{\lambda_s}}$  of the light source is held constant.

and,

2. a pronounced sensitivity of the above function to variations in pressure, position or motion between the transducer and the skin.

While the first of the above characteristics of external biosensor backscatter systems, i.e., the semilogarithmic nature of the relationship between oxygen saturation and measured light intensities, represents only a matter of small inconvenience, the second characteristic above is of major practical import. With the demonstration of sensitivity to position, pressure and motion variations of the backscatter mode of operation, the principal hoped-for advantage of external backscatter-mode biosensors over external transmission-mode biosensors for use in active personnel disappeared.

Thus, while external backscatter-mode biosensors retain their obvious advantages in terms of flexibility of positioning and relative comfort of application over conventional transmission-mode devices, if a truly operational external biosensor for use upon active personnel is to be developed, it will be necessary to develop techniques either for stabilizing the physical coupling of the transducers to the subjects or for continuously compensating for the variations in optical coupling so produced.

Attention to this well-defined and remaining problem area is recommended to other experimenters in this field.

## II SPECTROPHOTOMETRIC STUDIES OF HEMOLYZED BLOOD

### A. General

Extensive spectrophotometric studies of hemolyzed-blood samples were not anticipated prior to the onset of this program. However, experience with gasometric and spectrophotometric determinations of hemolyzed-blood samples performed during the first several months of the program by an excellent clinical chemistry laboratory demonstrated that the orders of accuracy attainable in clinical chemistry laboratories and satisfactory for medical diagnostic and therapeutic purposes are insufficient for the needs of a developmental program such as conducted under the subject contract.

During the first six months of this program, the Presbyterian Medical Center Cardiac Catheterization Laboratory performed the standard-of-reference oxygen saturation measurements against which all developing instrumentation was compared. This clinical laboratory, which is surely one of the outstanding laboratories of its type in the country, furnished senior personnel for this purpose, each of whom had over five years of continuous experience with both gasometric and spectrophotometric techniques. After careful assessment of the measurement deviation for aliquot samples by both gasometric and spectrophotometric techniques, efforts were instituted to develop an intra-laboratory standard-of-reference spectrophotometric method of a high order of accuracy.

The standard-of-reference measurement method evolved represents a distinct advance in the art of laboratory blood-oxygen saturation measurement. A universal calibration line for hemolyzed-blood samples was realized that eliminates eight of the ten steps previously required to make a single

oxygen-saturation determination upon a blood sample. Prior to this development, 100% oxygen saturation points and 0% oxygen saturation points were chemically created and measured to establish a calibration line for each and every blood specimen studied in the oximetry laboratories. With this newly developed and simplified procedure, accuracies of  $\pm 2\%$  oxygen saturation are attainable, with a standard Beckman Model B laboratory spectrophotometer, an accuracy comparing favorably with any reported in the world.

The details of these spectrophotometric studies of hemolyzed blood directed toward evolution of a high-accuracy simplified method for the standard-of-reference laboratory measurements follow.



## B. Theoretical Basis

The standard spectrophotometric method for determination of the oxygen saturation of hemolyzed-blood samples is based upon the difference in optical absorption properties of hemoglobin and oxyhemoglobin, which is subsumed by the Lambert-Beer's law for non-turbid pigmented solutions illuminated by monochromatic light.

Widespread experience prior to the onset of this program had demonstrated that to make reliable measurements of oxygen saturation in blood samples, it was first necessary to break apart the red blood cells, liberating the hemoglobin contained therein (a procedure referred to as hemolysis), thereby converting the suspension of red blood cells in plasma to a uniform solution of hemoglobin pigments. This hemoglobin solution consists of a mixture of oxygenated hemoglobin (Oxyhemoglobin,  $\text{HbO}_2$ ) and non-oxygenated hemoglobin (Reduced Hemoglobin,  $\text{Hb}$ ). The Oxygen Saturation of the solution is defined as that fraction of the total hemoglobin present in the oxygenated form.

Non-turbid hemoglobin solutions are absorbing media that follow the Lambert-Beer Transmission Law, which states that light traversing an absorbing medium suffers an exponential (logarithmic) reduction in its intensity. The propensity of an absorbing material to produce "extinction" of the light traversing it is quantitated in spectrophotometric notation as its "extinction coefficient". The extinction coefficients are wavelength dependent. Figure FR-1, for example, is a plot of extinction coefficients of the two pigments oxygenated hemoglobin and reduced hemoglobin against spectral wavelength. The differences in the absorption spectra of the reduced and oxygenated form of hemoglobin form the basis upon which the

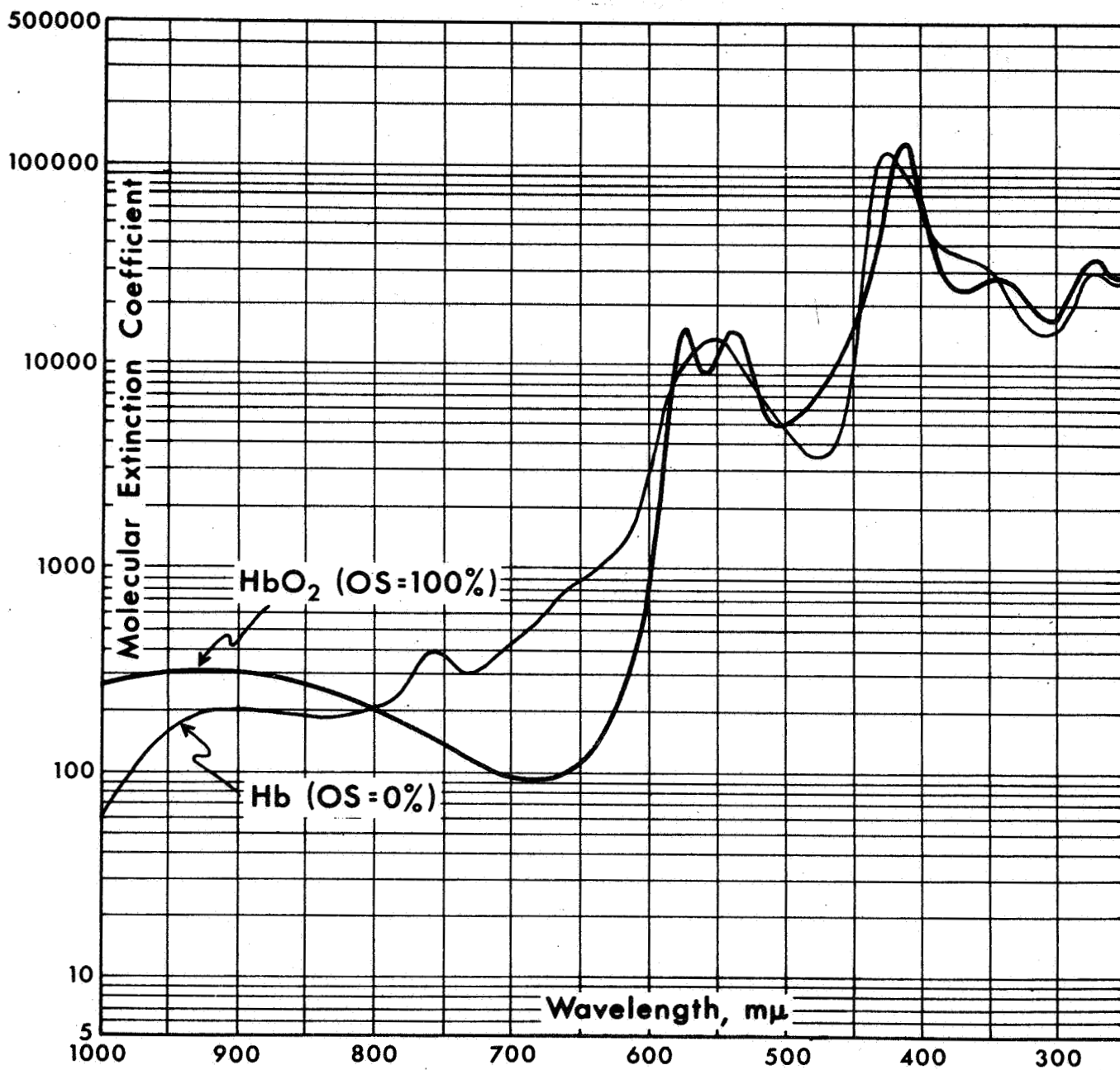


Figure FR-1. Spectrophotometric Studies of Hemolyzed Blood. Absorption spectra of oxyhemoglobin and reduced hemoglobin.

spectrophotometric determination of oxygen saturation is made.

The attenuation of light caused by a real sample of an absorbing material is a function not only of its extinction coefficient at the wavelength used, but is a function as well of the concentration of the material in the sample and the thickness of the sample. This is mathematically expressed in Equation 4, embodying Lambert's contribution in showing that the exponent is proportional to the optical path length (solution thickness), and Beer's contribution in showing that the exponent is proportional to the concentration of pigment for a given optical path length:

$$I = I_0 10^{-eCx} \quad \text{Eq. 4}$$

where

- I = Transmitted light intensity
- $I_0$  = Incident light intensity
- e = Extinction (or absorption) coefficient
- C = Concentration of pigment
- x = Optical path length (sample thickness).

If there are two non-interacting pigments in a solution, then their extinction-coefficient pigment-concentration products may be added as shown in Equation 5:

$$I = I_0 10^{-(e_1C_1 + e_2C_2) x} \quad \text{Eq. 5}$$

It is clear from the forms of Equations 4 and 5 that the logarithm of the ratio of transmitted light to incident light completely characterizes the optical-absorption properties of the solution.



The negative of the logarithm of Equation 5 is called the optical density, which for hemolyzed-blood solutions can be written as Equation 6:

$$\text{O.D.} = \epsilon_o C_o + \epsilon_r C_r \quad \text{Eq. 6}$$

where

$$\begin{aligned} \text{O.D.} &= \text{Optical density} \\ \epsilon_o &= \text{Extinction coefficient per HbO}_2 \text{ molecule} \\ C_o &= \text{Concentration of HbO}_2 \\ \epsilon_r &= \text{Extinction coefficient per Hb molecule} \\ C_r &= \text{Concentration of Hb.} \end{aligned}$$

Since hemoglobin concentration is equal to the sum of the Hb concentration and the HbO<sub>2</sub> concentration, Equation 6 may be rewritten as shown in Equation 7:

$$\text{O.D.} = \left[ (\epsilon_o - \epsilon_r) \frac{C_o}{C_r} + \epsilon_r \right] C \quad \text{Eq. 7}$$

An isosbestic wavelength is defined as a wavelength at which the extinction coefficients for Hb and HbO<sub>2</sub> are identical. Equation 7 may be written for this case as shown in Equation 8:

$$\text{O.D.}_i = \epsilon_i C \quad \text{Eq. 8}$$

By taking the ratio of Equations 7 and 8, a relationship can be established upon which to base a method for determining the oxygen saturation of hemolyzed-blood solutions. This is shown in Equation 9:

$$\frac{\text{O.D.}}{\text{O.D.}_i} = \left( \frac{e_o - e_r}{e_i} \right) \frac{C_o}{C} + \frac{e_r}{e_i} \quad \text{Eq. 9}$$

Equation 9 indicates that a linear relationship exists between oxygen saturation,  $C_o/C$ , of a hemolyzed-blood sample and the ratio of its optical densities at a non-isosbestic and an isosbestic wavelength. Strictly speaking, this relationship is valid only if the hemolyzed-blood solution is non-turbid and the only absorbing constituents are Hb and HbO<sub>2</sub>.

In practice, the transmission of light through a hemolyzed-blood sample is measured at an isosbestic wavelength and non-isosbestic (signal) wavelength. These two measurements are also performed with the cuvette filled with water rather than hemolyzed blood. The differences between the intensity measurements performed upon the hemolyzed-blood-filled cuvettes and the water-filled cuvettes establish the optical densities of the samples. The percent hemoglobin oxygen saturation can be found from the ratio of the two optical-density measurements.

### C. Improvement in Anaerobic Sampling

Oxygen-saturation measurements based upon the standard laboratory method discussed above have inherent limitations in attainable accuracy, particularly at low levels of oxygen saturation, which arise as a consequence of the operations involved in sample-preparation protocol. Attainment of the necessary degree of accuracy was implemented by developing a practicable improvement over the standard practice of using a glass syringe for whole-blood sample removal. An anaerobic sample capsule was designed to eliminate errors arising from air-entrainment which may occur both in the operation of sample withdrawal and in the introduction of a hemolyzing agent. The anaerobic sample capsule further obviates the need for the addition of mercury for mixing and the need for silicone syringe lubricant, both of which are potential sources of sample contamination.

The sample capsule, shown in Figure FR-2, consists of a measured section of Teflon tubing equipped at each end with a Luer-lok connector and a stop-cock valve. Hemolysis is accomplished by injection into the capsule of buffered Triton X-100 with a 5 inch, #20 needle through a capsule end-valve shielded with a 1 inch, #15 needle. Mixing is accomplished by means of a 1/8" brass cube housed in the capsule. Delivery of hemolyzed blood into 0.1 mm spectrophotometric-cuvette cells is accomplished through a #20 needle-equipped end-valve by a screw-driven pressure-plate which reduces the volume of the capsule, as shown in Figure FR-3.



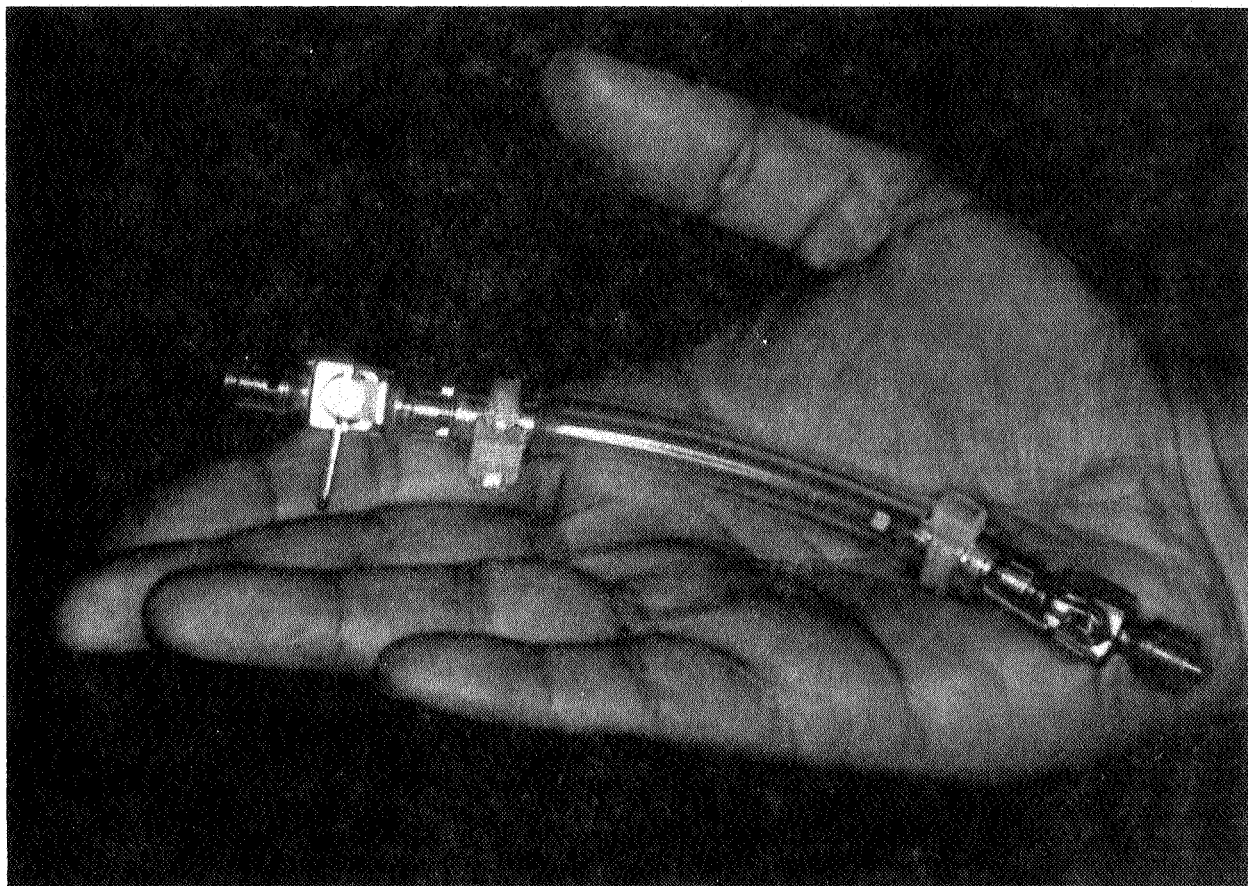


Figure FR-2. Spectrophotometric Studies of Hemolyzed Blood. Anaerobic sample capsule for obtaining whole-blood samples for oxygen saturation determination. The capsule consists of Teflon tubing end-equipped with Luer-Lok fittings and valves, and contains a brass cube for mixing hemolyzing agent with whole blood.

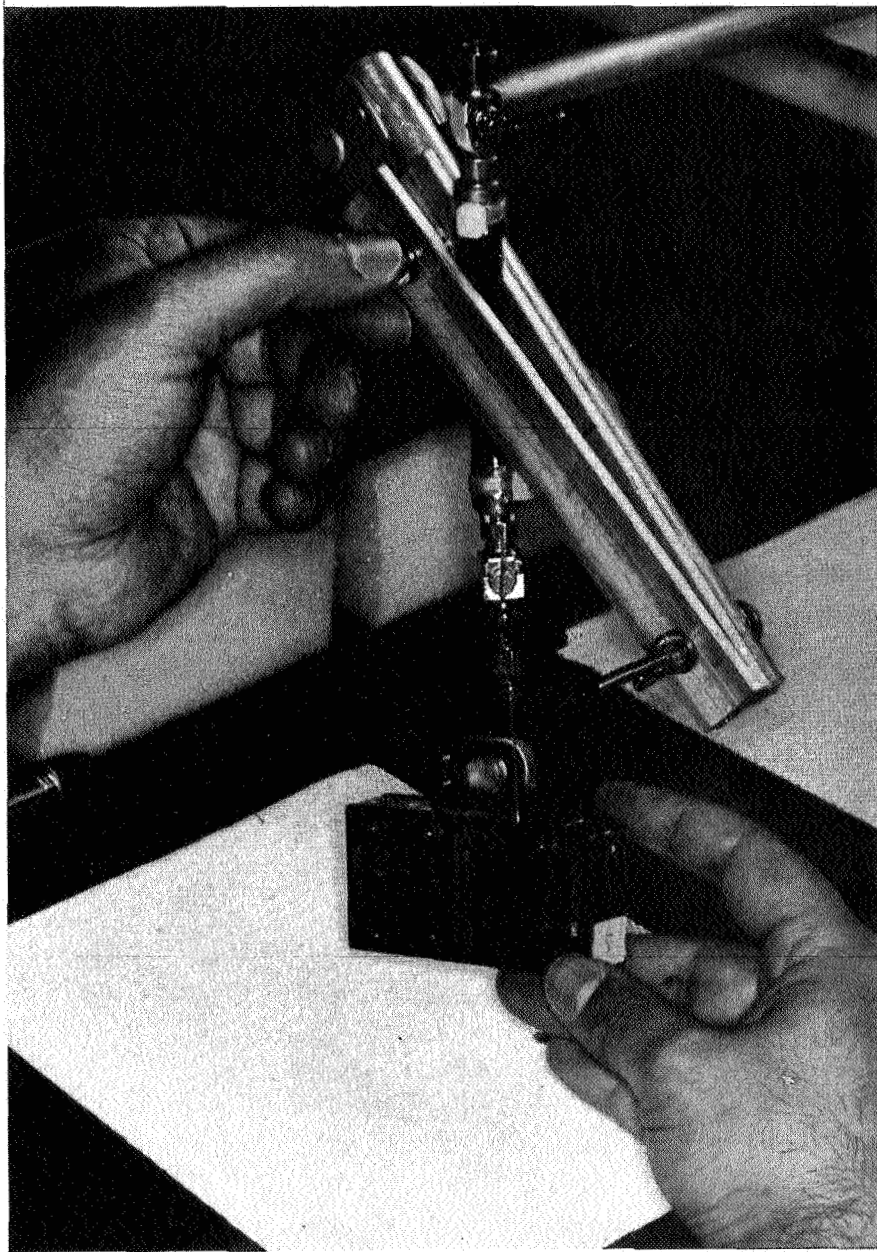


Figure FR-3. Spectrophotometric Studies of Hemolyzed Blood. Delivery of hemolyzed blood from anaerobic sample capsule to spectrophotometric cuvette.

#### D. Operational Oxygen Saturation Data

Optical density measurements were performed following the above sampling protocol on blood obtained post-operatively from a heart-lung machine. Because the rate of change of molecular extinction coefficient with wavelength is large for Hb, in the neighborhood of 506 m $\mu$  and for HbO<sub>2</sub> in the neighborhood of 480 m $\mu$ , small variations in spectrophotometer wavelength settings contribute significantly to the non-reproducibility of optical density measurements. On the Beckman Model B Spectrophotometer used, repeatability of successive wavelength settings was assured through the use of narrow band interference filters with peak transmissivity at the desired wavelengths. The optical density of hemolyzed-blood samples was measured in calibrated 0.1 mm four-cell Waters Model NAC-11 cuvettes, in which three cuvette cells were filled with aliquots of a given hemolyzed-blood sample and a fourth was consistently used as a distilled water reference cell. The optical density of each sample-containing cell was measured at 480 m $\mu$  and at 506 m $\mu$ , and respective ratios of O.D. 480/O.D. 506 were computed so that each O.D. 480/O.D. 506 ratio reported per blood sample is the average of three sets of measurements. The experimentally-determined ratio of optical density at 480 m $\mu$  to optical density at 506 m $\mu$  is reported in Figure FR-4 for forty blood samples of varying hematocrit brought to 100% oxygen saturation by humidified tank oxygen (95% O<sub>2</sub> - 5% CO<sub>2</sub>) in a pump-oxygenator system.\* The mean value of these oxyhemoglobin-intercept ratios is 1.352 with a standard deviation of  $\pm .011$  representing an equivalent oxygen saturation error of  $\pm 1.69\%$  O.S.

\* See Section III, Figures FR-18 through FR-23 for description of the pump-oxygenator flowthrough cuvette system used in these studies.

Optical Density at 480 Millimicrons				
Optical Density at 506 Millimicrons				
HbO <sub>2</sub>			Hb	
Paired Hb and HbO <sub>2</sub> Measurements	Hematocrit			
	1.343	40.5		
	1.363	32.0		
	1.359	47.0		
	1.364	40.0		
	1.357	32.0		
	1.370	32.0		
	1.364	32.0		
	1.363	32.0		
	1.363	32.0		
	1.345	37.5		
	1.335	37.5		
	1.340	37.5		
	1.343	37.5		
	1.340	37.5		
	1.356	30.5		
	1.344	37.0		
	1.367	46.5		
	1.338	41.0		
	1.351	57.5		
Unpaired Hb and HbO <sub>2</sub> Measurements	1.346	32.0	44.0	.692
	1.348	36.5	44.0	.685
	1.347	39.6	44.0	.696
	1.354	32.0	44.0	.700
	1.361	40.0	44.0	.696
	1.345	45.0	44.0	.689
	1.350	39.0	35.0	.690
	1.358	----	35.0	.693
	1.348	50.0	35.0	.688
	1.349	33.0	35.0	.693
	1.359	42.0	35.0	.697
	1.363	36.5		
	1.364	36.5		
	1.328	43.0		
	1.333	43.0		
	1.342	43.0		
	1.344	43.0		
	1.343	43.0		
	1.367	45.5		
	1.355	42.0		
	1.363	44.0		
Average N=40 1.352			Average N=30 .701	
S. D. $\pm$ .011			S. D. $\pm$ .009	
Equivalent %OS Error = $\pm$ 1.69%			Equivalent %OS Error = $\pm$ 1.38%	

Figure FR-4. Spectrophotometric Studies of Hemolyzed Blood. Experimentally-determined ratios O. D. 480/O. D. 506 for tank-oxygen oxygenated and tank-nitrogen deoxygenated hemolyzed-blood samples.

The standard deviation (S.D.) used in this report is defined in Equation 10.

$$\text{S.D.} = \sqrt{\frac{\sum (x - \bar{x})^2}{N - 1}} \quad \text{Eq. 10}$$

where

$x$  = an element of a set of  $N$  observations

$N$  = the total number of observations

$\bar{x} = \sum x/N$

and the standard deviation equivalent percent oxygen saturation error reported is  $\pm (\text{S.D.} \times 100)/(1.352 - .701)$ . For normal distributions of elements,  $x$ , 68.27% of the  $N$  observations lie between  $\bar{x} - \text{S.D.}$  and  $\bar{x} + \text{S.D.}$ , 95.45% lie between  $\bar{x} - 2 \text{ S.D.}$  and  $\bar{x} + 2 \text{ S.D.}$ , and 99.73% lie between  $\bar{x} - 3 \text{ S.D.}$  and  $\bar{x} + 3 \text{ S.D.}$

The 100% oxygen-saturation intercept of value of 1.352 presented in Figure FR-4 may be compared with our previously reported<sup>1</sup> mean O.D. 480/O.D. 506 ratio for six air-oxygenated samples of 1.362 with a standard deviation of  $\pm .018$ , and with our previous two tank-oxygenated values of 1.358 and 1.337. The 100% oxyhemoglobin O.D. 480/O.D. 506 ratio of 1.35 was reported in 1960 in a paper by Verel, Saynor and Kesteven<sup>2</sup>, in which the authors state that it, and the value of the 0% oxygen-saturation intercept ratio discussed below, are constants that need be determined from only a single sample of blood. Reference<sup>3</sup> is also made to our work in the

805 mμ isosbestic wavelength and 625 mμ non-isosbestic wavelength system which yielded a mean O.D. 625/O.D. 805 ratio for 19 tank-oxygenated blood samples of .972 with a standard deviation of  $\pm .051$ . The numerical value of the ratio in the 805-625 mμ wavelength system is, of course, not directly comparable to the value of the ratio in the 506-480 mμ wavelength system, but comparison of the standard deviations may reflect both an improvement in technique and the advantage of working in the latter system where the optical absorption of hemoglobin is approximately 25 times greater in the former.

Data were obtained bearing on the completely-deoxygenated hemoglobin oximetric readout-line intercept. The experimentally determined ratio of optical density at 480 mμ to optical density at 506 mμ is also reported in Figure FR-4 for thirty hemolyzed-blood samples of varying hematocrit brought to 0% oxygen saturation by humidified tank nitrogen (95% N<sub>2</sub> - 5% CO<sub>2</sub>) in the pump-oxygenator system. The mean value of these hemoglobin intercept ratios is .701 with a standard deviation of  $\pm .009$  representing an equivalent percent oxygen saturation error of  $\pm 1.38\%$  O.S. This value may be compared with our previously reported<sup>4</sup> mean O.D. 480/O.D. 506 ratio for two tank-nitrogen deoxygenated samples of .736 and .739 and with our mean ratio for six sodium-dithionite deoxygenated samples of .715 with a standard deviation of  $\pm .029$ .

The value of .7 is categorically reported by the 1960 workers cited above. As in the case of the HbO<sub>2</sub> intercept, indirect comparison may be made with our previously reported<sup>5</sup> mean O.D. 625/O.D. 805 ratio for 19 tank-nitrogen deoxygenated samples of 5.964 with a standard deviation of  $\pm .319$ .

### E. Experiments in Precision Limits

In an attempt to establish attainable limits of precision on the value of O.D. 480/O.D. 506 for Hb and HbO<sub>2</sub>, experiments were conducted in which multiple aliquots of a given sample were measured comparing the use of one sample cuvette and alternating wavelength settings, and the use of five cuvettes measured at a common 480-m $\mu$  and a common 506-m $\mu$  wavelength setting. The results are shown in Figures FR-5, FR-6 and FR-7.

In Figure FR-5, identical samples of HbO<sub>2</sub> were obtained by linking five sample capsules and tank-oxygenating the whole-blood flow through all of them for one hour. The five capsules were removed simultaneously, hemolyzed, and measured serially in one cuvette which was cleaned between successive measurements. The process required successive wavelength settings on the spectrophotometer and resulted in a mean O.D. 480/O.D. 506 ratio of 1.363 with a standard deviation of  $\pm .005$ , equivalent to a percent oxygen saturation error of  $\pm .77\%$ . Also shown in Figure FR-5 are the results of measurements on five aliquots of a second blood, tank-oxygenated for one hour, simultaneously hemolyzed, and introduced into five spectrophotometer cuvettes which were all measured at the same 480 m $\mu$  wavelength setting followed by measurement at the same 506 m $\mu$  setting. Somewhat increased precision is indicated in the mean O.D. 480/O.D. 506 ratio of 1.341 with a standard deviation of .004 corresponding to an equivalent percent oxygen saturation error of  $\pm .61\%$ .

Four experiments were performed in like manner for the tank-nitrogen deoxygenated Hb O.D. 480/O.D. 506 ratio in which serial sample processing and wavelength setting resulted in a



Optical Density at 480 Millimicrons  
Optical Density at 506 Millimicrons

Serial Measurement Protocol One Cuvette Alternate wavelength settings  Aliquots of Blood "A"		Simultaneous Measurement Protocol Five Cuvettes Common wavelength settings  Aliquots of Blood "B"	
	1.357		1.345
	1.370		1.335
	1.364		1.340
	1.363		1.343
	1.363		1.340
Average	1.363	Average	1.341
S. D.	$\pm .005$	S. D.	$\pm .004$
Equivalent %OS Error = $\pm .77\%$		Equivalent %OS Error = $\pm .61\%$	

Figure FR-5. Spectrophotometric Studies of Hemolyzed Blood. Precision attained in experimentally-determined ratios O. D. 480/O. D. 506 for oxyhemoglobin, serial optical-density measurement vs. simultaneous optical-density measurement protocol.



Hb

Optical Density at 480 Millimicrons  
Optical Density at 506 Millimicrons

Serial Measurement Protocol One Cuvette Alternate wavelength settings		Simultaneous Measurement Protocol Five Cuvettes Common wavelength settings	
Aliquots of		Aliquots of	
Blood "A"	Blood "C"	Blood "B"	Blood "D"
.702	.692	.711	.690
.710	.685	.701	.693
.705	.696	.705	.688
.714	.700	.706	.693
.717	.696	.699	.697
	.689		
Average .710	.693	.704	.692
S. D. $\pm .006$	$\pm .005$	$\pm .005$	$\pm .003$
Equivalent %OS Error = $\pm .92\%$	$\pm .77\%$	$\pm .77\%$	$\pm .46\%$

Figure FR-6. Spectrophotometric Studies of Hemolyzed Blood. Precision attained in experimentally-determined ratios O. D. 480/ O. D. 506 for hemoglobin, serial optical-density measurement protocol vs. simultaneous optical-density measurement protocol.

Optical Density Measurement Protocol	Blood Aliquots	Optical Density at 480 Millimicrons	
		Optical Density at 506 Millimicrons	
		HbO <sub>2</sub> Mean S. D. %OS Error	Hb Mean S. D. % OS Error
Serial	"A"	1.363 $\pm$ .77 %	.710 $\pm$ .006, $\pm$ .92%
	"C"		.693 $\pm$ .005, $\pm$ .77%
Simultaneous	"B"	1.341 $\pm$ .004, $\pm$ 61%	.704 $\pm$ .005, $\pm$ .77%
	"D"		.692 $\pm$ .003, $\pm$ .46%

Figure FR-7. Spectrophotometric Studies of Hemolyzed Blood. Summary of precision attained in experimentally-determined ratios O. D. 480/O. D. 506 for Hb and HbO<sub>2</sub>, serial optical-density measurement protocol vs. simultaneous optical-density measurement protocol.

five-aliquot mean value of .710 with a standard deviation of  $\pm .006$  or percent oxygen saturation error of  $\pm .92\%$ , and a six-aliquot second blood mean value of .693 with a standard deviation of  $\pm .005$  or  $\pm .77\%$  oxygen saturation error as shown in Figure FR-6. Associated simultaneous sample processing and common-wavelength data are also shown in Figure FR-6 for two different bloods indicating an O.D. 480/O.D. 506 ratio for one of  $.704 \pm .005$  corresponding to  $\pm .77\%$  and an O.D. 480/O.D. 506 ratio for the other of  $.692 \pm .003$  corresponding to  $\pm .46\%$  oxygen saturation error. These separate precision experiments are brought together in Figure FR-7 from which it may be concluded that wavelength-setting variation as a source of error is masked by the vagaries of other perturbations for Hb but is significant at 100% HbO<sub>2</sub>.

F. Effect of Oxygenating and Deoxygenating Gas Flow

Data are shown in Figures FR-8 and FR-9 bearing on the possible deleterious effect on whole blood arising from the mechanics of prolonged gas flowthrough. As indicated in Figure FR-9, the blood used in the work reported, obtained from a surgical heart-lung machine, appeared to undergo no detectable change in optical properties as evidenced also in the data of Figure FR-8 in which whole blood, over a four-hour period, was tank oxygenated, tank-nitrogen deoxygenated, and reoxygenated to a comparable value of O.D. 480/O.D. 506.

G. Effect of Amount of Hemolyzing Agent

The amount of hemolyzing agent, used in the whole-blood preparation protocol, is .05 cc of 33% Triton X-100 in .1 M Borax per 1.0 cc of whole blood. The effect on O.D. 480/O.D. 506 for  $\text{HbO}_2$  of a twofold addition of detergent is shown in Figure FR-10, indicating that a slight excess may be tolerated. Preliminary data were obtained indicating that inadequate detergent may result in incomplete hemolysis and may constitute a more serious source of error in the determination of O.D. 480/O.D. 506 ratios.

Optical Density at 480 Millimicrons		
Optical Density at 506 Millimicrons		
HbO <sub>2</sub> Oxygenation 1 hour O <sub>2</sub> flow	Hb Deoxygenation 2 hours N <sub>2</sub> flow	HbO <sub>2</sub> Re-oxygenation 1 hour O <sub>2</sub> flow
1.364	.699	1.361

Figure FR-8. Spectrophotometric Studies of Hemolyzed Blood. Experimentally-determined effect on optical properties of heart-lung machine hemolyzed blood: 1 hr. O<sub>2</sub> flowthrough, followed by 2 hrs. N<sub>2</sub> flowthrough, compared with 1 hr. re-oxygenation O<sub>2</sub> flowthrough.

Hematocrit	Optical Density of Hemolyzed Blood at 805 Millimicrons		
	HbO <sub>2</sub> 15 min. O <sub>2</sub> flow	Hb 45 min. N <sub>2</sub> flow	Partial HbO <sub>2</sub> No gas flow
25	.102	.102	.104
35	.1275	.1275	.129
40	.150	.150	.155
48	.164	.164	.168
62	.219	.219	.221

Figure FR-9. Spectrophotometric Studies of Hemolyzed Blood. Experimentally-determined effect on optical properties of hemolyzed heart-lung machine blood: 15 minutes O<sub>2</sub> flowthrough, followed by 45 minutes N<sub>2</sub> flowthrough, compared with no gas flowthrough.



Optical Density at 480 Millimicrons  
Optical Density at 506 Millimicrons

Standard Amount of Hemolyzing Agent Added: .05 cc Triton X-100 per cc whole-blood aliquots		Excess Amount of Hemolyzing Agent Added: .10 cc Triton X-100 per cc whole-blood aliquots	
	1.363		1.352
	1.364		1.358
Average	1.364	Average	1.355

Figure FR-10. Spectrophotometric Studies of Hemolyzed Blood. Effect of the addition of excess hemolyzing agent on experimentally-determined ratios O. D. 480/O. D. 506 for oxyhemoglobin.

#### H. Chemical vs. Physical Deoxygenation

A comparison was made in the determination of the O.D. 480/O.D. 506 ratio for nitrogen-deoxygenated and sodium-dithionite deoxygenated Hb employing a ten-aliquot approach similar to those discussed above. As shown in Figure FR-11, nitrogen deoxygenation resulted in a mean O.D. 480/O.D. 506 ratio of .692 with a standard deviation of  $\pm .003$  or a percent oxygen saturation error of  $\pm .46\%$  compared to .709  $\pm .012$  or  $\pm 1.84\%$  oxygen saturation error for dithionite. These data constitute evidence of turbidity formation which arises from chemical deoxygenation with sodium dithionite.



Optical Density at 480 Millimicrons  
Optical Density at 506 Millimicrons

Tank-Nitrogen Deoxygenated Hb Aliquots		Sodium-Dithionite Deoxygenated Hb Aliquots	
	.690		.711
	.693		.710
	.688		.704
	.693		.695
	.697		.727
Average	.692	Average	.709
S. D.	$\pm .003$	S. D.	$\pm .012$
Equivalent %OS Error $\pm .46\%$		Equivalent %OS Error $\pm 1.84\%$	

Figure FR-11. Spectrophotometric Studies of Hemolyzed Blood.  
 Comparison of experimentally-determined ratios O. D. 480/  
 O. D. 506 for physically vs. chemically deoxygenated hemoglobin.

## I. Summary

Careful attention to the technique recommended above for oxygen saturation determination in hemolyzed-blood samples permits use of a general calibration curve in which the O.D. 480/O.D. 506 intercept ratio for 100% O.S. is  $1.352 \pm .011$  and that the associated O.D. 480/O.D. 506 intercept ratio for 0% oxygen saturation is  $.701 \pm .009$ , resulting in a general line with slope 153.6 and standard deviation range +4.8 and -4.6. For accuracy greater than this it may be necessary to resort to determining an individual calibration curve for each blood sample.

The use of sodium dithionite as a deoxygenating agent produced turbidity in blood serum, adversely affecting the optical density measurements. The effect of the amount of hemolyzing agent used was investigated. The relation of wavelength selection to precision was demonstrated. Physical oxygenation and deoxygenation by ventilation with oxygen and nitrogen was found to have no deleterious effect on whole blood.

Further experimental work performed upon experimental animals and human subjects substantiated the applicability to freshly-drawn blood samples of the results reported here for heart-lung machine blood.

### III SPECTROPHOTOMETRIC STUDIES OF WHOLE BLOOD

#### A. General

As noted in the foregoing section, for a blood sample to obey the Lambert-Beer's transmission law, it is necessary to break apart the red blood cells of the sample, liberating the hemoglobin contained therein (a procedure referred to as hemolysis), thereby converting the suspension of red blood cells in plasma to a uniform solution of hemoglobin pigments. When hemoglobin pigments are not in uniform solution, but are packaged within individual red blood cells, light introduced on one side of a cuvette containing whole blood is lost to a detector on the opposite side of the cuvette not only through absorption by the blood pigments, but also through reflections from the surfaces of the red blood cells and through refraction.

An external biosensor for the measurement of blood oxygen saturation must deal with whole red blood cells within the body's tissues. Further, the effective tissue hematocrit (volume of blood per volume of tissue) is indeterminate and is varying in time both slowly - as a function of variation of skin perfusion and general body activity, and phasically, - as a function of the pulsatile nature of cardiac output and arterial blood flow. Accordingly, it is mandatory that the relationships generated between the oxygen saturation of whole blood within the tissues and the light intensities transmitted and received by the biosensor be insensitive to and independent of variations in hematocrit.

The relationship between light transmission and oxygen saturation of whole blood, as described in the literature<sup>6,7</sup>

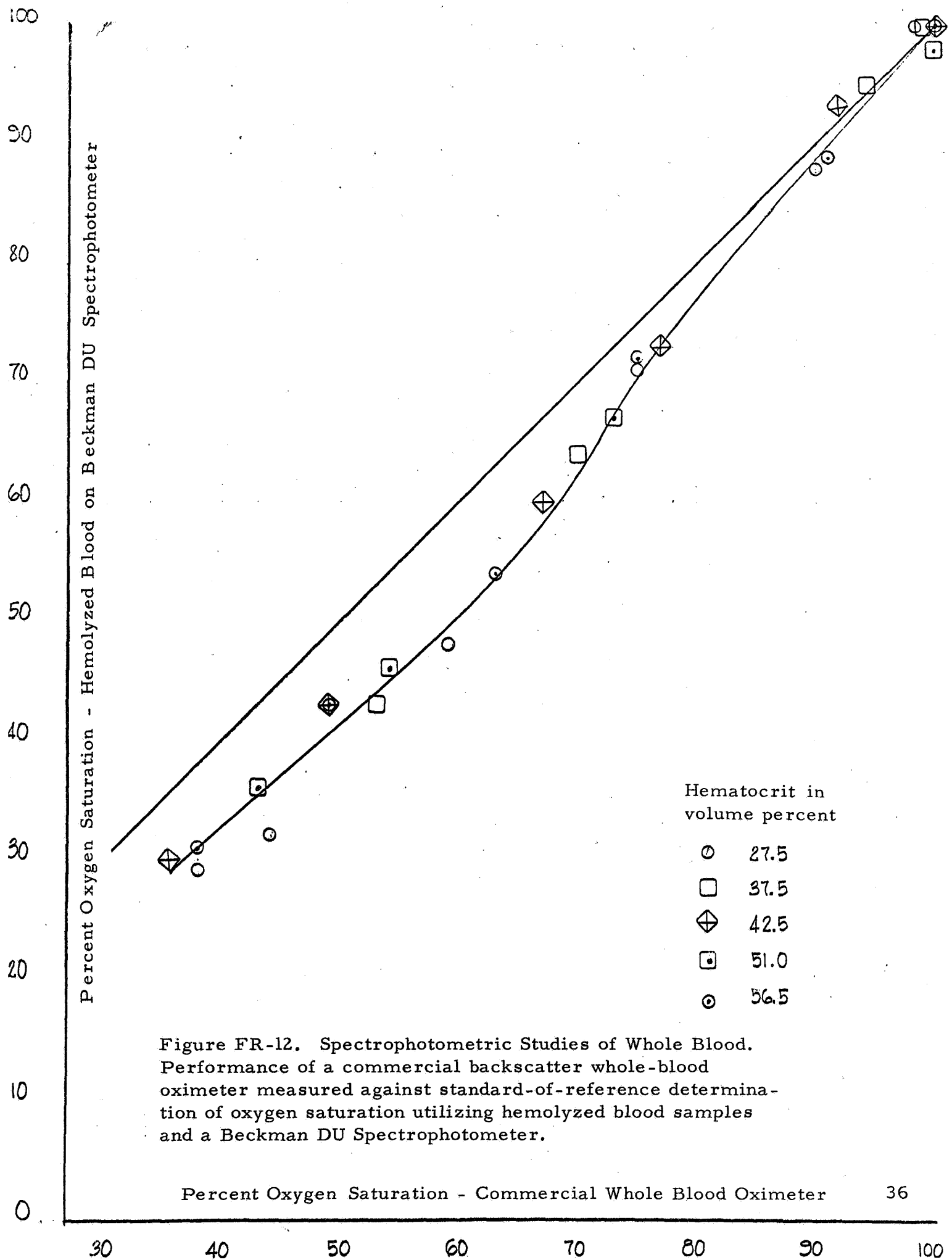
and referenced in the Proposal, are sensitive to hematocrit variations.

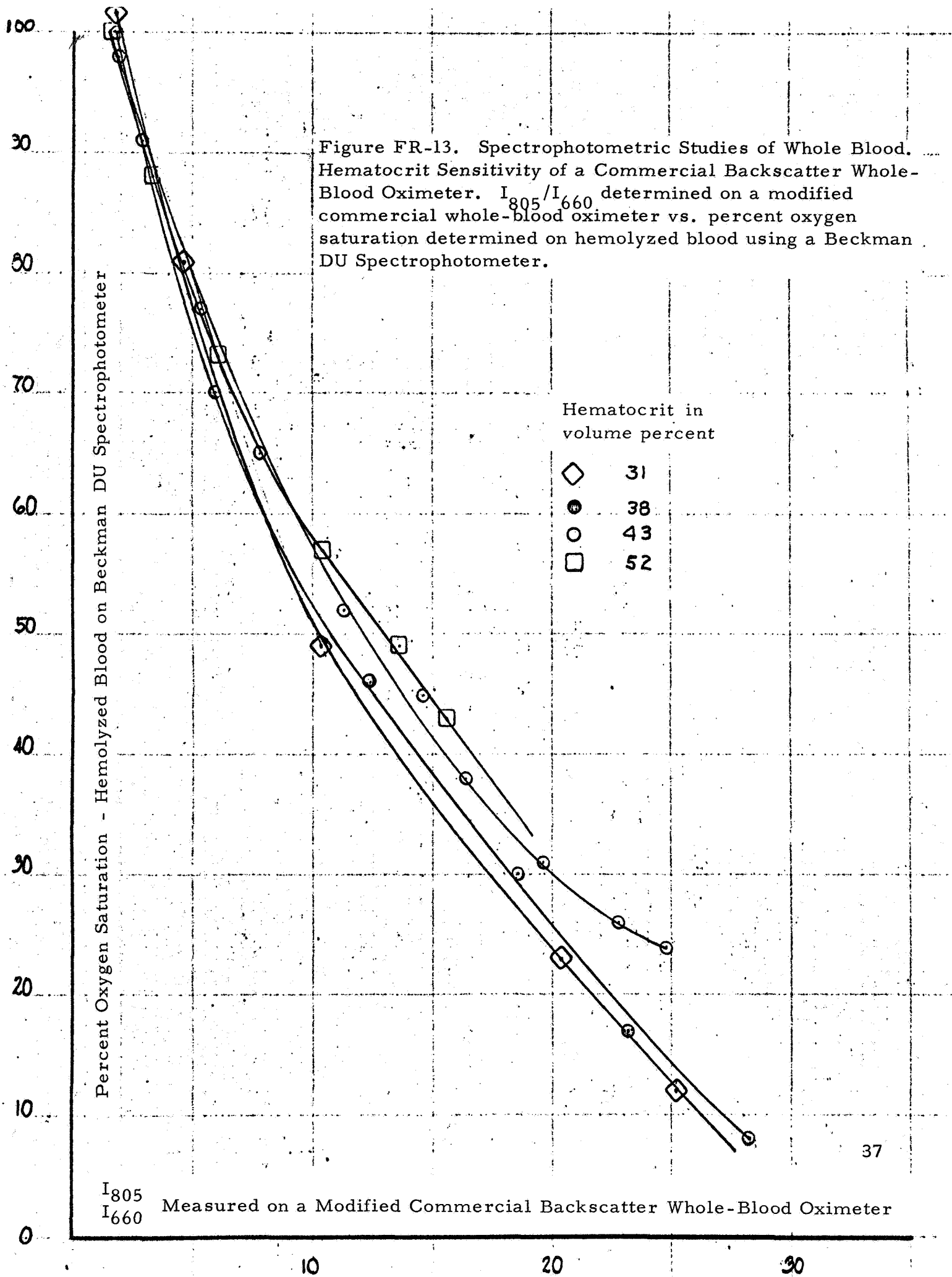
The relationships between backscattered light and oxygen saturation of whole blood as described in the literature<sup>8,9,10</sup> and as quoted in the original Proposal are hematocrit insensitive. The whole-blood oximetry studies originally proposed and planned were designed to corroborate these fundamental relationships described in the literature and to study the influence of optical geometries and other design characteristics of the measuring systems upon system performance in the relatively simpler and more readily manipulable whole-blood systems.

These studies took on increased scope and importance, however, when at the beginning of the program a commercial whole-blood sample oximeter which attempted to implement the fundamental backscatter relationships appearing in the literature became commercially available.\* As reported in Progress Report P-1/167, two such instruments were acquired and evaluated. Figure FR-12 illustrates the unsatisfactory general performance of the commercial system and Figure FR-13 illustrates the tendency toward hematocrit sensitivity of that system.

A major effort in both backscatter and transmission mode whole-blood oximetry was mounted; 1) in order to resolve the disparity between the fundamental backscatter data reported in the literature and the performance of the commercial backscatter oximeter implementing that data; 2) in order to verify the transmission data in the literature and to seek to evolve a technique for implementing a transmission system

\*American Optical Company, Buffalo, New York





independent of hematocrit; and 3) in order to get a firm first-hand purchase upon the relatively simpler whole-blood system that would be useful in establishing design characteristics for the more complicated and difficult to handle skin-tissue-blood systems.

In summary, it can be said that the whole-blood studies performed during this phase of the program demonstrated that with careful and proper selection of the optical characteristics of the measuring systems, a transmission-mode whole-blood oximetric system can be constructed which will relate the oxygen saturation of a blood sample of given hematocrit to the following classic expression as a straight line function:

$$\begin{aligned} \% \text{ O.S.} &= K_1 \cdot \frac{\text{O.D.}_{660}}{\text{O.D.}_{805}} + K_2 = K_1 \frac{\text{Log } \frac{I_{660} \text{ incident}}{I_{660} \text{ transmitted}}}{\text{Log } \frac{I_{805} \text{ incident}}{I_{805} \text{ transmitted}}} + K_2 \\ &= K_1 \frac{\text{Log}_{660} \text{ incident} - \text{Log}_{660} \text{ transmitted}}{\text{Log}_{805} \text{ incident} - \text{Log}_{805} \text{ transmitted}} + K_2 \end{aligned}$$

Eq. 11 (= Eq. 1)

While the above expression can be satisfied as a straight line function for specific blood samples of various hematocrits, the slopes of the resultant straight lines are hematocrit dependent and not universal. A method for implementing the relationships between these two optical densities independent of hematocrit is now available and has recently been independently reported from another laboratory.<sup>11</sup>

It was further demonstrated that with careful and proper selection of the optical properties of the measuring systems, backscatter-mode whole-blood oximetric systems can be fabricated which will relate the oxygen saturation of whole-blood samples

to the following expression:

$$\text{O.S.} = K_1 \cdot \frac{I_{660} \text{ backscattered}}{I_{805} \text{ backscattered}} + K_2$$

Eq. 12 (= Eq. 2)

where the ratio  $\frac{I_{805} \text{ source}}{I_{660} \text{ source}}$  is held constant. This relationship can be made a straight line relationship insensitive to hematocrit.

The transmission-mode and backscatter-mode whole-blood data presented herein indicate that the measurement accuracy of whole-blood systems can be made comparable to that achieved with hemolyzed-blood systems. Both transmission-mode and backscatter-mode whole-blood oximetric apparatus developed in this laboratory provided accuracies in determining the oxygen saturations of whole-blood samples of  $\pm 2\%$  O.S. relative to Van Slyke analysis and hemolyzed-blood spectrophotometric analysis.



## B. Whole-Blood Transmission-Mode Studies

A typical curve, characteristic of the relationship between whole-blood oxygen saturation vs. the ratios of the logarithms of optical densities at 660 mμ and 805 mμ (the reciprocal of optical-density ratio) is shown in Figure FR-14. It is of the form

$$\% \text{ O.S.} = K_1 \frac{OD_{805}}{OD_{660}} + K_2 \quad \text{Eq. 13 (= Eq. 1)}$$

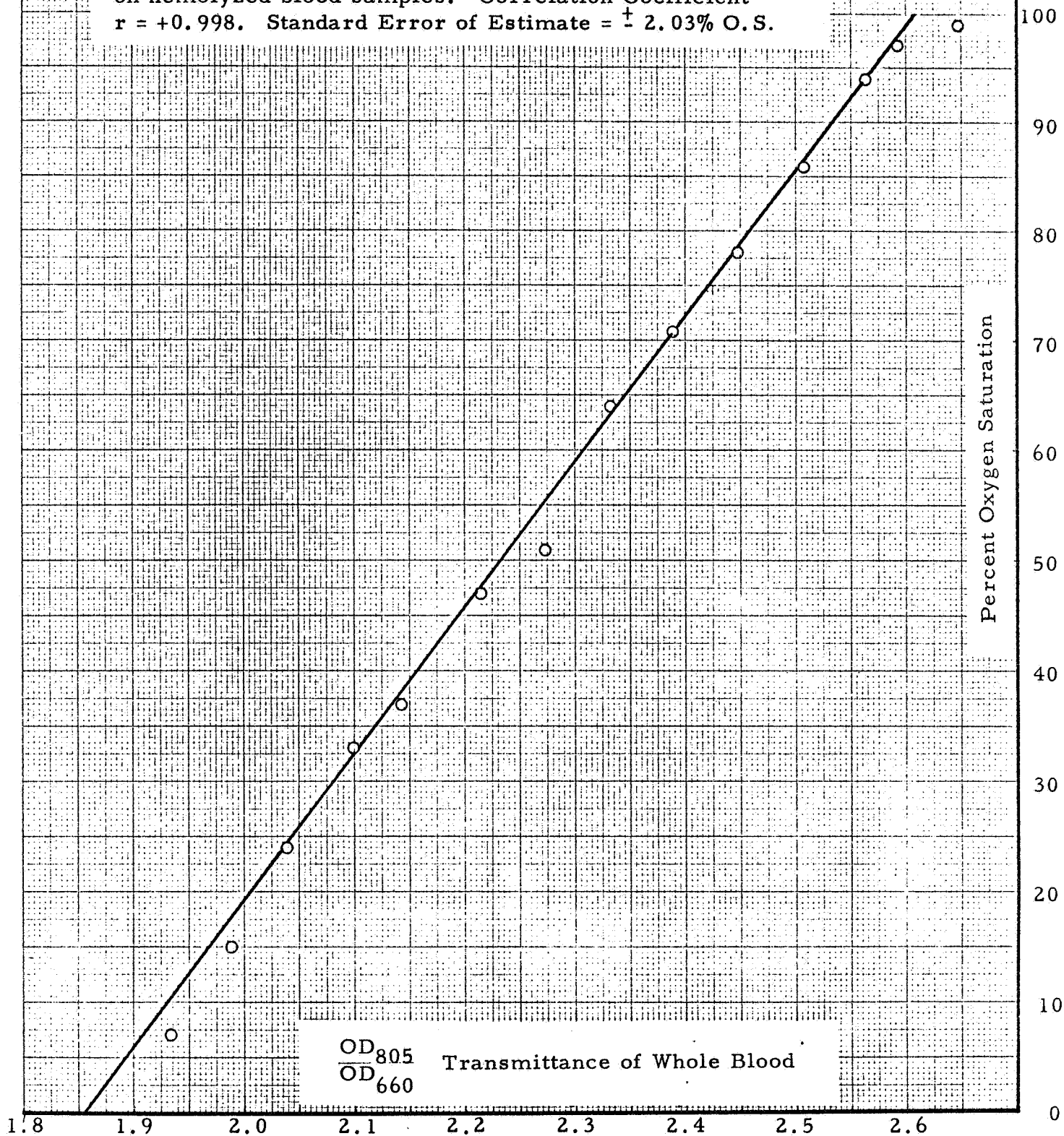
and is linear within a correlation coefficient  $r \pm 0.998$  through the range of 0% to 100% oxygen saturation when compared to hemolyzed samples of the same blood measured spectrophotometrically. The blood sample depicted in this curve had a constant hematocrit of 37 volume percent.

The instrument used to conduct transmission studies is schematically illustrated in Figure FR-15. It consists of two monochromatic light sources with center frequencies of 660 mμ for the signal wavelength and 805 mμ for the isosbestic wavelength.

When oxygen saturation is plotted versus optical densities of transmitted light for blood samples of varied hematocrit (Fig. FR-16), a family of straight lines, each with a different slope, is obtained.\* However, by incorporating the relationships between the extinction coefficients as a function of hematocrit for whole blood into the idealized equations relating optical density to oxygen saturation for hemolyzed

\* The scatter in data points of Figure FR-16 was caused by an optically incorrect gasket in the original cuvette, which, when replaced, resulted in a marked decrease in data point deviation, as typified by Fig. FR-14.

Figure FR-14. Spectrophotometric Studies of Whole Blood, Transmission Mode: Oxygen Saturation vs.  $OD_{805}/OD_{660}$ . Data taken on transmission cuvette apparatus shown in Figure FR-15. Cuvette thickness (optical path length through blood) = 1 mm. Hematocrit = 37 vol. %. Percent oxygen saturation was determined spectrophotometrically on hemolyzed blood samples. Correlation Coefficient  $r = +0.998$ . Standard Error of Estimate =  $\pm 2.03\%$  O.S.



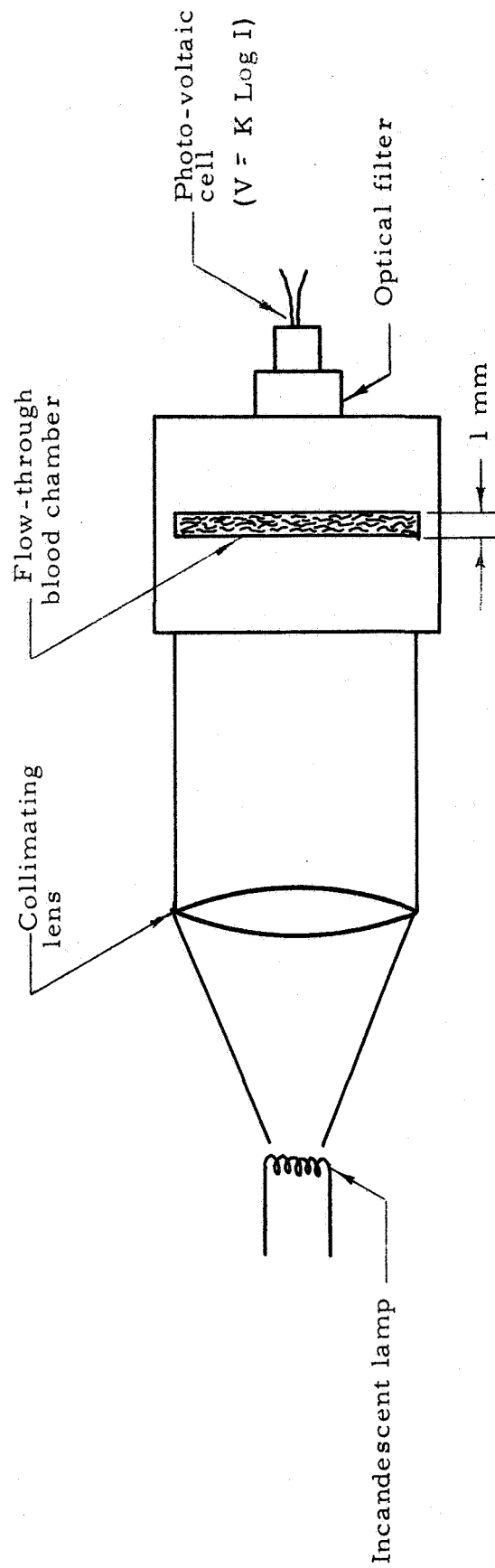
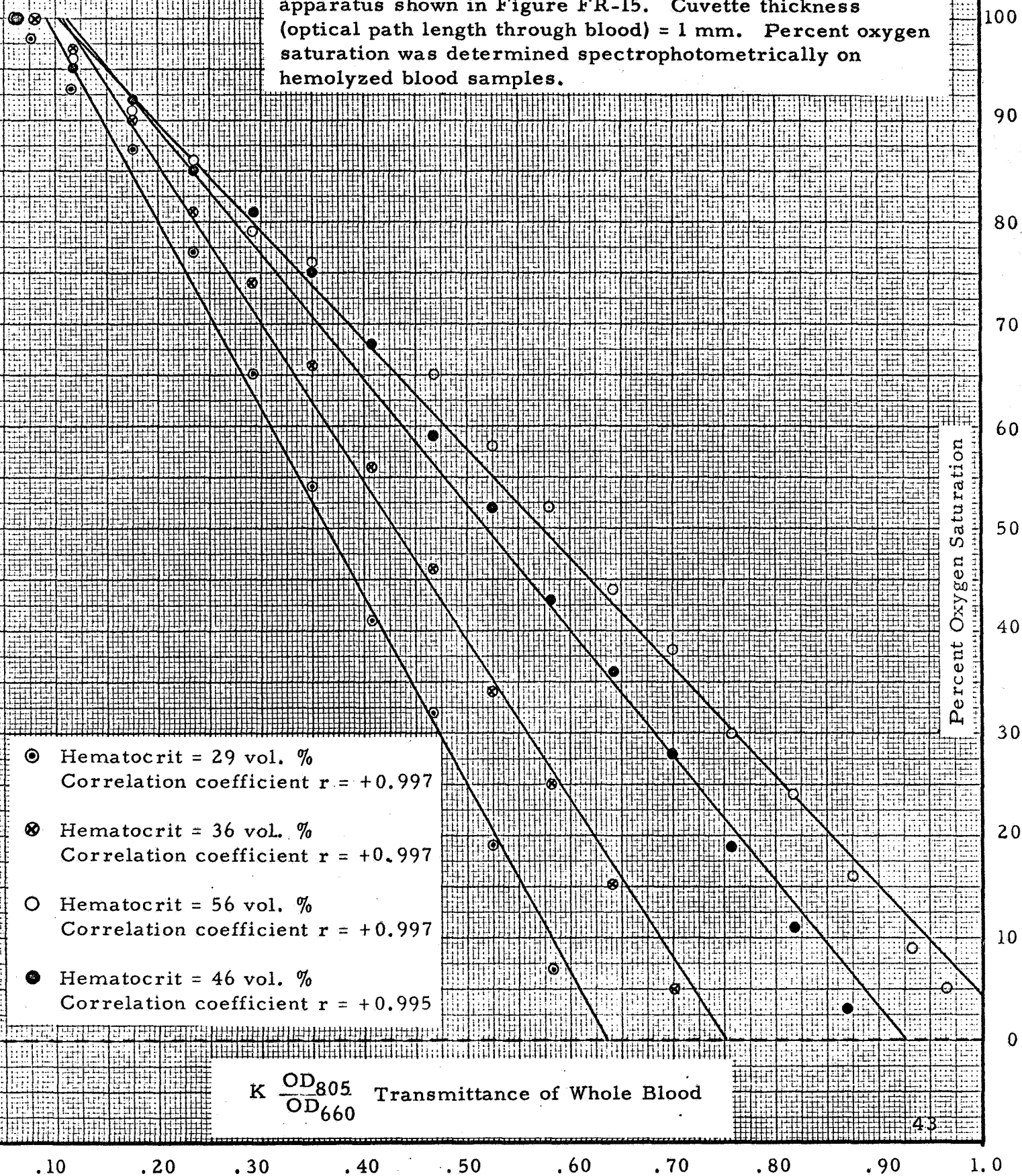


Figure FR-15. Spectrophotometric Studies of Whole Blood: Schematic Diagram of the Transmission Cuvette Oximetric Apparatus.

Figure FR-16. Spectrophotometric Studies of Whole Blood, Transmission Mode: Percent Oxygen Saturation vs.  $OD_{805}/OD_{660}$ . This data was obtained with transmission cuvette apparatus shown in Figure FR-15. Cuvette thickness (optical path length through blood) = 1 mm. Percent oxygen saturation was determined spectrophotometrically on hemolyzed blood samples.



blood, Anderson and Sekelj independently demonstrated that with a properly configured optical geometry, it is possible to relate optical densities to oxygen saturation of whole blood, independent of hematocrit. This relationship can be instrumentably implemented.

An interesting relationship was found to exist between the change in slope of the oxygen saturation vs. optical density characteristic and hematocrit in that this rate of change is linear, as shown in Figure FR-17. Data of other investigators verify, but do not highlight, this characteristic.

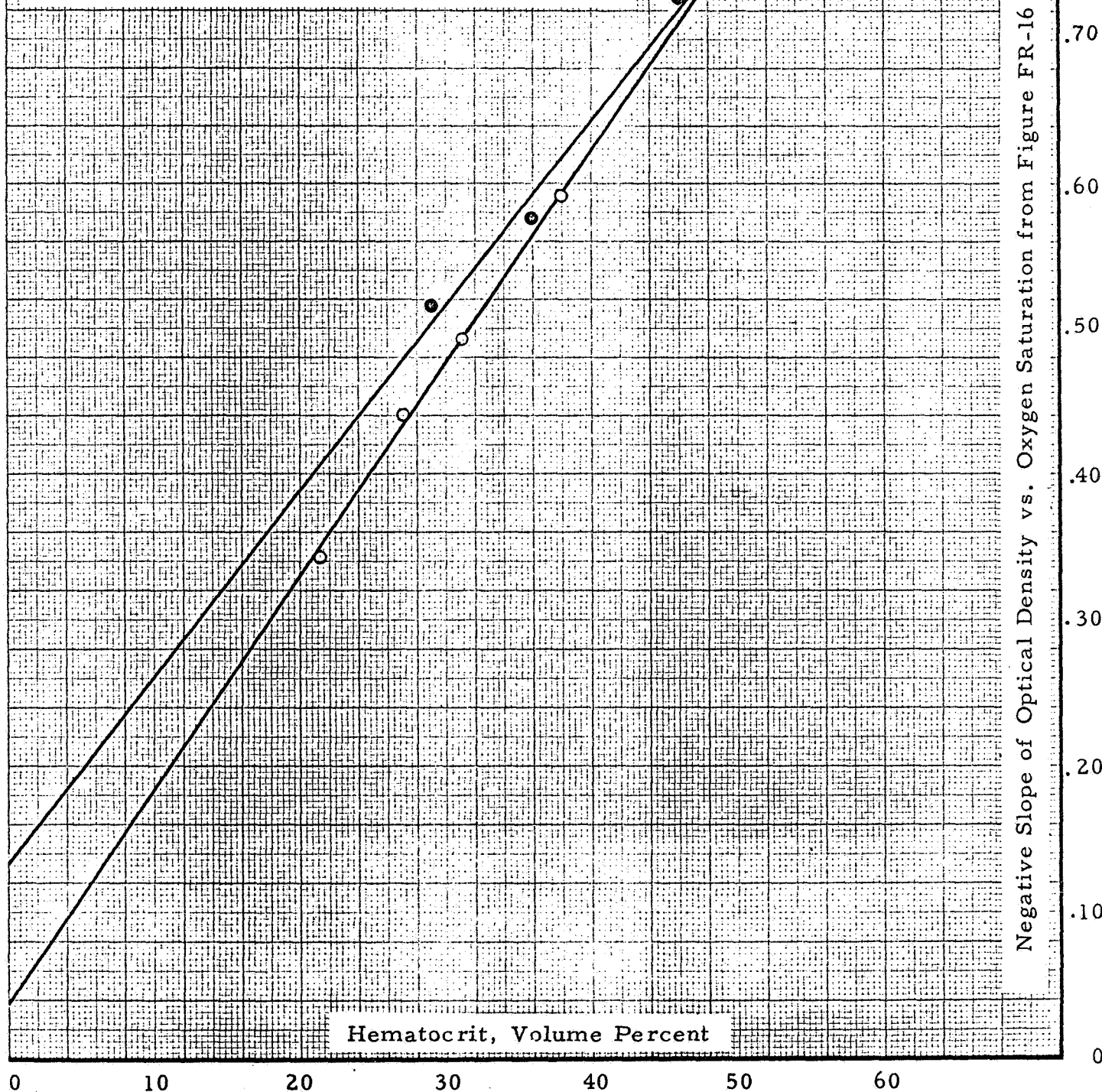
Figure FR-17. Spectrophotometric Studies of Whole Blood, Transmission Mode: Negative Slope of Optical Density vs. Oxygen Saturation (from Figure FR-16 and Reference 11).

$$\frac{\partial \frac{OD_{660}}{OD_{805}}}{\partial OS} \text{ vs. hematocrit}$$

⊙ = Figure FR-16

○ = Reference 11 data

Negative Slope of Optical Density vs. Oxygen Saturation from Figure FR-16 and Reference 11



Hematocrit, Volume Percent

### C. Whole-Blood Backscatter-Mode Studies

The backscatter system utilized to attain the desired relationship between oxygen saturation of whole blood and backscattered light intensities is shown in Figures FR-18 through FR-23. The optical geometry of this system is shown in Figure FR-18. The pump-oxygenator, cuvette and flow circuit used is shown in Figure FR-19.

Reasonably well collimated light from a tungsten source is piped onto the bottom of a one-inch diameter brass cuvette, one centimeter deep. The bottom of the cuvette, shown in Figure FR-22, is covered with a glass plate sealed with an "o" ring. The inside of the cuvette has a bright machined finish. Blood is brought into the top of the cuvette to within two millimeters of the glass bottom via a one-half inch thin-wall brass tube, and removed from the cuvette via two one-quarter inch holes tangential to the brass top of the cuvette as shown in Figure FR-20 and Figure FR-22. The backscattered light, at an angle of  $45^{\circ}$ , is focused onto a photoresistor through an interference filter, whose pass bandwidth is about five millimicrons. The angular distribution of backscattered light was roughly checked and, except for a Brewster's angle effect at the glass-air interface of the cuvette cover plate, no gross variation from uniform angular distribution was observed. The  $45^{\circ}$  angle was chosen for reasons of simplified mechanical construction.

Since the only isosbestic wavelength available in the near infra-red portion of the spectrum occurs at 805 m $\mu$ , this wavelength was selected for experimental implementation of Equation 2. A Clairex photoresistor type 707L was selected

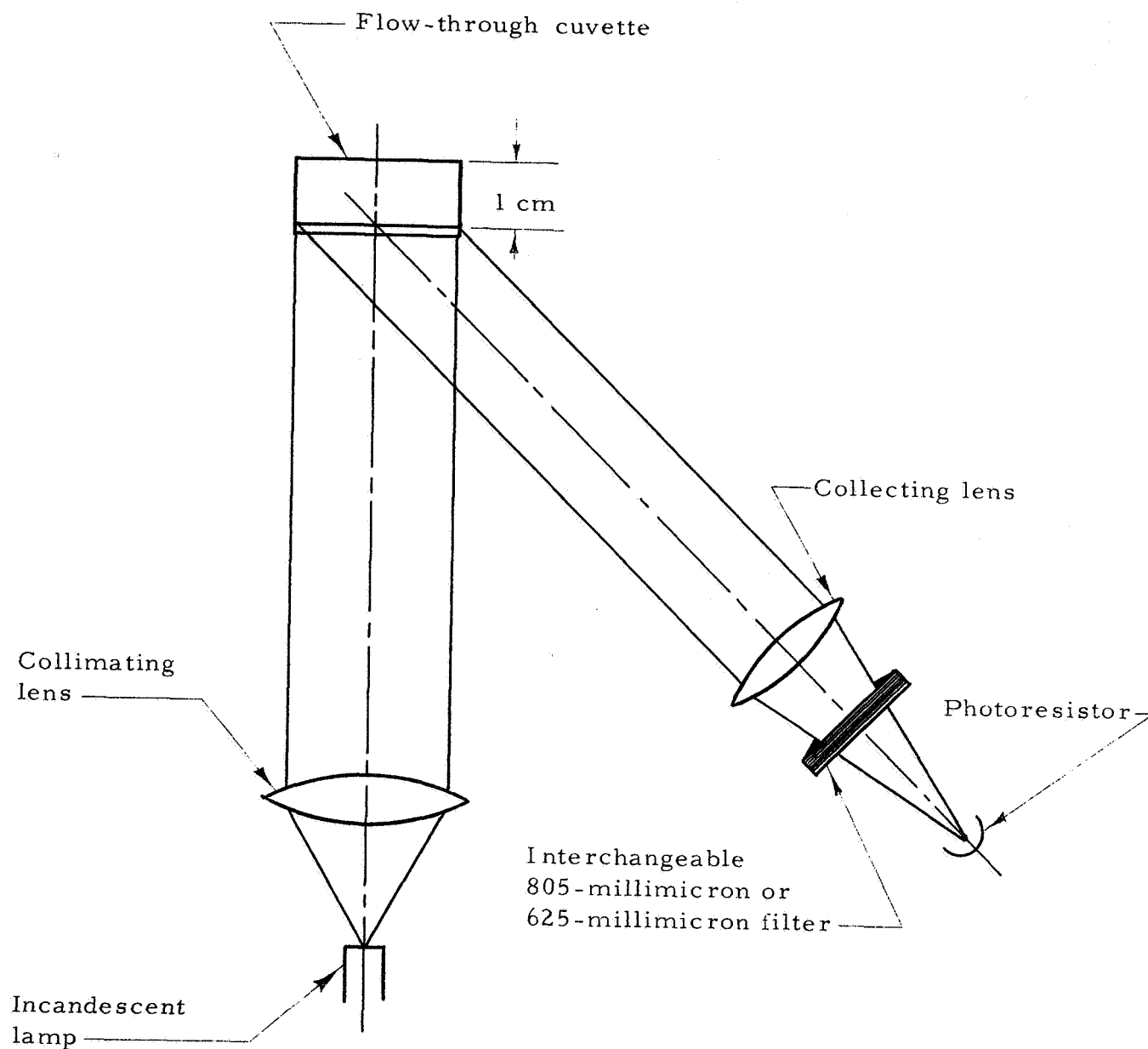


Figure FR-18. Spectrophotometric Studies of Whole Blood, Backscatter Mode: Schematic diagram of congruent optical system in pump-oxygenator flowthrough cuvette apparatus. (See also Figs. FR-19, FR-20, and FR-21).



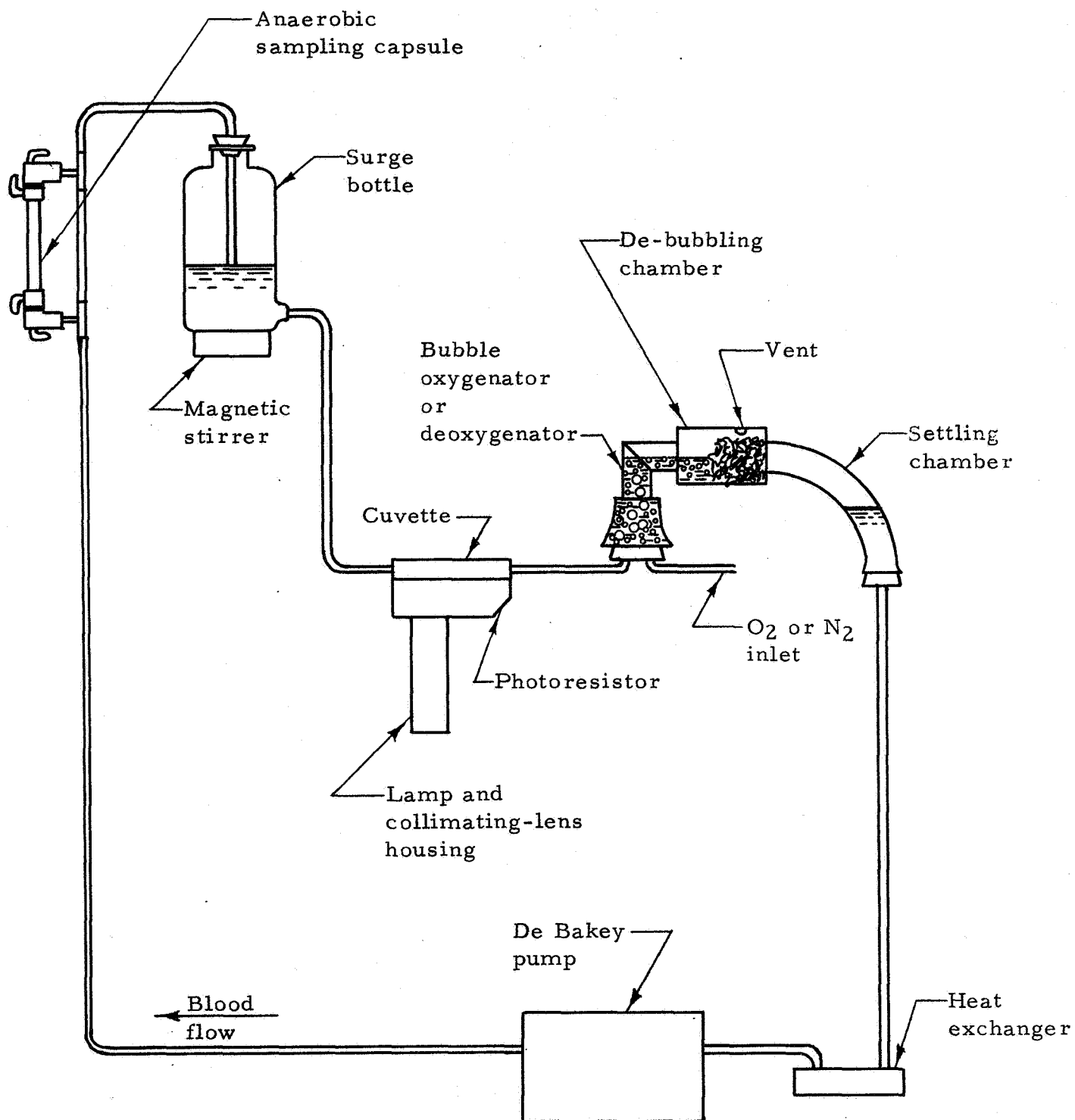


Figure FR-19. Spectrophotometric Studies of Whole Blood, Backscatter Mode: Schematic diagram of pump-oxygenator flowthrough cuvette system. (See also Figs. FR-18, FR-20, and FR-21).

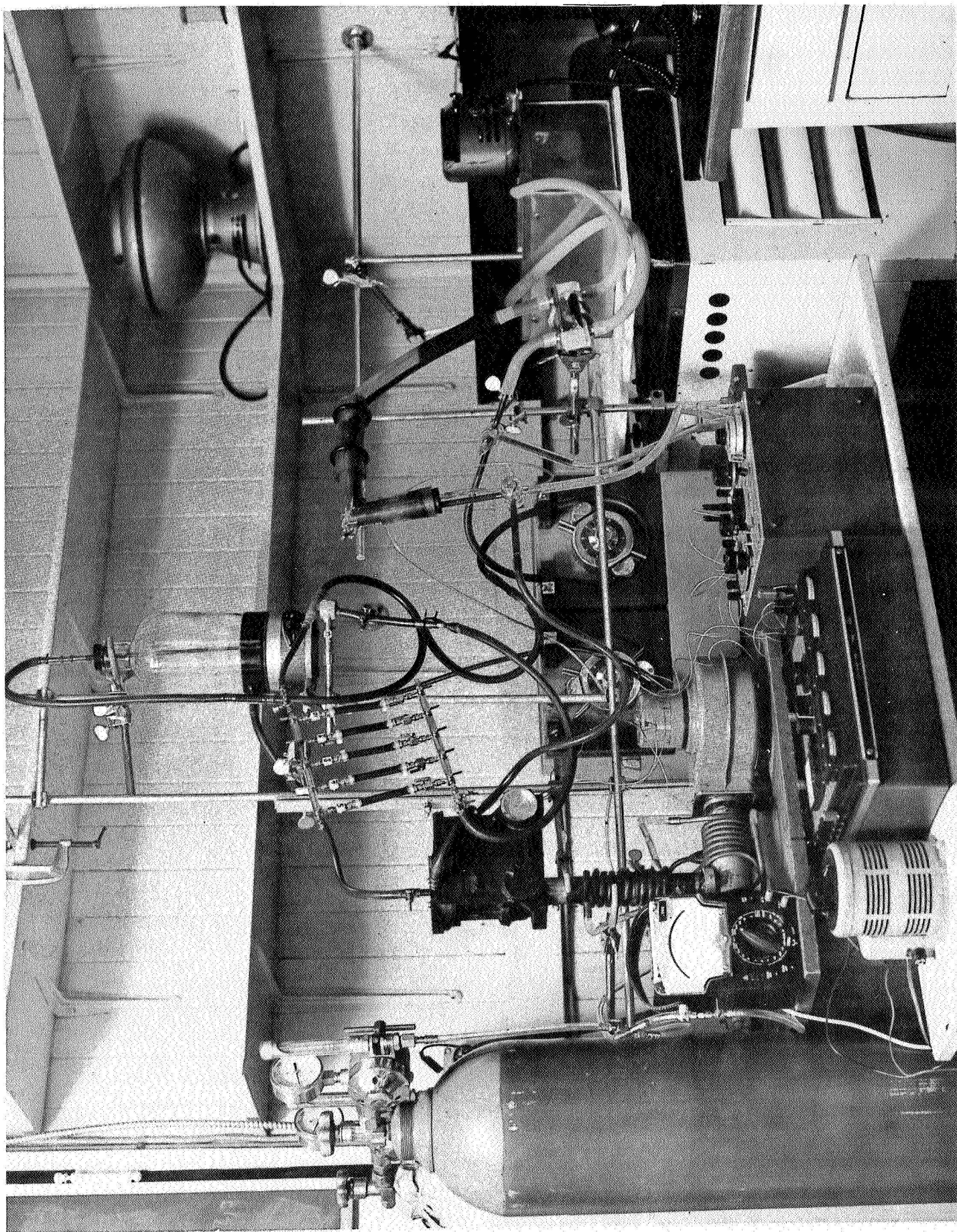


Figure FR-20. Spectrophotometric Studies of Whole Blood, Backscatter  
Mode: Pump-oxygenator, cuvette and flow circuit.





Figure FR-21. Spectrophotometric Studies of Whole Blood, Backscatter Mode: Detail of pump-oxygenator flowthrough cuvette apparatus showing cooled lamp housing and equipment for measuring the intensity of light backscattered from whole blood.



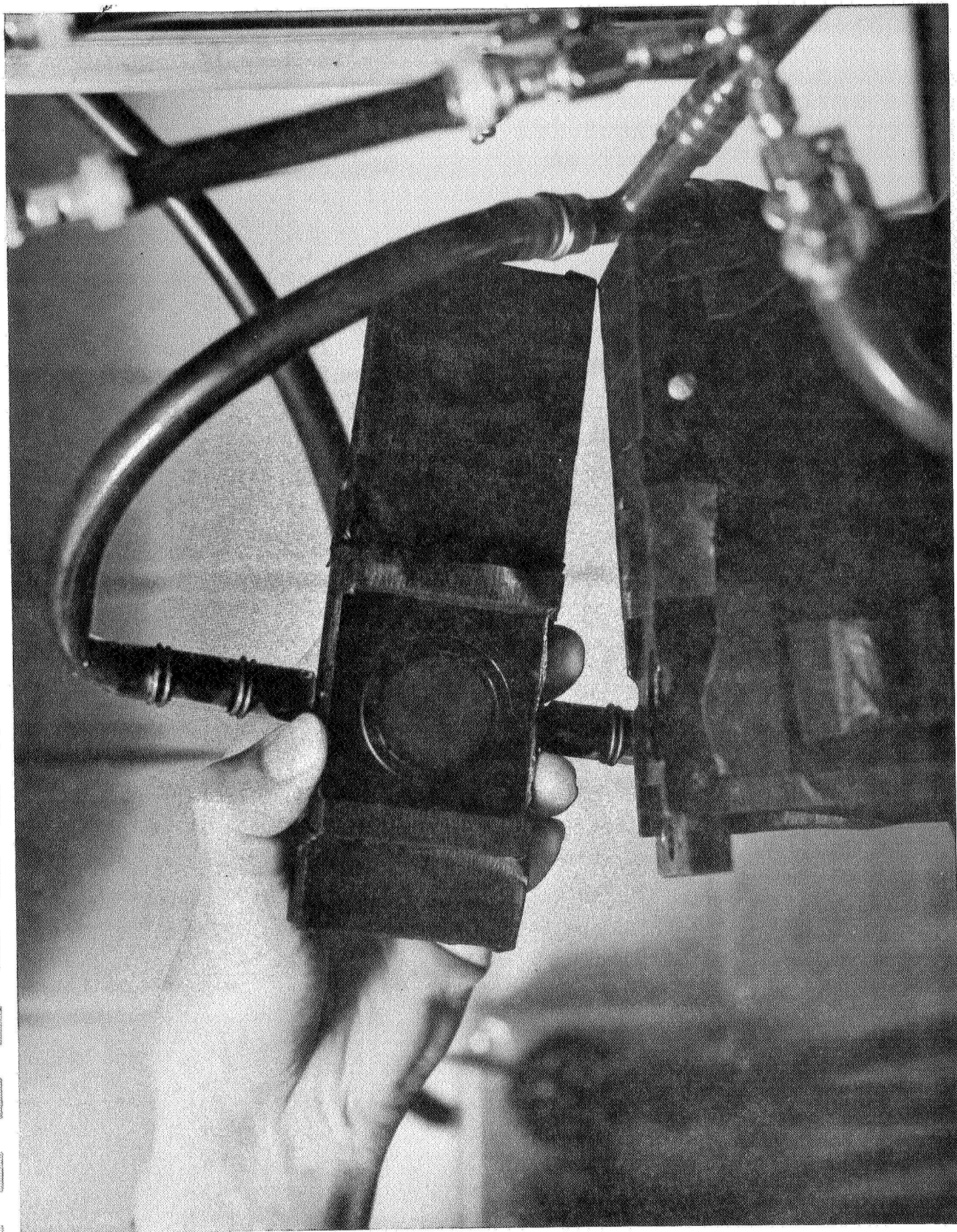


Figure FR-22. Spectrophotometric Studies of Whole Blood, Backscatter Mode:  
Detail of pump-oxygenator flowthrough cuvette apparatus showing whole-blood  
cuvette for backscatter measurements shown schematically in Figure FR-18.



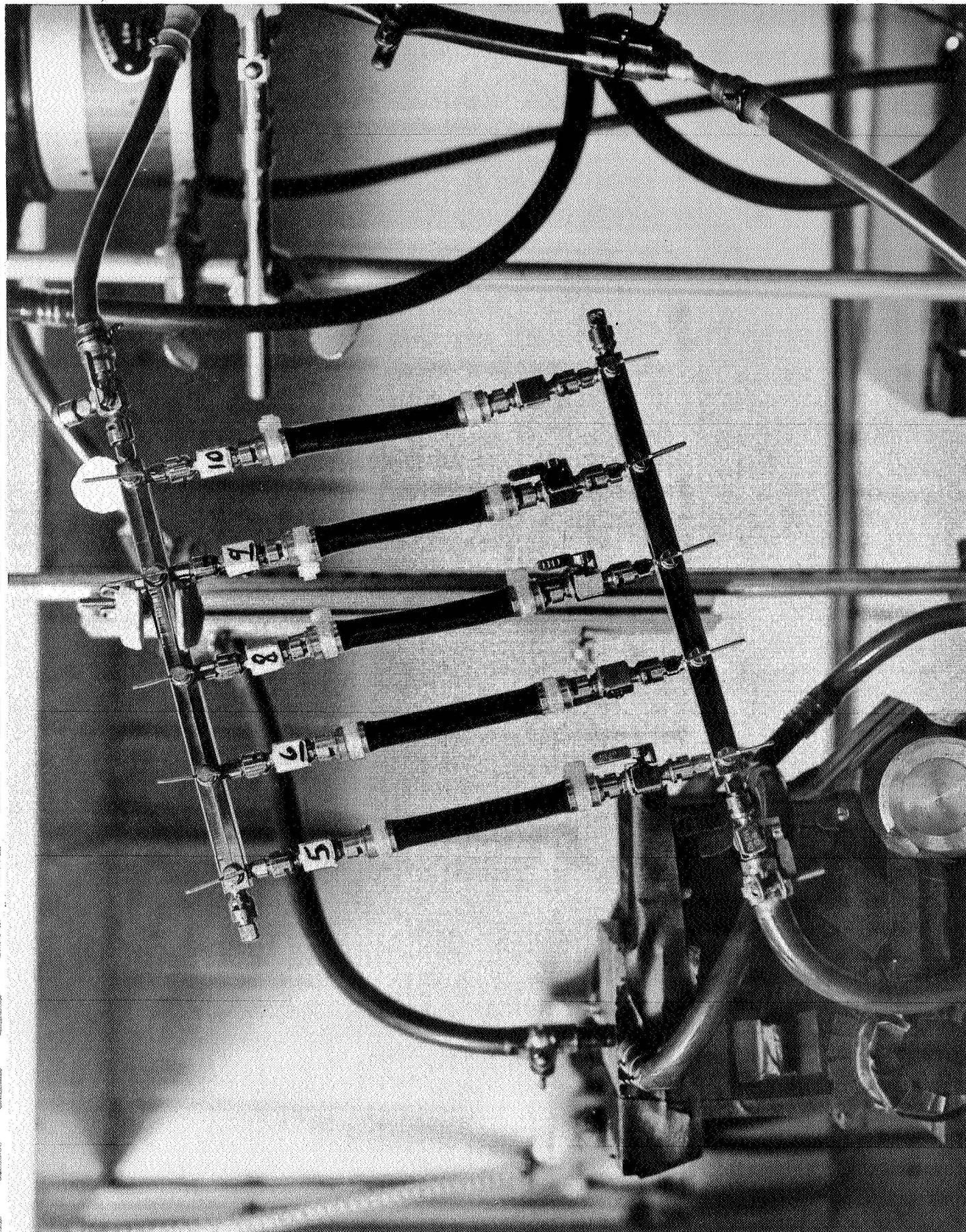


Figure FR-23. Spectrophotometric Studies of Whole Blood, Backscatter Mode:  
Detail of pump-oxygenator flowthrough cuvette apparatus showing anaerobic  
sample capsules, removable, for reference oxygen saturation measurement  
on hemolyzed blood samples.

on the basis of spectral response for use at the 805 mμ wavelength. Because the optical absorption coefficient for HbO<sub>2</sub> at 625 mμ is equal to the optical absorption coefficient at 805 mμ, this wavelength was selected as the non-isosbestic wavelength. A Clairex photoresistor type 704L was selected for use at 625 mμ, also for reasons of spectral response and linearity.

Whole blood was varied in oxygen saturation and circulated through the cuvette by the system shown schematically in Figure FR-19. The blood was circulated by the DeBaKey-type pump through the specially made anaerobic sample capsule manifold shown in Figure FR-20 and FR-23. These capsules are removable, and the blood contained therein could be removed for subsequent hemolysis and reference oxygen-saturation measurement on a Beckman Model B Spectrophotometer. Magnetic stirring at the reservoir maintained a homogeneous source of blood for the cuvette. The blood was then gravity-fed, with a constant head pressure, through the cuvette into an oxygenating-deoxygenating chamber. The hemoglobin oxygen content was raised by bubbling humidified oxygen with 5% CO<sub>2</sub> through the blood, or lowered by bubbling with humidified nitrogen with 5% CO<sub>2</sub>. A chamber packed with antifoam-sprayed stainless steel wool then removed the bubbles. From a settling chamber, the blood flowed through a heat exchanger which kept the blood at 37°C, and the flow cycle was completed at the DeBaKey pump. The blood-cycling system was carefully checked and significant hemolysis or turbidity was not introduced into the system by operating periods of several hours.

Results obtained with the backscatter-mode whole-blood pump oxygenator are presented in Figures FR-24, FR-25 and FR-26. A plot of oxygen saturation as a function of the ratio of backscattered intensities at 805 mμ and 625 mμ for varying hematocrits from 33 to 50 volume percent is shown in Figure

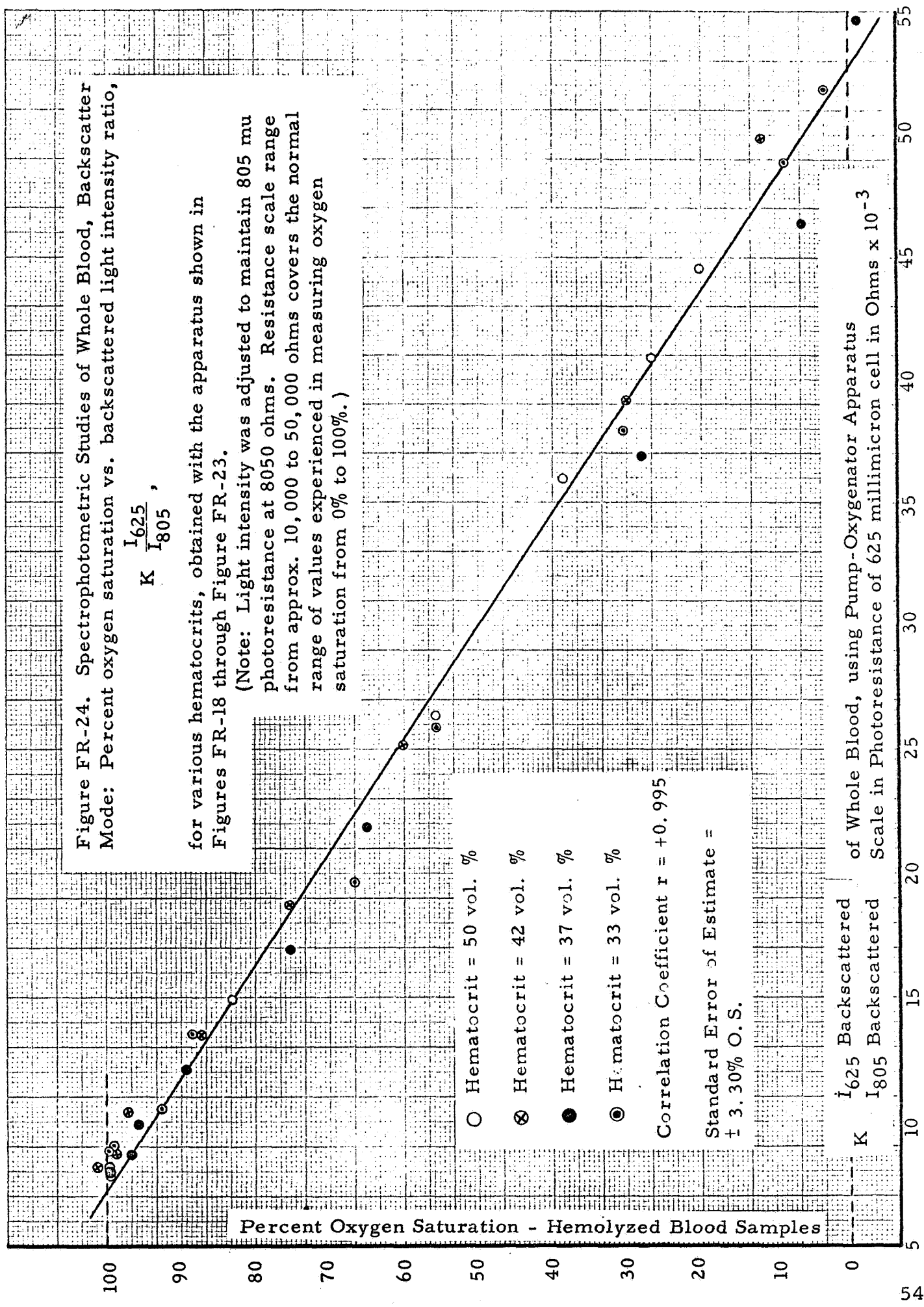
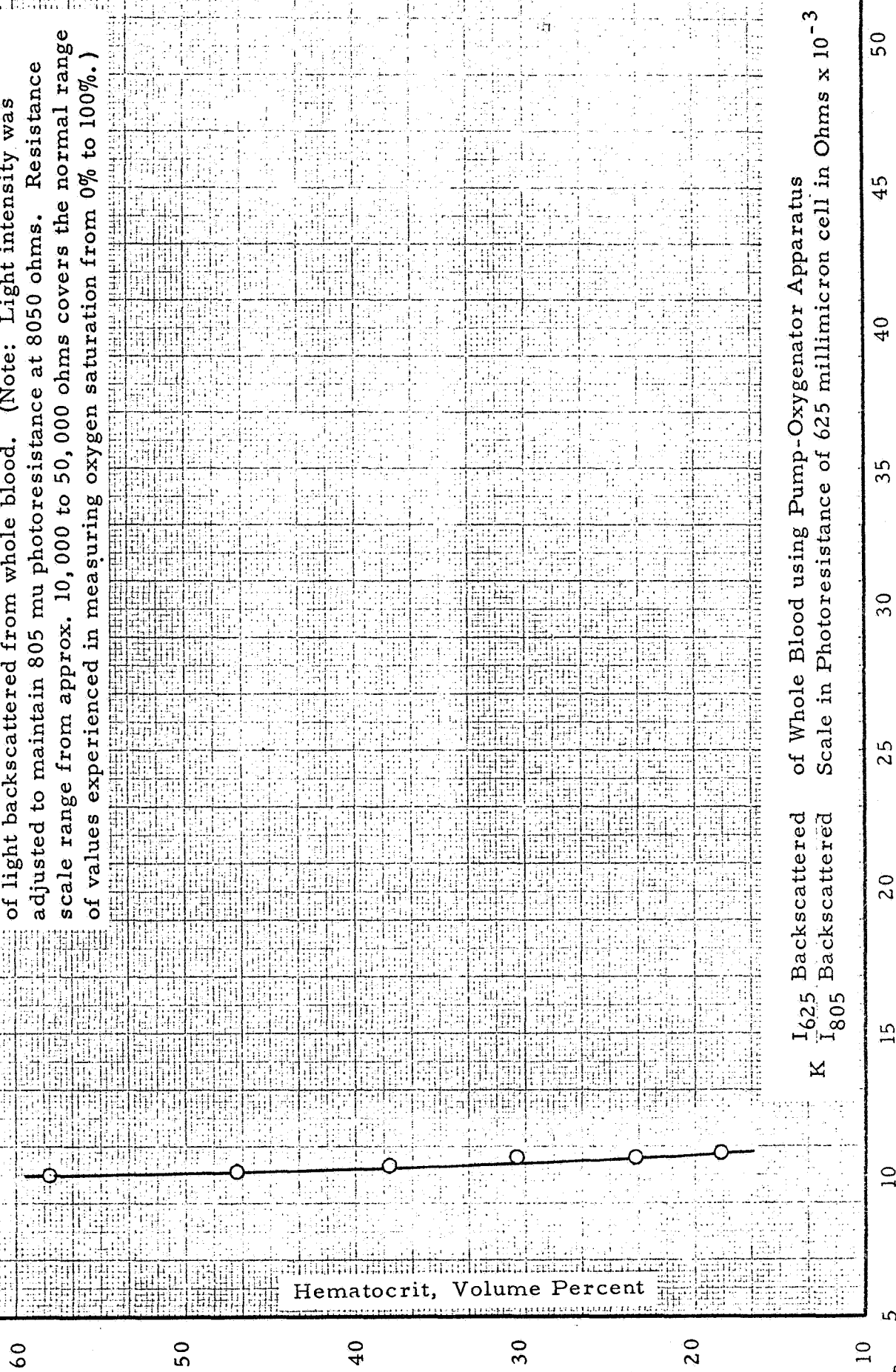




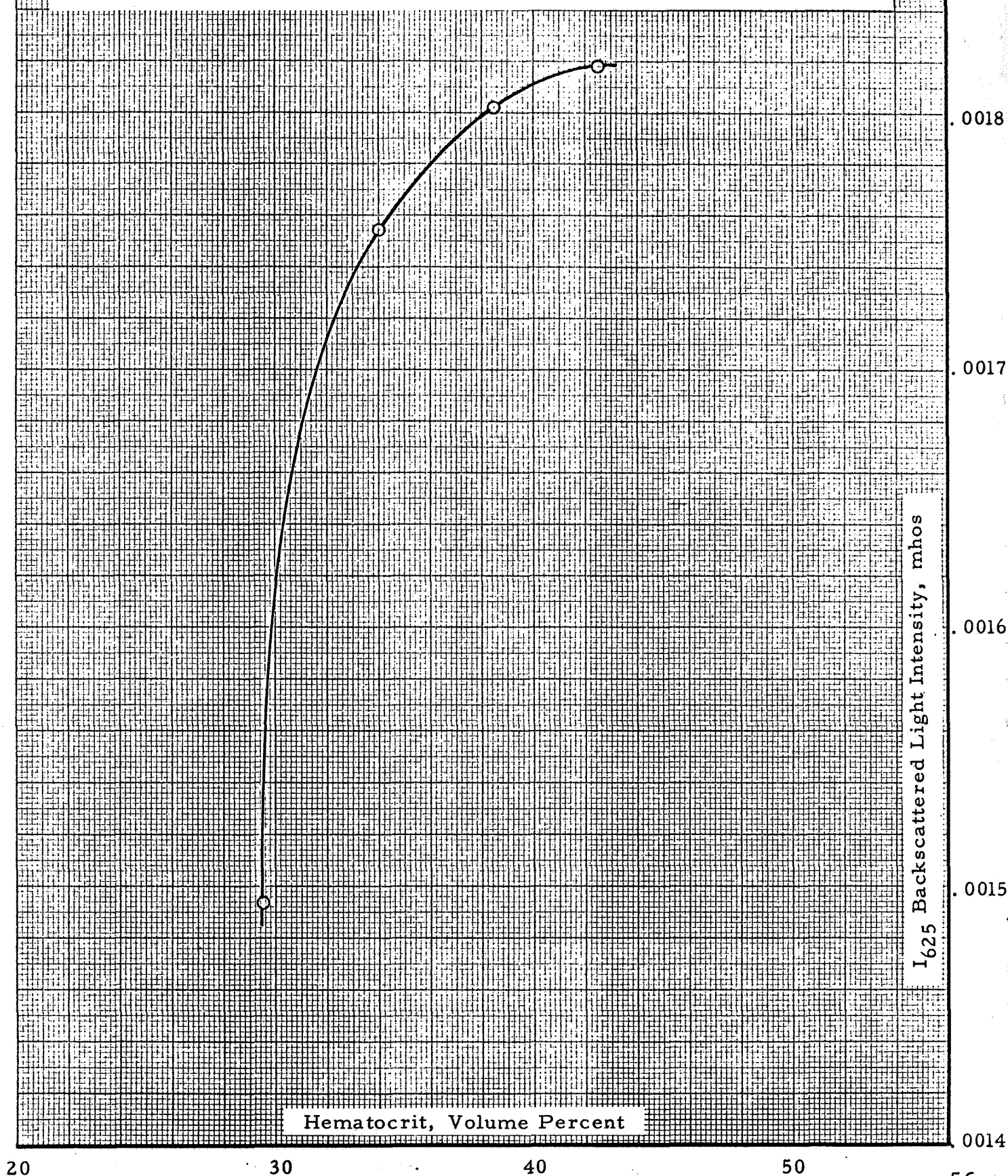
Figure FR-25. Spectrophotometric Studies of Whole Blood, Backscatter Mode: Hematocrit vs.  $K(I_{625}/I_{805})$  at 100% Oxygen Saturation. This curve illustrates hematocrit independence for the ratio of two-wavelengths of light backscattered from whole blood. (Note: Light intensity was adjusted to maintain 805 mu photoresistance at 8050 ohms. Resistance scale range from approx. 10,000 to 50,000 ohms covers the normal range of values experienced in measuring oxygen saturation from 0% to 100%.)



$I_{625}$  Backscattered of Whole Blood using Pump-Oxygenator Apparatus  
 $K$   $I_{805}$  Backscattered Scale in Photoresistance of 625 millimicron cell in Ohms  $\times 10^{-3}$



Figure FR-26. Spectrophotometric Studies of Whole Blood, Backscatter Mode: Hematocrit vs.  $I_{625}$  at 100% Oxygen Saturation. This curve illustrated hematocrit dependence for one-wavelength light backscattered from whole blood.



Hematocrit, Volume Percent

$I_{625}$  Backscattered Light Intensity, mhos

FR-24.

The function presented in these graphs approximates the linear expression

$$\text{O.S.} = K_1 \cdot \frac{I_{625} \text{ backscattered}}{I_{805} \text{ backscattered}} + K_2$$

Eq. 14 (= Eq. 2)

where  $\frac{I_{805} \text{ source}}{I_{625} \text{ source}}$  is held constant, within a standard deviation of  $\pm 3.3\%$  oxygen saturation over the range from 0% to 100% oxygen saturation.

The ratio of back-reflected light at these two wavelengths to hematocrit over the range 18 to 50 volume percent for 100% oxygen-saturated whole-blood is presented in Figure FR-25. This shows the ratio to be relatively hematocrit independent as does the data of Figure FR-24.

The same results are not obtained for single wavelength characteristics of oxygen saturation vs. hematocrit. Figure FR-26 shows the alinearity of the back-reflected light transfer function for the non-isosbestic wavelength over hematocrit ranging from 25 to 45 volume percent for 100% oxygen-saturated whole blood. As can be seen in this figure, the rate of change for relatively low hematocrits is rapid and for hematocrits approximately greater than 40 volume percent, backscattered light becomes considerably more independent of hematocrit for the single wavelength system. This data highlights the significance of taking the ratio of two wavelengths to eliminate the hematocrit effect in the resulting oxygen-saturation characteristic.

#### D. Conclusions

Determination of blood oxygen saturation performed upon whole blood in backscattered and transmission flowthrough cuvettes provide measurements of roughly the same order of accuracy and repeatability as that associated with hemolyzed blood determinations. A standard deviation of  $\pm 2-3\%$  O.S. is possible under controlled laboratory conditions in apparatus where the known optical and geometrical factors adversely affecting system accuracy are taken into account. Backscatter measurements made on whole blood in the system fabricated and described above indicate a means of instrumentation independent of hematocrit variations and a linear response between oxygen saturation and the ratio of backscattered light. Transmission oxygen-saturation measurements can be made on whole blood independent of hematocrit variations but with the limitation of following a non-linear and complicated function.

#### IV SPECTROPHOTOMETRIC STUDIES OF THE SKIN-TISSUE SYSTEM

##### A. General

Studies of the spectrophotometric properties of skin, both in-vivo and in-vitro, were conducted during the first twelve months of the program. It was anticipated that data from these studies would be brought together with the spectrophotometric data from whole-blood studies to establish design criteria for the experimental biosensor systems and to specify transducer topology, configuration and operating parameters. Four different kinds of measurement techniques were utilized: (1) standard spectrophotometric transmittance measurements on excised skin samples, (2) microscopic and photomicrographic visible and infra-red fixed-focus studies of intact skin, (3) congruent backscatter spectrum studies of living and dead skin, and (4) contact photographic studies of living and dead skin.

As was anticipated in the Proposal and later demonstrated in the studies reported in the previous section, a congruent optical geometry of backscatter operation could be developed for whole blood in which oxygen saturation of whole-blood samples was linearly related to the relative intensities of backscattered light at a signal and isosbestic wavelength independent of hematocrit variations. If the skin could be treated from an operational point of view as a transparent cuvette, the relationships suspected and verified in the previous section could then be directly implemented in a body surface external biosensor. The first two groups of studies upon the skin reported below were designed to explore the relative transparency of the skin at wavelengths of operational interest.

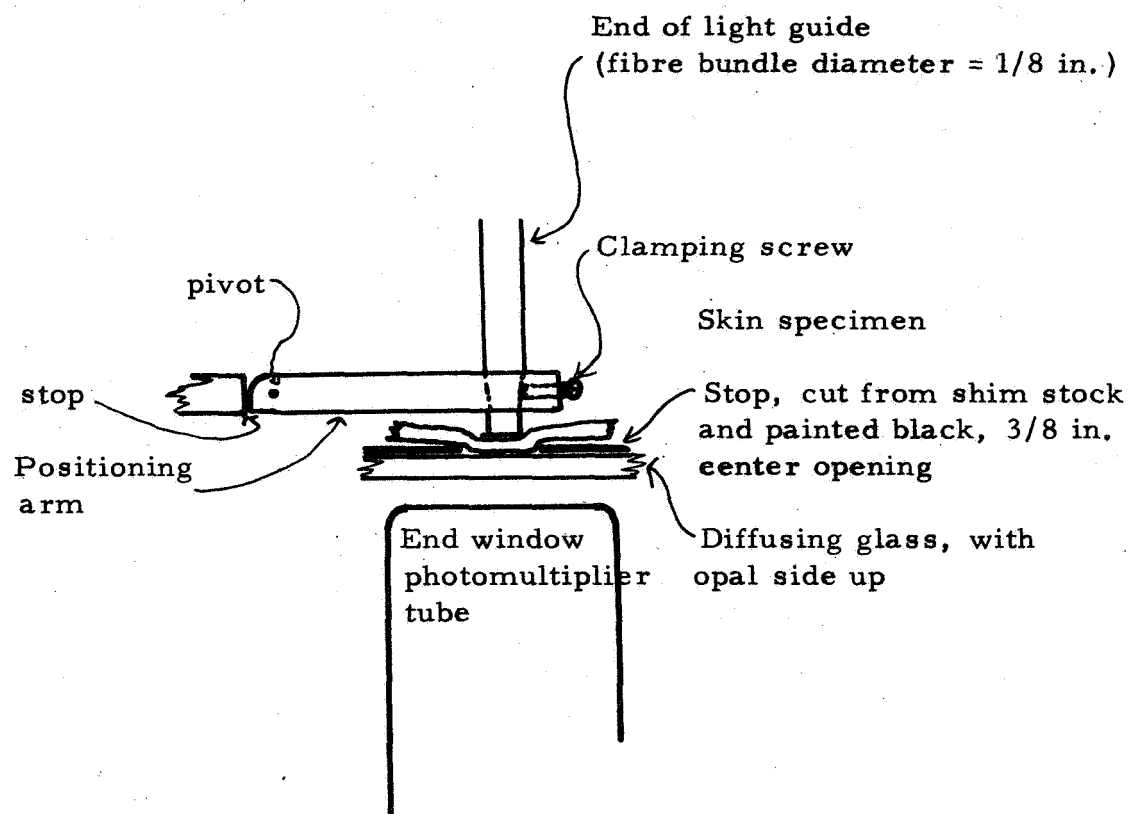
## B. Studies on Transmittance of Excised Human Skin

1. Specimens: Samples of skin were resected from individuals coming to post mortem examination. The samples were well washed with isotonic saline and dried between absorbent tissue prior to measurement. Elapsed time for an absorption spectrum measurement on a single sample was about five minutes, so the skin tissue did not have time to dry out.

2. Apparatus: A (Leiss) monochromator prism-eye image was focused onto the end of a 1/8" light guide, and the other end of the light guide was used as a light source. The geometry of measurement is illustrated in Figure FR-27. The primary light source was a tungsten-band filament incandescent lamp run at 6 volts and held constant by a Sola voltage-regulating transformer. The entrance slit of the monochromator was set to 0.5 mm and the exit slit to 0.6 mm. A flint-glass prism was used as the dispersing element.

3. Procedure: With no sample in place, a Photovolt model 520M photometer was read at 25  $m\mu$  intervals throughout the wavelength range 400 to 1000  $m\mu$ . Then, each excised skin sample was placed between the light guide and the diffusing glass and the measurements repeated. Once a sample was positioned, it was not touched until all of the photometric readings on it were completed.

In this experiment the reference measurement (the  $I_0$  measurement) was taken without a skin sample in the photometric gap. The aperture size was taken large enough so that, when no skin sample was in place, all of the light from the guide fell on the open portion of the diffusing glass with the following exception: because there were two glass-air interfaces in the photometric gap, approximately 8% of the photo-



All skin samples compressed to 0.023 in. thickness for measurement.  
 Reference readings made with air gap of 0.023 in.  
 All measurements carried out in total darkness

Figure FR-27. Spectrophotometric Studies of the Skin-Tissue System: Geometry for Transmittance Measurements on Excised Skin.

metric light was lost when no sample is in place. When the sample was in place, the refractive index discontinuity at the glass interfaces was reduced, though not necessarily removed.

4. Results: Representative curves obtained by the method described above are presented in Figure FR-28.\* The specimens shown illustrate generally parallel curves which tend to flatten out at wavelengths greater than 650 mμ. The transmittance of the specimens illustrated is in the neighborhood of 50% above 650 mμ, dropping off steeply at shorter wavelengths.

The curves obtained are consistent with the absorption of melanin, melanoid and similar pigments. The results are consistent with reflectance studies performed with more primitive techniques by Edwards and Duntley in 1938.<sup>12</sup>

It is of interest that the skin specimens demonstrated

---

\* Identification of Skin Specimens in Transmittance Studies

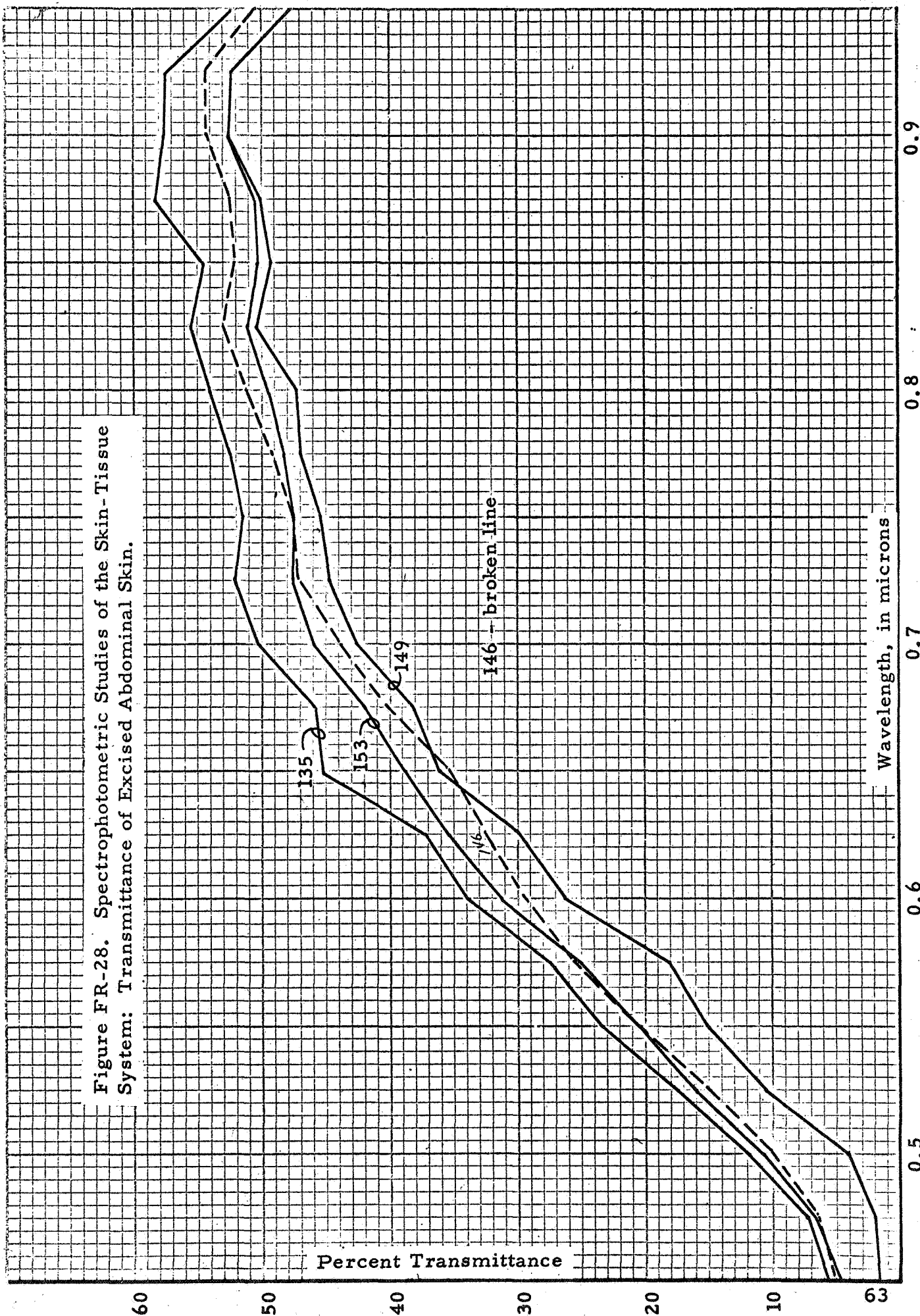
A64-135    AMB. Caucasian. Age 56 years. Coronary atherosclerosis. Severe myocardial infarction.

A64-146    RK. Caucasian. Age 3 years. Congenital heart disease, mitral stenosis.

A64-149    JOD. Caucasian. Age 60 years. Post operative aortic graft. Necrosis of small and large bowel.

A64-153    KE. Caucasian. Age 2 years. Anomalous pulmonary venous return, right atrial septal defect.

Figure FR-28. Spectrophotometric Studies of the Skin-Tissue  
System: Transmittance of Excised Abdominal Skin.





a transmittance of roughly 50% in the longer wavelengths. A thin non-absorbing diffuser placed in a photometric gap, such as the one described, would be expected to show a diffuse transmittance of about 50% with one-half the light passing to the photometer and one-half of the incident light being returned to the upper surface.

### C. Microscopic and Photomicrographic Visible and Infrared Fixed-Focus Studies of Intact Skin

The 50% transmittance at longer wavelengths exhibited by the excised skin samples in the transmittance studies suggested a highly turbid diffusing media. Accordingly, fixed-focus microscopic and microphotographic studies were initiated to assess the optical turbidity through efforts to visualize subcutaneous vascular structures.

#### 1. Microscopic Studies

Using illumination at 545 mμ from a filtered mercury lamp, and a Zeiss microscope fitted with a 4 x epi-illumination objective (used with 0° illumination and crossed polarizers) and an 8xKpl ocular, attempts were made to visualize the terminal capillary loops in the skin of a living human hand. This wavelength is excellent for visualizing hemoglobin-containing structures because it coincides well with the beta peak of oxyhemoglobin. However, it proved possible to visualize only the most external extremities of the capillary loops. This was attributed to the highly scattering nature of skin at this wavelength. Because of the strong dependence of the scattering phenomenon on wavelength, measurements were conducted at longer wavelengths by means of infrared photography.

#### 2. Infrared Photomicrographic Studies

Using a "constant-focus" camera, attempts were made to demonstrate subcutaneous vascular structure by means of Xenon-flash photomicrography using a band of wavelengths between 700 and 900 mμ. In this wavelength range, the absorption coefficients of reduced and oxidized hemoglobin are appreciable.

Thus, to the extent that skin is transparent in the infrared region of the spectrum, subcutaneous vascular structures should be photomicrographically resolvable.

Repeated attempts at photographing the subcutaneous vascular structures were unsuccessful. Only "shadows" of large surface venous channels were demonstrated. These studies demonstrated the skin to be a highly "turbid" optical media which cannot be treated as transparent from an operational point of view.

#### D. Congruent Backscatter Spectrum of Living and Excised Skin

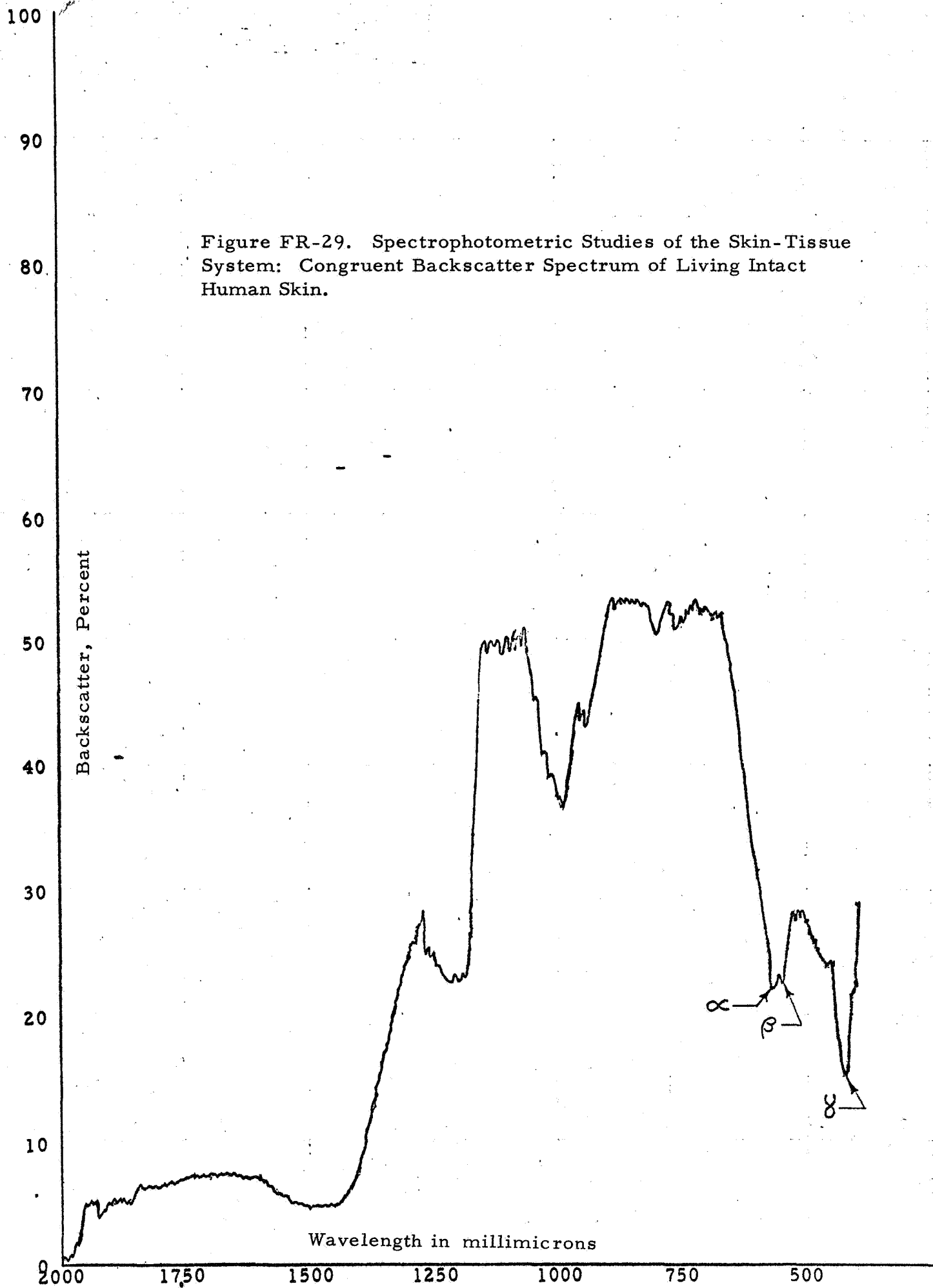
To determine the reflectance of light as a function of wavelength, experiments were performed upon living and excised dead skin with a Carey Model 14 Spectrophotometer.

For the experiments performed, the spectrophotometer was fitted with a Carey Reflectance Head and a photomultiplier phototube with good visible response but poor response in the infrared.

The Reflectance Head diffusely illuminated a sample area of approximately one-half square inch by means of an integrating sphere. Backscattered illumination leaving the illuminated area of the sample area at right angles was transmitted to the monochromator optics of the spectrophotometer by an optical system. The backscatter index of a sample was determined by automatic comparison of the light backscattered from it compared with that backscattered from a magnesium carbonate block reference standard.

##### 1. Backscatter Spectrum of Living Skin

Figure FR-29 shows a typical congruent backscatter spectrum taken from the palmar surface of the hand of an intact living white subject. Note that the alpha and beta absorption peaks of oxyhemoglobin are clearly defined. Toward the blue end of the spectrum the gamma hemoglobin absorption peak is also apparent. Through the near infrared about 50% of the light is reflected, as compared with the magnesium carbonate standard. At 1000  $m\mu$  there appears to be an absorption band of unknown origin. Further into the infrared the backscatter falls approaching zero.



The physical geometry of the instrument near the sample window prevented its use in measuring the backscatter spectrum of most of the body parts of living subjects. However, backscatter measurements of the surface of the palm of the hand of both caucasian and negro individuals were performed. The influence of increased perfusion of the skin was explored. In these studies, increased skin perfusion was attained through vigorous rubbing of the skin site of measurement. Data of four skin measurements is presented in Figure FR-30.

## 2. Measurements of Excised Skin

In addition to congruent backscatter measurements made upon volunteers, measurements were made on samples of abdominal skin from cadavers designated 146, 149 and 153. All of the adhering fat was dissected from the excised skin samples, and the samples were thoroughly washed in isotonic saline. Prior to being prepared for the measurements, the samples had been stored deep-frozen for intervals of some weeks. The backscatter of each sample was measured both on a white background (magnesium carbonate painted onto a block of aluminum) and on a black background (flat black enamel on aluminum). Typical data from three caucasian cadavers, designated 146, 149 and 153, is presented in Figure FR-31.

## 3. Experimental Data

The data was presented by the spectrophotometer as chart graphs with wavelength on the horizontal axis. For the purpose of presentation, the charts were read at wavelengths of interest, and the readings tabulated as below. The estimated accuracy with which the charts could be read is  $\pm 5\%$ .

$\lambda$	G	Gf	$\Delta$	L	Lf	$\Delta$	A	Af	$\Delta$	W	Wf	$\Delta$
415	13	14.5	-1.5	16	13.5	2.5	15.5	15.5	0	15.5	14.5	1
480	20.5	25	-4.5	32	26	6	26.5	26.5	0	26	24.5	1.5
506	21	26	-5	32	25	7	27.5	28	-0.5	28	25	3
540	19	21	-2	26.5	17	9.5	21.5	25	-3.5	21.5	19.5	2
555	19	20	-1	25.5	16.5	9	21.5	26	-4.5	23	18	5
576	21	23	-2	26	16.5	9.5	20	21	-1	21	18.5	2.5
625	39	42	-3	57	59.5	-2.5	55	57	-2	57	59	-2
660	57	47.5	9.5	59	58.5	0.5	57	58	-1	58	58	0
700	57	51.5	5.5	60	50.5	0.5	57	59	-2	58	59	-1

Figure FR-30. Spectrophotometric Studies of the Skin-Tissue System: Backscatter, Palmar Skin of Living Subjects.

$\lambda$	146 wh	146 bl	$\frac{\Delta}{R_{bl}}$	149 wh	149 bl	$\frac{\Delta}{R_{bl}}$	153 wh	153 bl	$\frac{\Delta}{R_{bl}}$
415	20	27	-.26	21	19	.10	49	58	-.16
480	58	43	.35	59	33	.79	65	66	-.02
506	65	64	.02	59	48	.23	66	66	0
540	65	63	.03	62	59	.05	69	70	-.02
555	65	62	.05	65	65	0	77	72	.07
576	59	63	-.06	66	64	.03	72	72	0
625	73	66	.11	70	67	.04	80	79	.01
660	78	68	.15	73	68	.07	82	80	.03
700	79	68	.16	74	69	.07	83	79	.05

Figure FR-31. Spectrophotometric Studies of the Skin-Tissue System:  
Backscatter, Excised Abdominal Skin.



In the following tables, the capital letters refer to the subjects; i.e., A, G, L and W. W is a negro subject. The symbol "f" indicates measurements after flushing by rubbing the palm.  $\Delta$ , for the living subjects, is the difference between the unflushed and flushed readings. For the excised skins,  $\Delta / R_{b1}$  is the difference, in percent backscatter between skin on a white background and on a black background, divided by the percent backscatter on a black background.

The backscatter of the black background alone was found to be approximately five percent all through the measured spectrum.

#### 4. Experimental Results

A. In the region of the spectrum between 600 and 700  $m\mu$ , the palmar skin of living caucasian subjects backscattered slightly over half of the amount of light reflected by a magnesium carbonate standard.

B. Flushing the skin of a living subject by rubbing did not have a consistent or significant effect upon the amount of light backscattered.

C. The backscatter of the skin of a living negro subject (W) at wavelengths 660 and 700  $m\mu$  was not demonstrably different than that of white subjects.

D. There was very little difference between the backscatter of excised skin mounted on a white background and the same skin mounted on a black background.

E. In the spectral region 600 to 700  $m\mu$ , the backscatter of excised white abdominal cadaver skin was 10 to 20 percent higher than the backscatter of living skin in situ.

## 5. Interpretation of Results

The foregoing studies tended to confirm what had been anticipated in the Program Proposal with regard to the absence of absorbing pigments other than oxyhemoglobin and hemoglobin in the intact skin at wavelengths over 650 mμ. These studies also confirmed the similarity in optical properties for skins from various individuals and various races at these longer wavelengths and the high degree of consistency with regard to relative spectral transmittance for wavelengths greater than 650 mμ.

The highly diffuse and turbid optical behaviour of skin, however, suggested difficulties in implementing a congruent-type of backscatter biosensor transducer. The geometry of the backscatter systems which were demonstrated (Section III) to linearly relate backscattered light intensities to the oxygen-saturation of whole-blood samples, were essentially congruent in character. In the foregoing congruent optical geometry studies of a mixed skin-tissue-blood system, however, a preponderance of light (80-90%) returned from the illuminated area was seen to be non-information bearing, while all of the oxygen saturation information was contained within the remaining 10-20% variation of light intensity level. Whether or not this preponderance of non-information-bearing light from the bloodless skin-tissue could be treated as a d.c. offset signal (on top of which [subtracted from] is the oxygen-saturation information-bearing signal from the blood within the skin tissues) or whether this large non-information-bearing signal had to be treated as "noise" depended upon its stability. While these preliminary studies suggested that the ratios of these large non-information-bearing signals would prove to be time varying and hence "noise", in-vivo experimental studies directed to this question were conducted with specially built experimental biosensor systems as reported in Section V-D.

## E. Photographic-Photometric Studies

### 1. General

An alternative to the congruent backscatter geometry was the annular geometry suggested in the original Proposal. To construct a suitable annular transducer, the dimension of the illumination aperture, the receptor aperture, and the width of the baffle separating the two, must be specified. Specification of these dimensions requires consideration of the following:

- a. The attenuation of light, at wavelengths appropriate to oximetric measurements, during its transit in skin, blood, and other tissue between the apertures;
- b. The attenuation of light, at the above wavelengths, by bloodless skin and tissue;
- c. The amount of attenuation of light, at the above wavelengths, due specifically to the presence of blood in tissue (which might be inferred from the difference between 1 and 2 above);
- d. The intensity of practical systems for supplying near-monochromatic light and the sensitivity of available and appropriate detectors.

### 2. Methods

The distribution of light backscattered around a site of light input into the skin was studied by means of "contact photographs". The device for making these photographs is illustrated in Figure FR-32. Monochromatic light was brought by means of a light guide to the skin through a hole punched in the center of a 2-1/4" by 3-1/4" sheet of

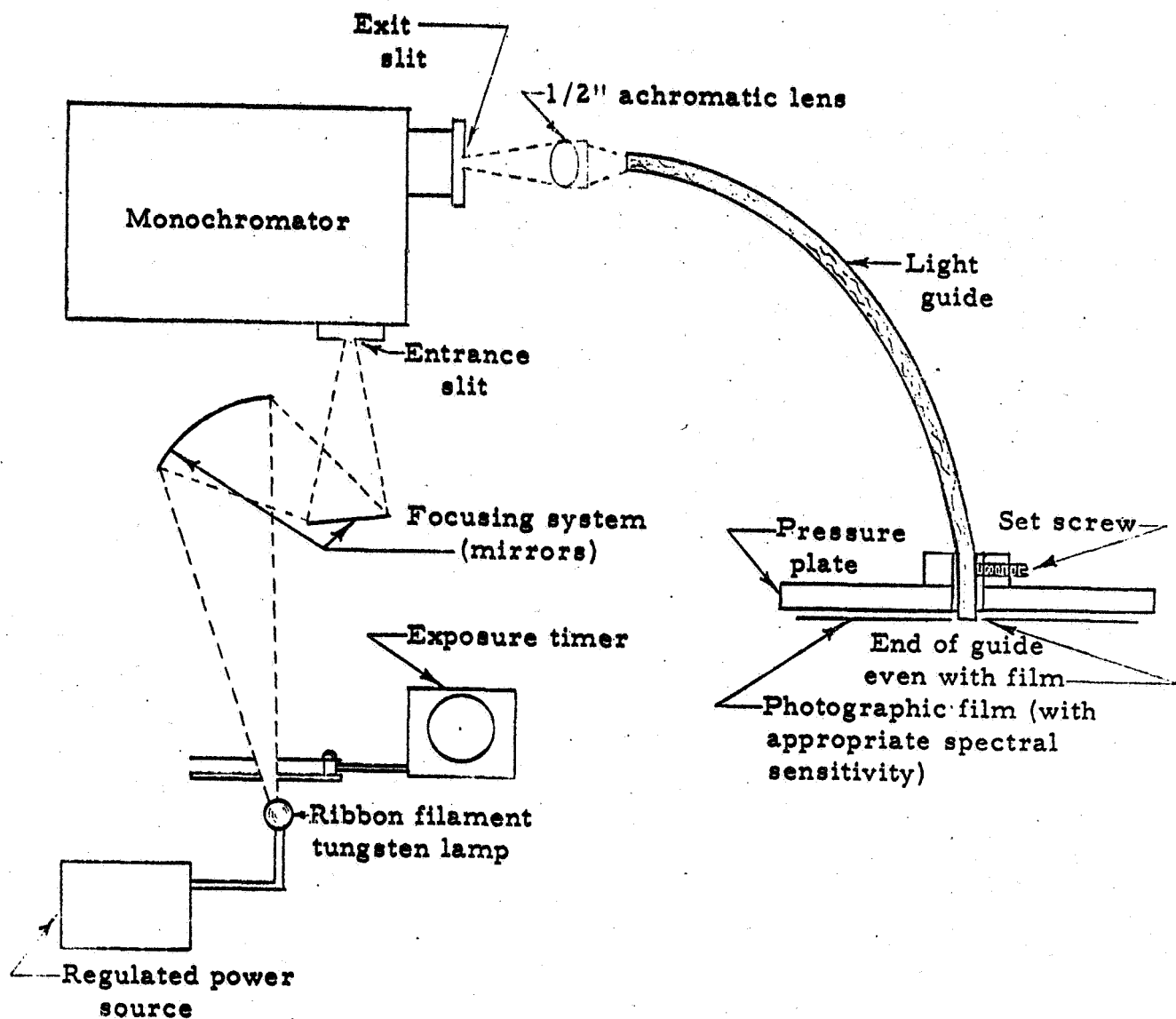


Figure FR-32. Spectrophotometric Studies of the Skin-Tissue System: Schematic Diagram of Apparatus for Skin-Contact Photographs.

cut film. The film was held in contact with the skin by a specially constructed pressure plate. Kodak Panatomic X film was used for visible wavelengths, and Kodak Infrared film was used for infrared wavelengths.

These experiments were designed to demonstrate the extent and the degree of diffuse transmittance and backscatter of light through the skin and superficial tissues. Quantitative analysis of the photographic negatives so made entailed reference to the characteristic of the photographic emulsion (the density vs. log exposure curve, or a similar plot). Inasmuch as this characteristic is a function of the procedure of film development, a calibration was made for each batch of films developed together.

In order to obtain a longer exposure range, a rotating sector wheel initially used in these studies was replaced with a neutral-density step tablet. The attenuation provided by the step tablet was wavelength dependent, thus an independent calibration of the step tablet was necessary at each wavelength used. The wavelengths of light studied were 506, 625, 660 and 805 m $\mu$ . 506 m $\mu$  and 805 m $\mu$  are isosbestic points between oxygenated and deoxygenated hemoglobin. 625 m $\mu$  and 660 m $\mu$  are wavelengths where the difference between the absorption coefficients of reduced and oxygenated hemoglobin are appreciable. 660 m $\mu$  represents a maximum difference.

The exposure time required to obtain comparable darkening of the various films at the various wavelengths varied because the efficiency of the system for supplying monochromatic light is a function of wavelength, as is the sensitivity of the photographic emulsions. Experiments indicated that the transmittance of the light guide is also a wavelength function. The determination of the wavelength dependence of light guide

transmittance was determined by coupling the guide to a photographic emulsion by means of an integrating sphere.

Interpretation of the photographic negatives showing the light-distribution patterns was initially attempted using a scanning microdensitometer. In the course of manually interpreting the microdensitometer tracings, it became evident that the light patterns were generally unsymmetric. Thus, a large number of radial scans were required for each negative in order to quantitatively state the radial distribution pattern giving responsible limits of error. Using the manual procedure, each point on each radial distribution trace had to be referred to the characteristic calibration curve in order to be interpreted as a light intensity. Interpretation of a single photographic negative required much more time than was warranted by the resulting quantitative information.

After the initial manual microdensitometric quantitative analyses had been completed, it was felt that the great preponderance of information desired could be extracted from the remaining photographs by visual assessment.

### 3. Experimental Data

Using various experimental protocols, over one hundred calibrated photographic negatives were made of light distribution patterns in living and dead skin. Differences in the backscattering characteristics between the skin system alone and the living skin-blood system were necessary for biosensor transducer design, for in this way "signal-to-noise" of the transducer could be maximized.

Representative photographic negatives are shown in Figures FR-33 and FR-34. Figure FR-33 is a contact photograph

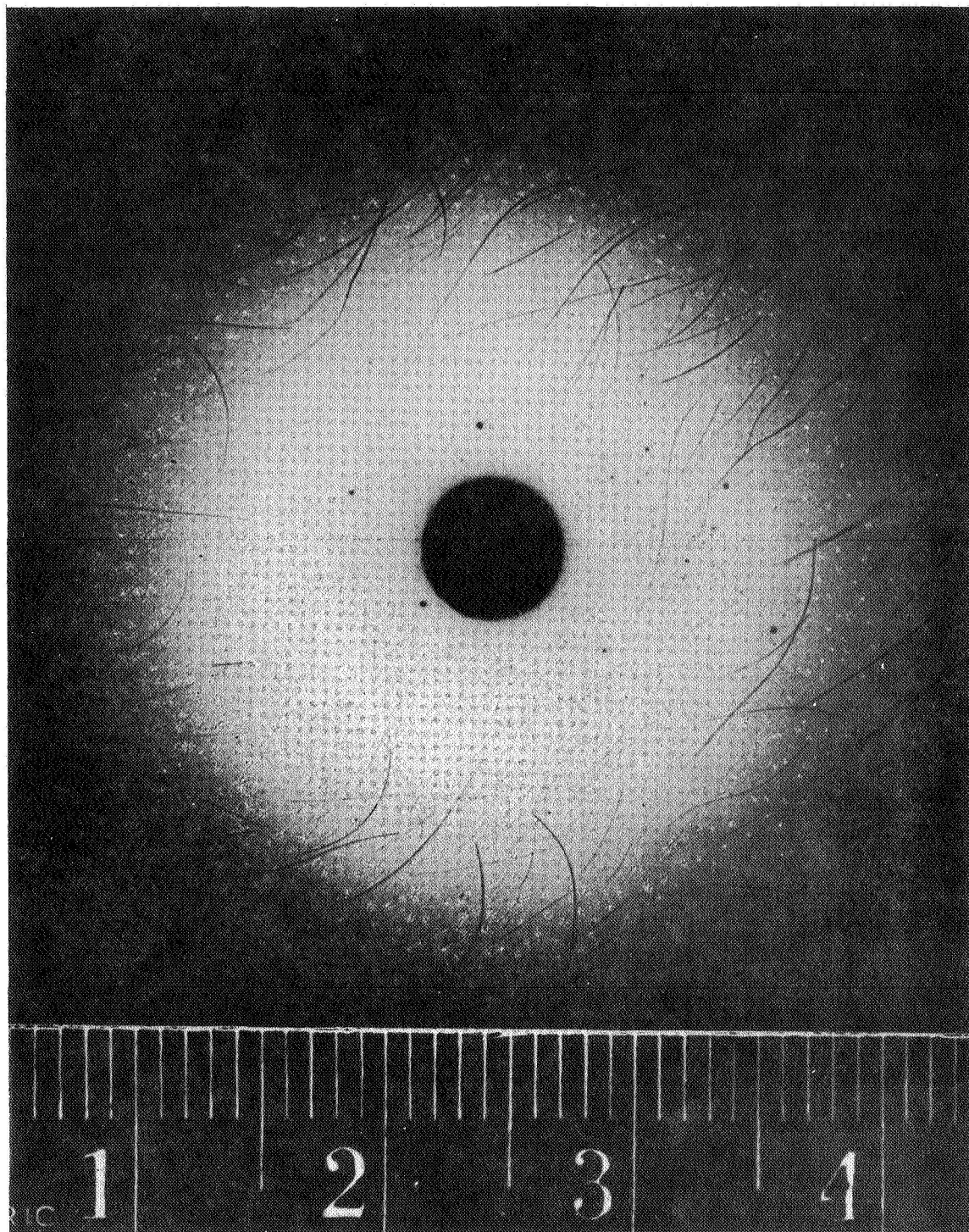


Figure FR-33. Spectrophotometric Studies of the Skin-Tissue System: Contact Photograph of Living Skin. Photographic enlargement of light distribution pattern in the skin on the forearm of an intact living white subject. The scale is in centimeters. Light of wavelength 660 mu was used. Some detail has been lost in reproduction. The light areas at the periphery are not explained, though they may represent aggregates of sebaceous material.

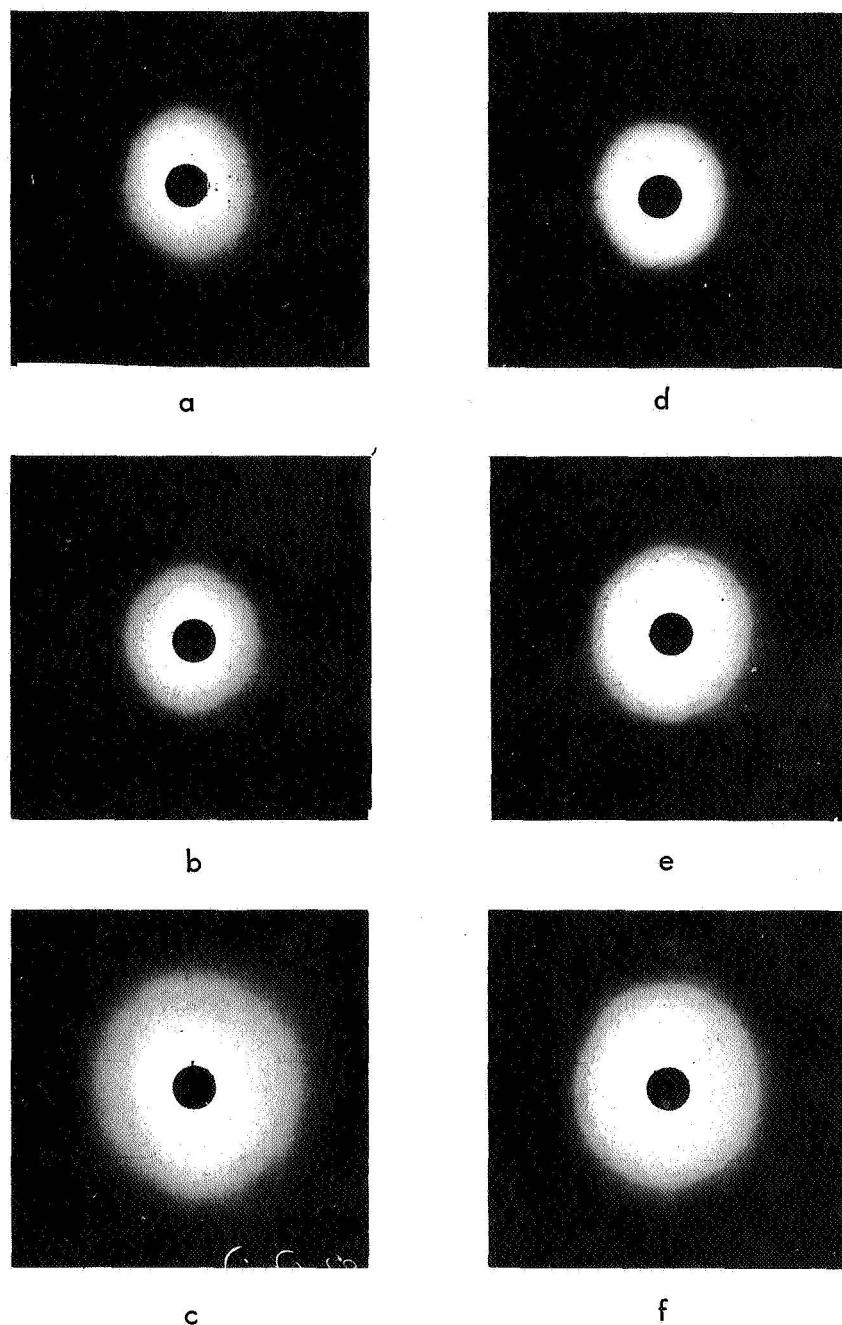


Figure FR-34. Spectrophotometric Studies of the Skin-Tissue System: Comparison, at three wavelengths, of the Diffusion Pattern in Living and in Dead Skin. a, b, and c: Light distribution pattern in live skin of the forearm of an intact white human subject. d, e, and f: corresponding patterns in excised abdominal skin. a and d: 660 mu. b and e: 725 mu. c and f: 800 mu. Some of the gradation present in the negatives has been lost in the reproduction process - thus the extent of the patterns as discussed in the text is not clearly represented.



of a male forearm taken at 550 mμ. Figure FR-34 is a comparison, at three different wavelengths, of the light diffusion patterns in living intact skin (containing active blood flow) and in dead skin. The live skin photographs in Figure FR-34 were made on the forearm of a young adult female of Scandinavian descent; the dead skin was taken from the abdomen of a 56 year old white male of similar pigmentation shortly after death. The dead skin was mounted on India ink gelatin to avoid reflections from the mounting material.

Exposures were all of the same duration (one minute). No attempt was made to compensate for the various wavelength dependent variables, such as photographic sensitivity, monochromator energy output, and lamp color temperature.

#### 4. Experimental Results

a. The extent of the light pattern as a function of wavelength on a given dead skin: These experiments indicate that the shorter wavelengths are attenuated considerably more rapidly than the longer wavelengths. Thus, (on white subjects) there is photographically detectable light at radii of one-half inch at 805 mμ, but at 506 mμ the light pattern is only barely detectable at radii of one-eighth of an inch.

b. The extent of the light pattern as a function of wavelength on live skin: As above, specifically, the shorter wavelengths are attenuated much more notably than the longer wavelengths.

c. The extent of the pattern in dead skin with and without the subcutaneous fat: Prior to dissecting away the fat, the pattern, at all wavelengths, extended much further laterally than after the removal of the fat.

d. The effect of heat flushing on the patterns:

A visible degree of increased skin-blood flow (creating a "flushed" skin) could be obtained on a living subject by heating with an infra-red lamp. This skin flushing could not be detected in the light distribution patterns at any wavelength.

e. The effect of moderate and heavy skin pigmentation:

Exposures which were sufficient to demonstrate the light distribution pattern on a white subject were quite similar to those obtained in a negro of moderate pigmentation. However, in the case of one negro subject having very deep pigmentation, only a barely discernable pattern was produced.

f. The effect of varying sample site:

Comparable measurements were made on living subjects on the forehead, on the arm, on the stomach, and, in one negro, on the cheek. For a given subject, at a given wavelength, there was very little difference between the light patterns at the various sites.

5. Conclusions

a. The isosbestic point at 506 m $\mu$  is probably not operable with an annular sensor.

b. Wavelengths between 600 and 805 m $\mu$  are operable with an annular sensor.

c. The tissue underlying the skin is an important part of the optical path of the light leaving the skin surface at source-detector distances of more than one-half inch.

d. For annular transducers with a radius of one-

half inch and a thickness of one-eighth inch, optical efficiencies (ratio of light in to light out) of the order of  $10^{-4}$  can be anticipated at the operations and wavelengths studied. If the annulus is one-eighth of an inch in diameter rather than one-half inch, an additional two orders of magnitude in light efficiency can be anticipated.

#### F. Methods for Increasing Skin Blood Flow

In order to maximize signal-to-noise levels available to the experimental external biosensor systems and to insure that arterial oxygen saturation rather than mixed arterial and venous blood oxygen saturation was being detected, an investigation into methods of inducing excessive skin blood flow, i.e. "flushing" of the skin, was conducted.

Successful histaminization of the skin by iontophoresis was accomplished on human subjects and on experimental animals utilizing the following protocol outlined by W. G. Zijlstra and G. A. Mook of Assen, Netherlands:<sup>13</sup>

1. A piece of filter is wetted with a fresh 0.6% aqueous solution of histamin phosphate.
2. The paper is applied to the skin and the positive electrode attached to it.
3. The negative electrode is grasped by the patient.
4. The electrodes are connected to the iontophoresis apparatus.
5. By turning the potentiometer, the current is regulated at 1 to 2 mA, according to the patients's convenience. The duration of the iontophoresis is two to four minutes for the forehead and four to eight minutes for other places on the skin. (The minimum durations mentioned hold for children.) The current through the patient should be gradually increased or decreased; don't switch off suddenly.
6. Immediately after iontophoresis some edema is often present. The histaminized spot is at first white rather than red. In about 10 minutes edema subsides and the field becomes intensely red. The disappearance of edema is favored by subsequent compression of the skin and by light massage.

The response of the biosensor systems to increased perfusion thus induced on experimental animals is discussed in Section V, page 123.

A study of the increase in skin-blood flow induced by application of Trafural, a nicotinic acid ester derivative, was conducted and indicated that while considerable skin flushing could be effected, it was accompanied by excessive edema, rendering the method unsuitable.

## V. EXPERIMENTAL BACKSCATTER-MODE EXTERNAL BIOSENSOR SYSTEM DEVELOPMENT AND PERFORMANCE

### A. General

The spectrophotometric studies of whole blood reported in Section III and the spectrophotometric studies of skin reported in Section IV were brought together to form the foundation for design of several experimental backscatter-mode external biosensor systems. These systems were experimentally applied to the measurement of blood oxygen saturation in simulated skin-tissue-blood systems, experimental animals, open-heart surgery patients and human volunteer subjects. During these experimental studies of systems performance, actual blood oxygen saturation was experimentally varied over a wide range of values and the measurement indications of the biosensor systems were compared with standard-of-reference blood oxygen saturation measurements performed by the refined technique reported in Section II.

During this phase of the program, there was an essential, continuous and dynamic interplay between the development and refinement of each of the biosensor systems and the data acquired with each system, which data, in turn, furnished the basis for progressive biosensor system development and refinement.

The design and fabrication of the experimental external biosensor systems with their various transducers and the extensive data acquired to evaluate their performance and refine these systems are described in this section. The progressive step-by-step development of these systems will not be presented in detail, nor will the great bulk of experimental data acquired. Rather, the experimental systems will be described and illustrated in their most refined forms and representative data acquired with these forms of the experimental systems will be presented.

## B. Skin-Tissue-Blood Simulator Cuvettes

Experience obtained during the spectrophotometric studies of whole blood utilizing the pump oxygenator and flowthrough cuvettes shown in Figures FR-18 through FR-23 suggested that a cuvette that was a model or optical analogue of the actual in-vivo skin-tissue-blood (STB) system would be extremely useful in the development of the experimental external biosensor systems. The utility of such a skin-tissue-blood simulator (STBS) cuvette was twofold.

First, with regard to design and refinement of transducers, amplifiers and various other components of the biosensor systems, the STBS cuvettes permitted rapid determination of the order of magnitude of various key parameters that were essential for design. Through the use of the STBS, comparisons of the performance of one design with respect to another could be readily performed. Secondly, the simulated systems were of utility during actual in-vivo use of the experimental biosensor system, for they permitted the rapid and accurate assessment of instrumentation operating points. Thus, the skin-tissue-blood system simulators did not supersede or replace in-vivo measurements, but were used to optimize transducer and other component design and performance and to periodically establish instrumentation stability, reliability and calibration.

The general specifications for the cuvettes that were to simulate the skin-tissue-blood system were:

1. Light transmission and scattering characteristics of the same general order of magnitude as skin;

2. Suitable for pumping whole blood through in multiple small moving streams, as generated by the pump-oxygenator flow system shown in Figures FR-18 through FR-23;
3. No entrapment of or damage to erythrocytes or other blood constituents.

The specific design specifications for the cuvettes were derived from the earlier spectrophotometric studies of whole blood and skin, reported in Sections III and IV.

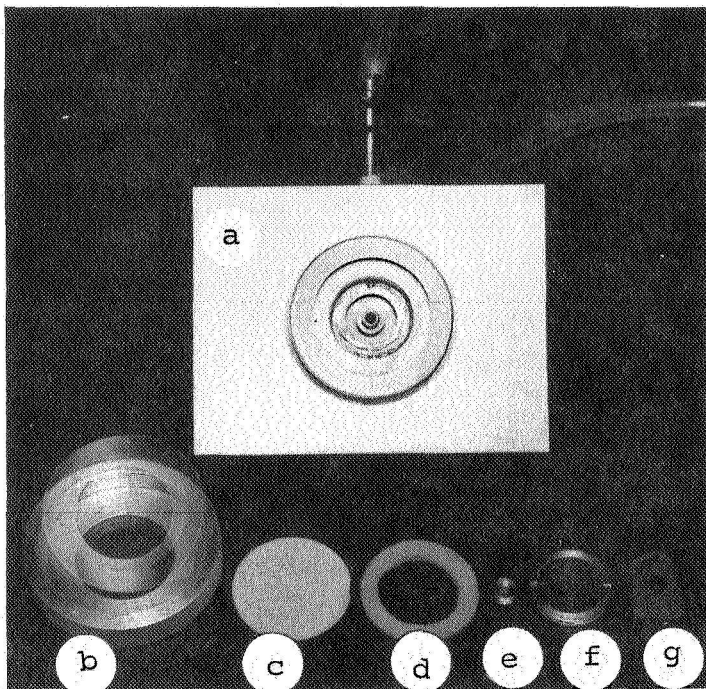
Two skin-tissue-blood system simulator cuvettes were engineered and fabricated.

The first of these, shown in Figure FR-35, had a cover plate fabricated from 60 mesh (0.3 millimeter) fritted-glass imbedded in a plastic to provide a diffusing surface similar to the skin. To simulate optical scattering by tissue, a cavity under the cover plate was filled with small siliconized glass beads, 0.5 to 1.2 millimeters in diameter, through which whole blood was pumped. This cuvette was designated the STBS-I.

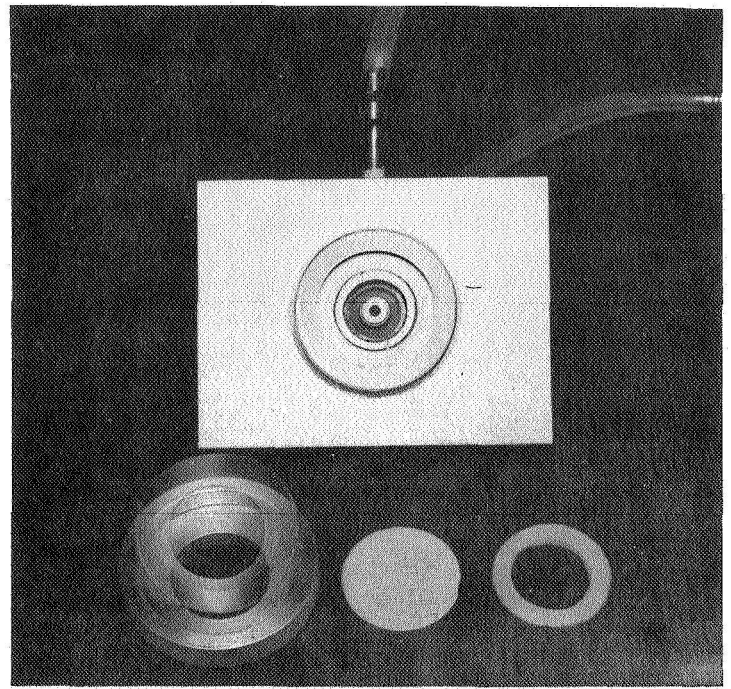
A second skin-tissue-blood simulator cuvette, STBS-II, was designed and fabricated from a solid piece of extra coarse fritted glass (Figure FR-36). This cuvette was designed for use with dye as the liquid absorbing medium instead of blood. Dyes having appropriate spectral characteristics were used in varying concentrations to establish specific stable instrument operating points over the entire range of blood oxygen saturation values. For establishing instrument operating points, the ready accessibility and chemical stability of dyes made them in some respects more useful than blood of varying oxygen saturations.



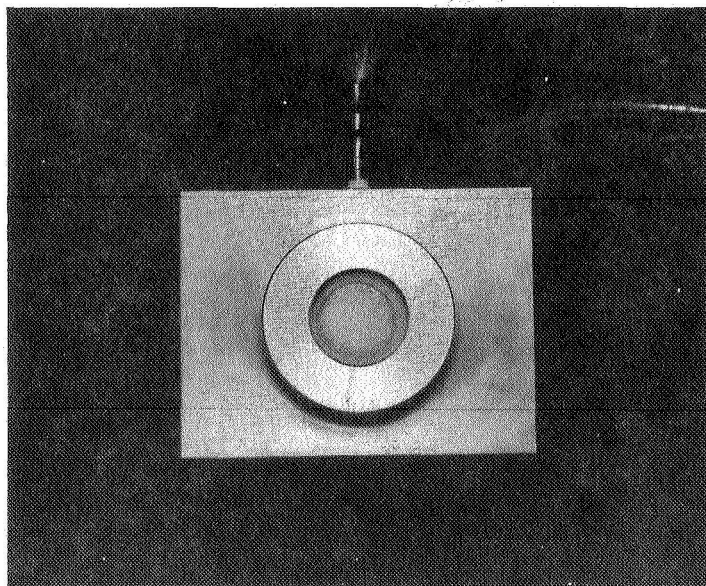
1



2



3



4

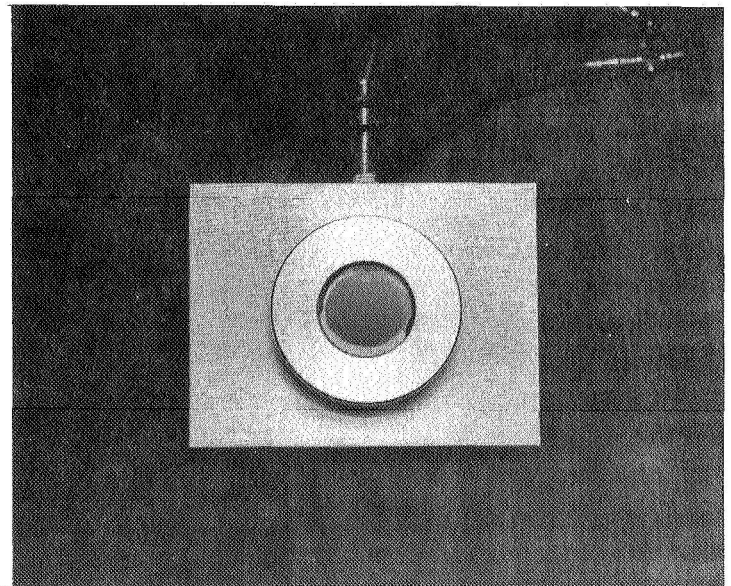


Figure FR-35. Skin-Tissue-Blood Simulator Flowthrough Cuvette (STBS-I).

(1) Disassembled view

- a) Cuvette housing
- b) Cover retaining ring & plastic gasket
- c) Diffuser window
- d) Gum rubber window gasket
- e) Outlet wier filter cap
- f) Inlet filter retaining ring
- g) Inlet filter screen

(2) Partial assembly

(3) Assembly with 0.5 to 1.2 mm siliconized glass beads in blood cavity (without diffuser window)

(4) Complete assembly: cavity filled with blood shown through clear plastic window

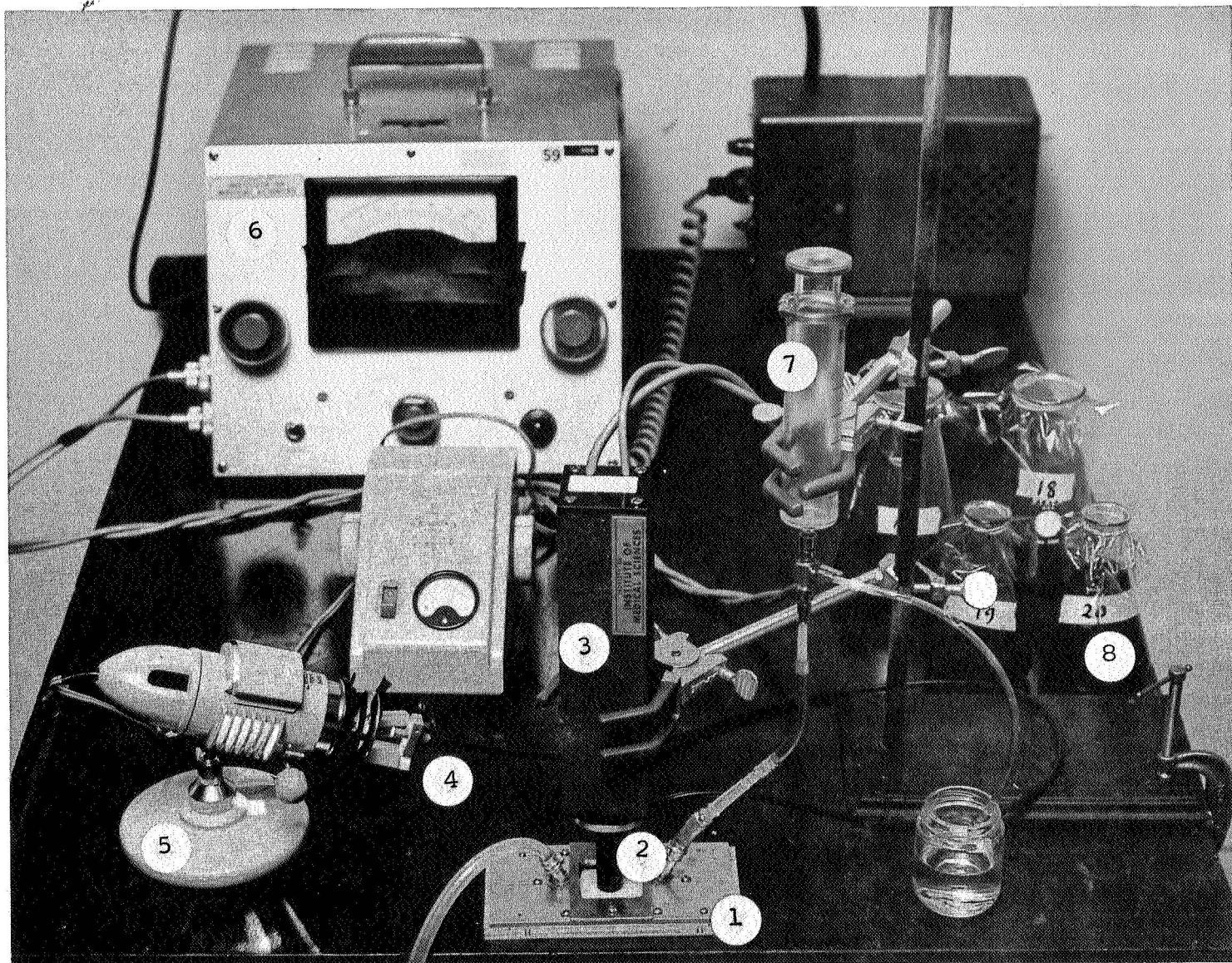


Figure FR-36. Skin-Tissue-Blood Simulator Flowthrough Cuvette (STBS-II): shown with annular lucite transducer (ALT) and dc photomultiplier biosensor system.

- (1) Skin-tissue-blood simulator cuvette (STBS-II)
- (2) Annular lucite transducer (ALT)
- (3) Photomultiplier - SI Response
- (4) Glass fiber flexible light guide
- (5) Illuminator with 660 nm filter
- (6) Photometer
- (7) Dye injection syringe
- (8) Flasks containing dye solutions of varying concentration

The STBS-II originally used with dyes underwent modification for use with whole blood and was brought into closer approximation to the optical properties of the in-vivo skin-tissue-blood system. This improved cuvette was designated the STBS-III.

In the experimental studies utilizing the simulator cuvettes, the cuvettes were inserted into the flow circuit of the pump-oxygenator flow system cited above in which controlled changes in oxygen saturation, hematocrit, and temperature were imposed upon the circulating blood. During these experiments, blood samples were obtained for standard-of-reference measurements by the technique reported in Section II for comparison with the performance of the experimental external biosensor systems.

## C. Experimental External Biosensor Systems

### 1. General

In conception, the operational biosensor was to have a disc-shaped coin-sized transducer applied directly to the surface of the skin. The biosensor was to contain provision for an illuminator which would transmit light into the skin and provision for the photodetection of light backscattered from blood within the skin. It was recognized that operation with discrete portions of the ultra-violet, visible, or infra-red electromagnetic spectrum could be implemented either through the use of monochromatic laser light sources, through optical filtering of broad-band light sources or by means of optical filtering of broad-band backscattered light.

Design goals for the operational biosensor system were as follows:

- a. freedom of placement: to be used on any skin surface, i.e., forehead, arm, chest, etc.;
- b. comfort to subjects;
- c. minimum restriction of subject mobility;
- d. high-measurement accuracy over entire range of blood oxygen saturation;
- e. continuous measurement with rapid dynamic response to follow changes in blood oxygen saturation moment-by-moment;
- f. measurements displayed directly as percent oxygen saturation so that no calculations or interpretations required;

- g. stability and reliability;
- h. simplicity and infrequency of required calibration; no need to squeeze blood from the skin or otherwise manipulate the subject to obtain zero settings or calibrate;
- i. accuracy independent of variations in subject skin color, tissue hematocrit, etc.;
- j. minimal size, weight and power requirements, consistent with spacecraft and aircraft operations.

Although characteristics pertinent to an operational biosensor, such as items f and j above, were not deemed essential for the experimental systems, the above list provided a point of departure for experimental systems design and fabrication.

Two experimental backscatter-mode external biosensor systems were developed for use with a variety of transducers and investigated: (1) a chopped-light system; (2) a d.c. photomultiplier photometer system.



## 2. Chopped-Light Apparatus

The chopped-light apparatus (CLA,<sup>\*</sup> Figures FR-37 and FR-38) developed delivered two incident beams of broad-band light from a tungsten filament light source, through narrow band interference filters (previously evaluated during whole-blood studies reported in Section III), thence through a flexible fiber optics bundle to the surface of the skin. Light could be chopped at frequencies variable from d.c. to 400 cps.

Three fiber bundle sizes were interchangeable in the apparatus, having diameters of 0.62", 0.125" and 0.250".

While a wide variety of filters were interchangeable in the apparatus, initially 660 mμ and 805 mμ filters were incorporated. A 910 mμ filter was procured for use as the signal wavelength in studies exploring the usefulness of this portion of the electromagnetic spectrum in further reducing the problem of pigmentation variation between subjects.

Provision was made for close-coupling photodetectors of several types directly to the skin or remotely through light pipes. A wide variety of photodetectors were evaluated in order to establish the suitability of their signal-to-noise characteristics, optical and geometrical coupling factors, amplifier circuitry requirements and frequency response. Photodetectors assessed included silicon junction diodes, Cadmium Selenide photoconductors, a new molecular circuit photodiode Darlington amplifier molecular circuit module and an S-21 response photomultiplier.

Where remote photodetector coupling was considered, separate fiber bundles were used for light source and photo-

---

<sup>\*</sup> designated OCLA in Progress Reports

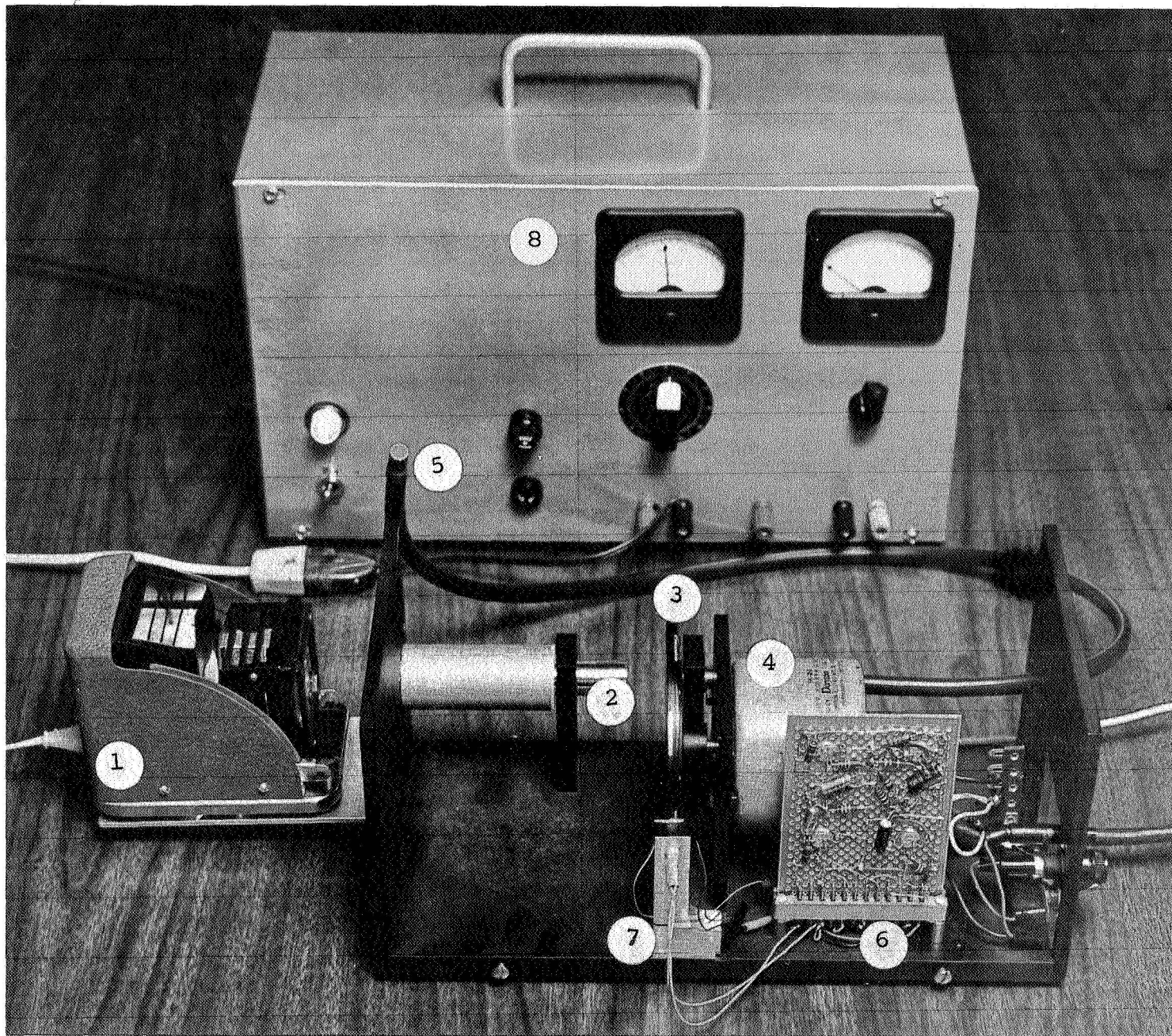


Figure FR-37. Experimental External Biosensor System: Chopped Light Apparatus (CLA), view without cover.

- (1) Projector housing
- (2) Projector objective
- (3) Filter wheel
- (4) Filter wheel drive motor
- (5) Glass fiber flexible light pipe
- (6) Synchronizing circuits
- (7) Synchronizing track photodetectors and illuminator block
- (8) Power supply



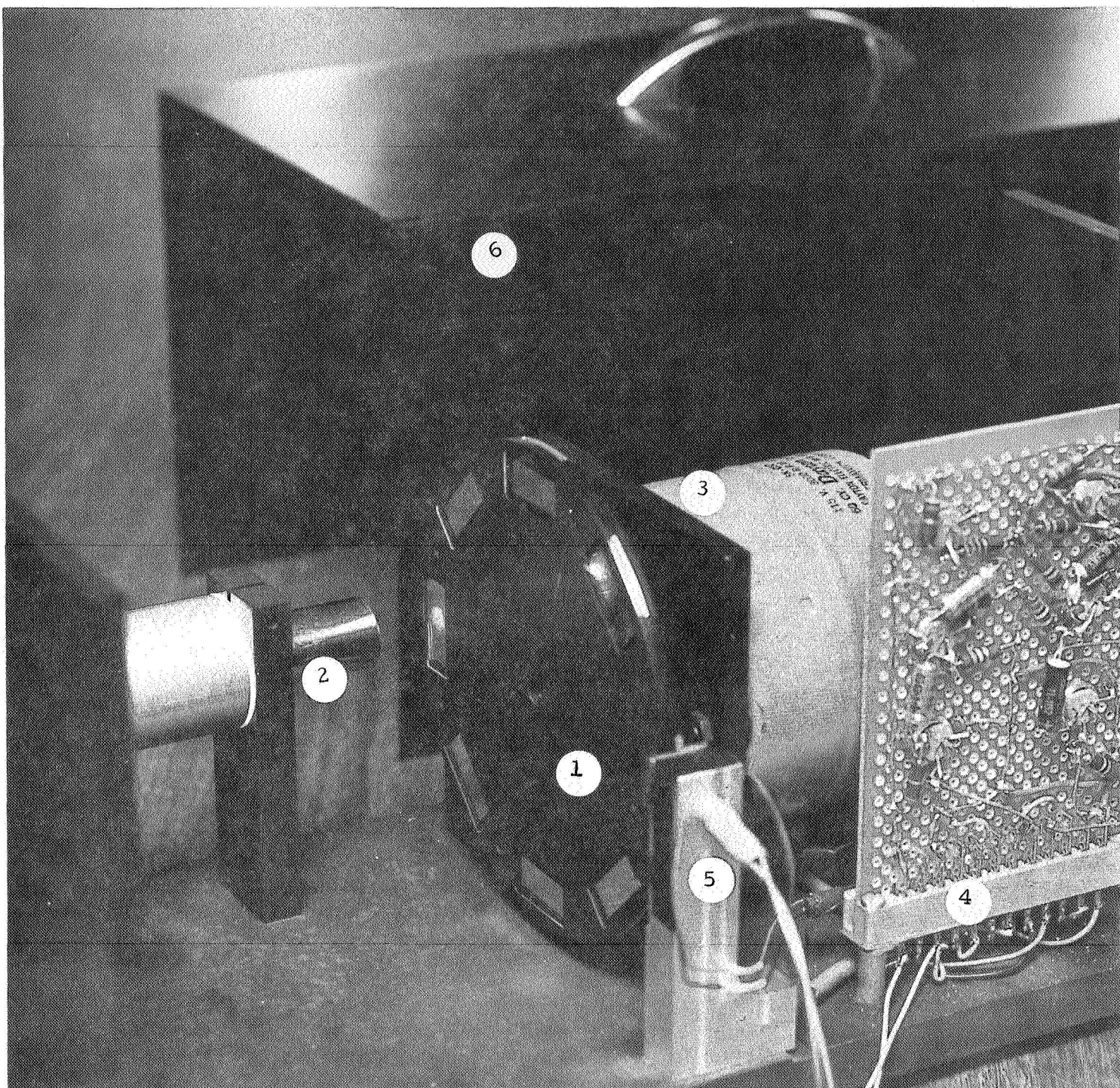


Figure FR-38. Experimental External Biosensor System: Chopped Light Apparatus (CLA), partial view.

- (1) Filter wheel - contains alternate 660 nm and 805 nm filters
- (2) Projector optics
- (3) Filter wheel drive motor
- (4) Synchronizing circuits
- (5) Synchronizing circuit photodetector and synchronizing track illuminator support block
- (6) Cover



detector pathways.

Gating circuits for signal sampling were provided to permit variable electronic sampling relative to and coincident with the two wavelength signal periods. Waveforms of the chopped 660 mμ and 805 mμ light and synchronizing pulses are shown in Figure FR-39.

The apparatus was made highly portable to permit easy movement of it between the laboratory, operating room, recovery room, heart catheterization laboratory and other locations where experiments were carried on.

The chopped-light apparatus (CLA) was used both with a congruent geometry transducer utilizing an integrating sphere and with a close-coupled detector contiguous field geometry transducer (CFT, Figure FR-40), both of which are described below.

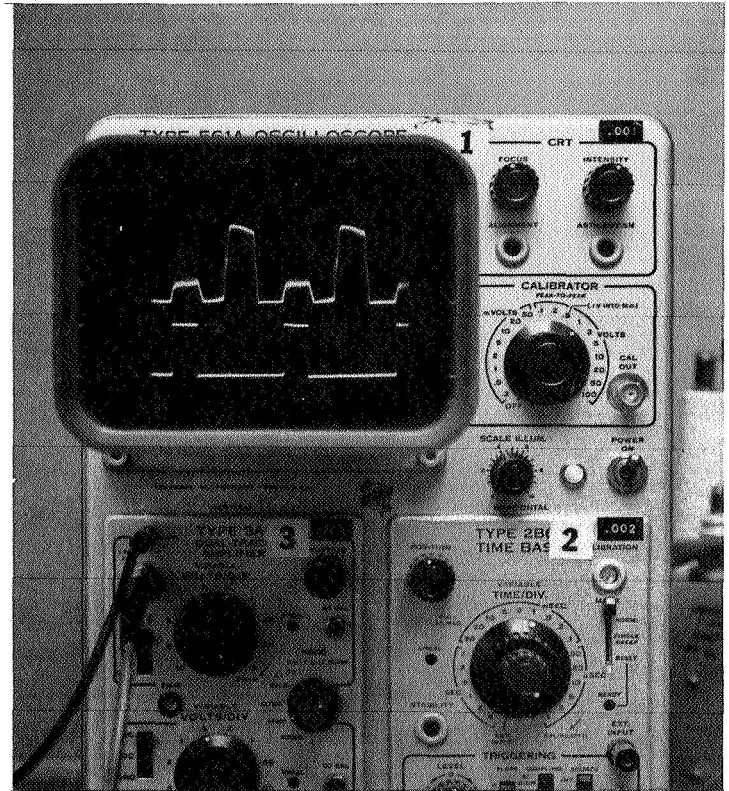
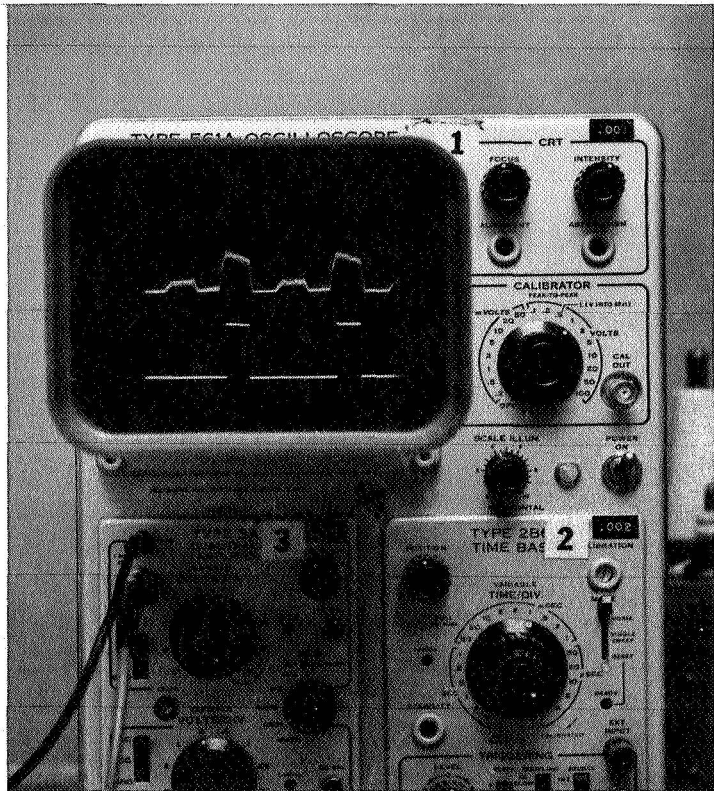


Figure FR-39. Experimental External Biosensor Systems: Chopped light apparatus monochromatic light output and synchronizing pulse waveforms. Left oscillogram: upper trace 805 millimicrons (small pulse) and 660 millimicrons light intensity; lower trace 660 millimicrons synchronizing pulse. Right oscillogram: upper trace 805 millimicrons (small pulse) and 660 millimicrons light intensity; lower trace 805 millimicrons synchronizing pulse.

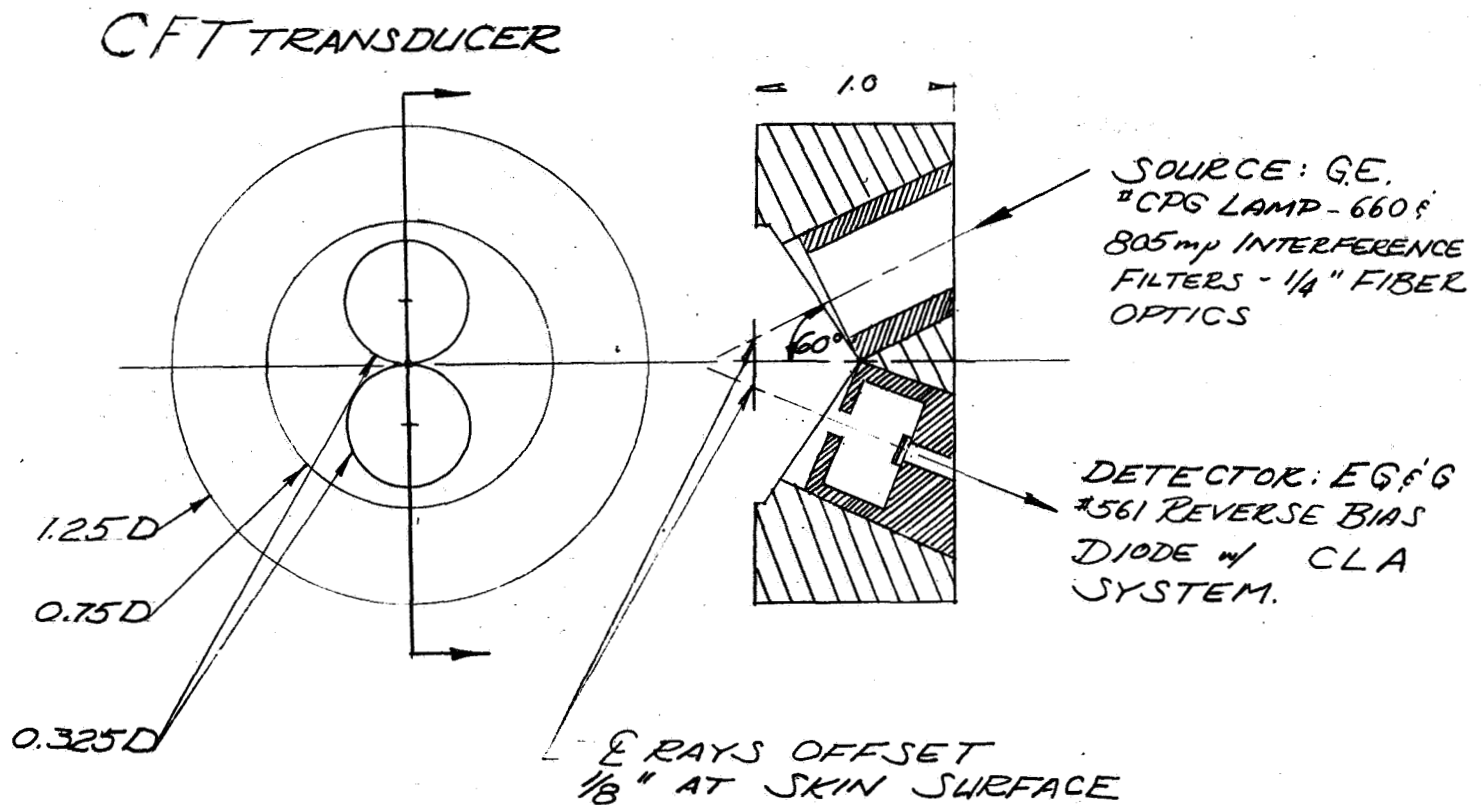


Figure FR-40. Experimental External Biosensor System: Diagram of Contiguous Field Transducer (CFT).

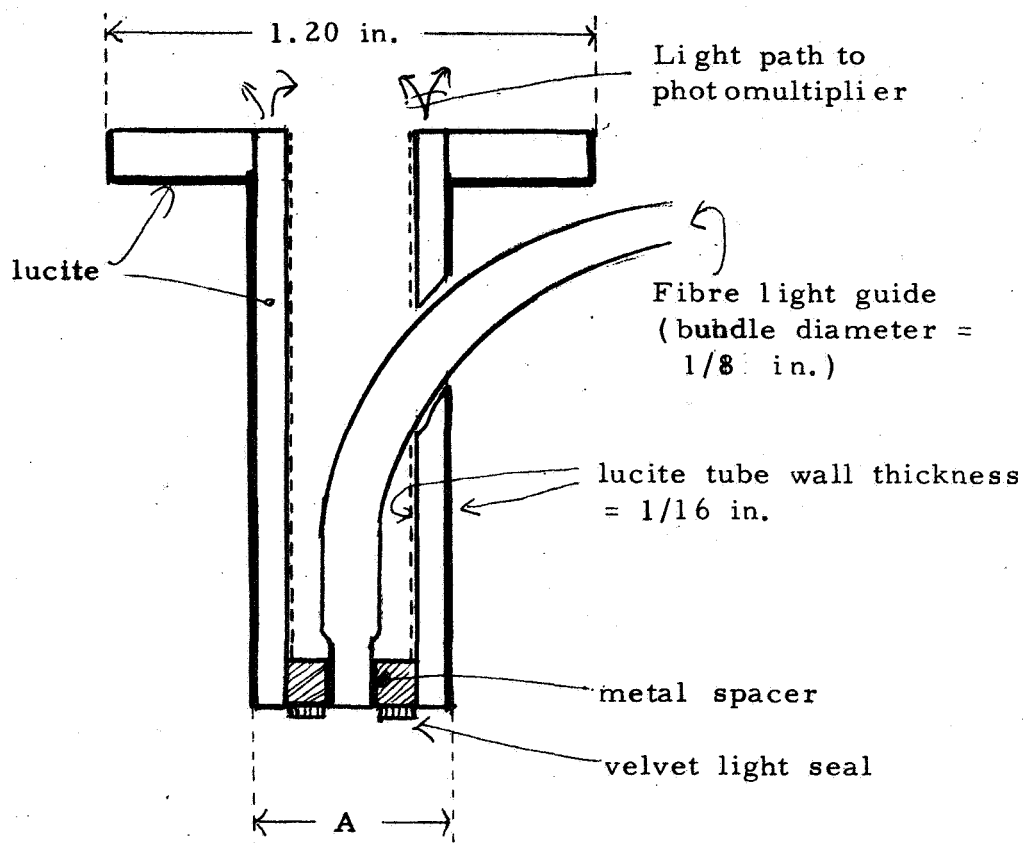
### 3. d.c. - Photomultiplier Apparatus

An alternative light source and detector apparatus utilized a broadband light source and photodetector element consisting of an S-1 response photomultiplier tube and a commercial photometer, shown in Figure FR-36. This system was used in conjunction with annular transducers of the designs shown in Figure FR-41 (designated the Annular Lucite Transducer, ALT)\* and Figure FR-42 (designated the Multiple Bundle Annular Transducer, MBAT). This d.c. photomultiplier apparatus had provision for either pre-filtering the transmitted light or transmitting while light and filtering the back-scattered light. Heat dissipation at the lamp was provided to eliminate interference filter heat damage. The system was semi-automated to permit remote switching of interference filters and to provide a zero calibration by means of light shutters.

### 4. Biosensor Transducers Configuration

As reported in Section III, the apparatus which was developed to obtain linear transfer functions between back-scattered light and oxygen saturation of whole blood, independent of hematocrit variations, utilized a congruent optical geometry (Figure FR-18), in which the light source and the detector "looked at" the same blood surface area. The congruent optical geometry transducer developed for the experimental external biosensor system made use of an integrating sphere and a fibre optics bundle. In this transducer, the incident pre-filtered light was brought via the fibre optics

\* designated ATO in Progress Reports



A: small sensor -- 1/2 in.  
 medium sensor 5/8 in.  
 large sensor - 7/8 in.

Figure FR-41. Experimental External Biosensor System: Diagram of Annular Lucite Transducer (ALT). Thick lines represent surfaces coated first with acrylic water-base white paint ( $\text{TiO}_2$  and silicate pigments) and then with black photographic lacquer. Dotted lines represent surfaces coated only with acrylic white paint.

# MBAT TRANSDUCER

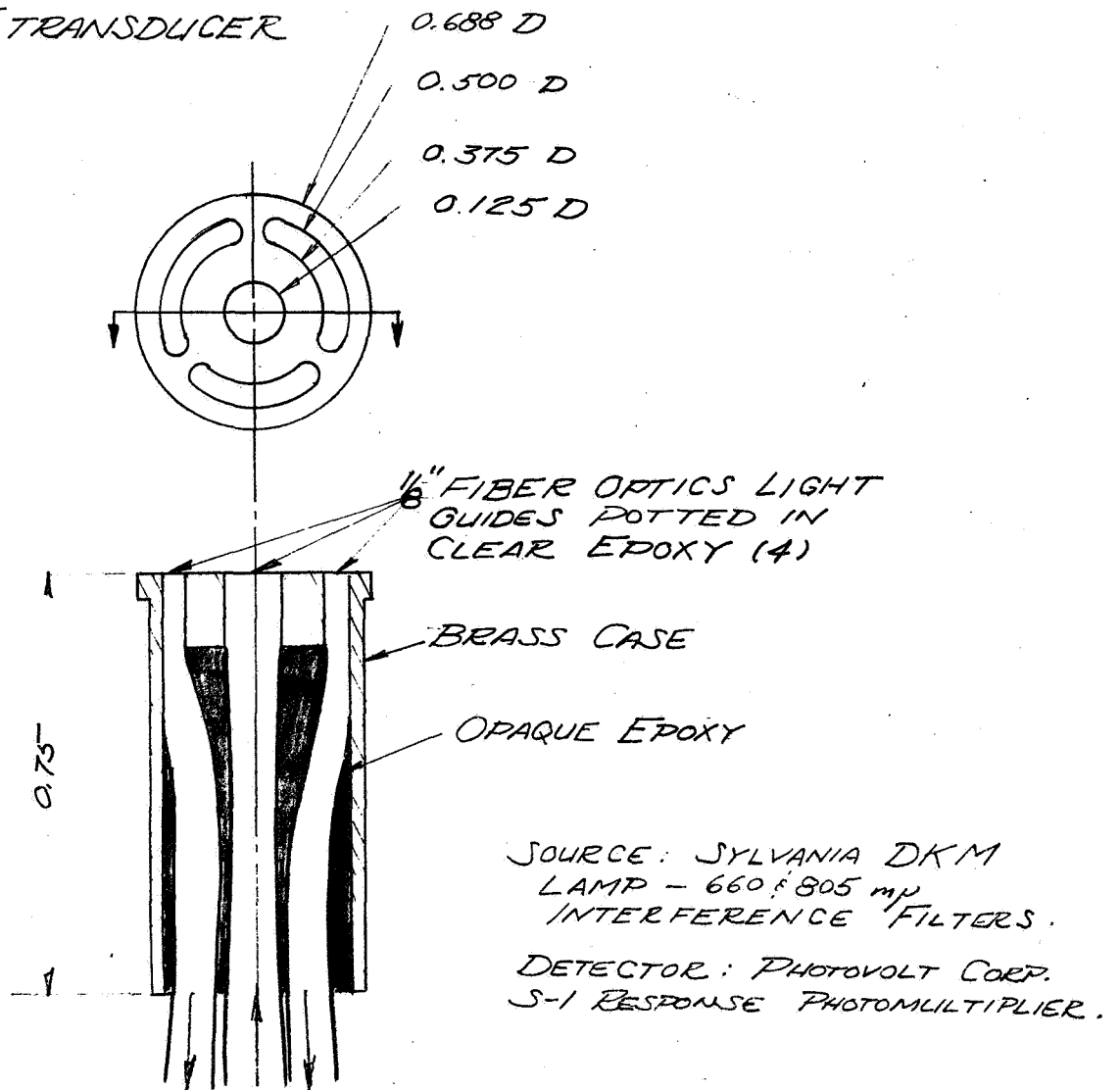


Figure FR-42. Experimental External Biosensor System: Diagram of Multiple Bundle Annular Transducer (MBAT).

bundle through the center of the integrating sphere onto the skin sample area. A photodetector was mounted on the periphery of the sphere. Provision was also made for the alternative of bringing white light to the center of an integrating sphere and filtering the back-reflected light returned to the detector. This configuration had the advantage of permitting the filters to be static, and, through the use of a mirrored chopping disc, permitting a longer period when monochromatic light was incident upon the photodetectors relative to the time light was blocked.

In addition, backscatter-mode transducers that approached the congruent optical configuration were designed and investigated. In these latter transducers, the field-of-view of the source and the detector were offset to reduce the contribution of direct-reflected light detected.

One such transducer (utilized with the chopped-light apparatus [CLA]) is shown in Figure FR-40. Designated the contiguous field transducer (CFT)\*, it approached the congruent optical condition by minimal separation of the illuminated and detected field of view by means of a 1/8" offset of the transmitted and backscattered ray center-lines at the skin surface.

\* designated QCT in Progress Reports

Two further alternative transducer configurations made use of an optical stop between the incident light and the detector field of view. These transducers were designated the Annular Lucite Transducer (ALT), illustrated in Figure FR-41, and the Multiple Bundle Annular Transducer (MBAT) illustrated in Figure FR-42. In the Annular Lucite Transducer, ALT, pre-filtered narrow-band light was transmitted down a central flexible fibre-optics light guide and light was returned through the walls of a hollow lucite pipe which was directly coupled to an S-1 response photomultiplier tube. In the MBAT transducer, a central fibre optics light guide carried either pre-filtered narrow-band radiation or white light to the center of the sensor disc. The distal portion of a large diameter fibre-optics light guide was dispersed and the individual optical fibres were randomly fanned out to form an annulus surrounding the central fibre bundle in the transducer head. The light collected by this annulus was carried back through the large diameter fibre optics bundle to an S-1 response photomultiplier tube. Filters were interposed or not in this optical path depending upon whether the light transmitted through the central fibre optics bundle had been pre-filtered.

These various backscatter-mode biosensor transducer configurations, each of which approached to a greater or lesser extent a congruent optical geometry configuration, were investigated with the hope that they would prove to perform in a manner approaching the transfer functions proved-out for a congruent optical geometry for whole blood, i.e.,

$$\text{O.S.} = K_1 \cdot \frac{I_{660} \text{ backscattered}}{I_{805} \text{ backscattered}} + K_2 \quad \text{Eq. 15 (= Eq. 2)}$$

where the ratio  $\frac{I_{805}}{I_{660}}$  of the light source was held constant

while having satisfactory sensitivity and signal-to-noise characteristics.



D. Experimental External Biosensor System Studies  
Utilizing a Congruent Optical Geometry

As reported in Section III and noted above, the apparatus developed to obtain linear transfer functions between backscattered light and oxygen saturation of whole blood, independent of hematocrit variations, utilized a congruent optical geometry. The integrating sphere external biosensor transducer described in Section V-C4 above was developed to experimentally explore the effect of a congruent optical geometry upon systems performance on the surface of the intact skin.

Some concern over the signal-to-noise characteristics of a congruent external biosensor applied to intact skin was originally manifest in the Program Proposal and this concern was further heightened during the skin-tissue studies, reported in Section IV, when it was quantitated that whole blood within the skin attenuated the light backscattered from the mixed skin-tissue-blood in-vivo system only a maximum of 10-20% (i.e. at 100% O.S.) of the total backscattered light. The following studies were generated to ascertain whether the non-information-bearing light component returned from the skin and tissue alone could be treated as a d.c. light level or whether this light underwent time-varying changes inseparable from the light intensity changes due to the blood within the skin, and consequently had to be treated as "noise".

If the external biosensor congruent transducer were to implement the transfer function observed for the congruent geometry with whole blood, i.e.,

$$\text{O.S.} = K_1 \cdot \frac{I_{660} \text{ backscattered}}{I_{805} \text{ backscattered}} + K_2 \quad \text{Eq. 16 (= Eq. 2)}$$

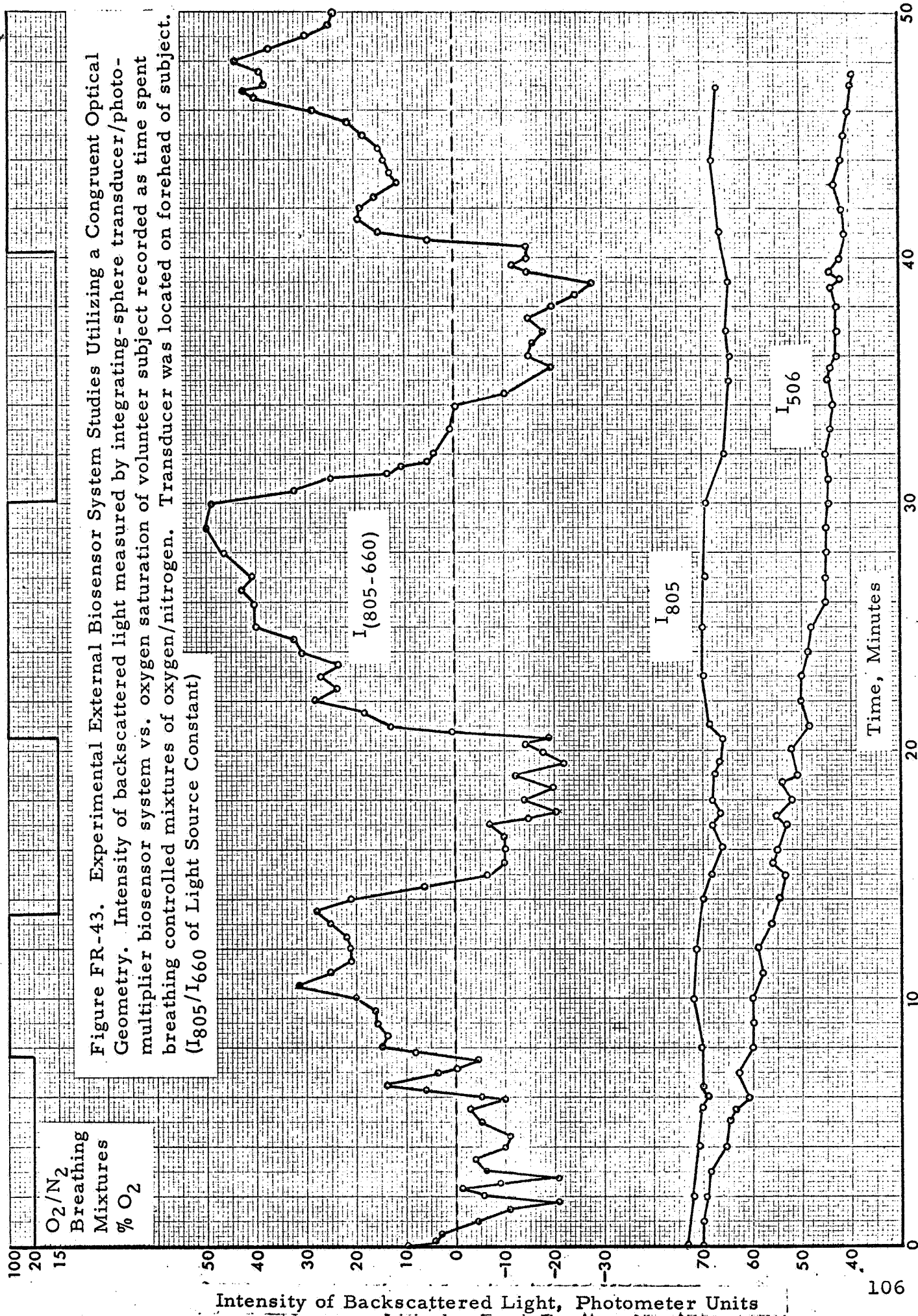
where the ratio  $\frac{I_{805}}{I_{660}}$  of the light source was held constant,

then the output of the system for a constant value of oxygen saturation (even with variations in physical and optical coupling of the transducers to the skin) would be constant.

In that case, the ratios of the non-information-bearing light component scattered back from the skin and tissues alone would be constant... and thus could be treated as a d.c. level rather than "noise". If, on the other hand, the output of the congruent geometry system during periods of constant oxygen saturation proved to be time-varying and sensitive to changes in physical and optical coupling, then the non-information-bearing component of light backscattered from the skin and tissues could not be differentiated from the information-bearing component, and the non-information-bearing component would have to be minimized in order to explore possible transfer functions relating oxygen saturation to information-bearing light signals.

Studies of the relationship of congruent geometry system performance at constant levels of oxygen saturations were performed utilizing the integrating sphere transducer described above and both the chopped-light system and the d.c. photomultiplier systems. The transducer was applied to the forehead of volunteer human subjects while oxygen saturation was maintained constant at one of three levels by breathing either 100% oxygen, room air (20% oxygen), or 15% oxygen.

A record of the best experimental result obtained is illustrated in Figure FR-43. This record shows the time sequence of backscattered light intensity levels at 805 and 506 mμ and presents the difference between the light intensities at 660 and 805 mμ, a difference initially set at zero. The subject was maintained at constant oxygen saturation levels that were varied in a step-wise fashion. The time history of the gas mixtures breathed by the subject are presented at the top of the record.



In this study, every effort was made to maintain the physical coupling of the transducer to the skin as constant as possible. Previous studies, in which the physical coupling between the transducer and skin had been purposely varied, resulted in extremely large and clearly unacceptable perturbations in system output.

As can be seen in Figure FR-43, even under the most stable physical situation obtained, considerable variation in system output is observed during periods of constant oxygen saturation. These variations were correlated with very minor perturbations in physical coupling.

The very large non-information-bearing light component backscattered from the skin and tissues alone in the congruent optical geometry was found to constitute "noise" rather than a d.c. offset. The signal-to-noise ratio for this geometry was found to be intolerable (approximately 1:7), consequently, major efforts were made to investigate non-congruent transducer geometries in which the "noise" generated by the skin could be minimized and satisfactory signal-to-noise ratios obtained. The results of these investigations are presented in the remainder of the report.

E. Experimental External Biosensor System Studies  
Performed on Skin-Tissue-Blood Simulator Cuvettes

Experiments were performed with the skin-tissue-blood simulator cuvettes to evaluate and compare the relative sensitivity\* of various transducer configurations and dimensions independent of the variables associated with actual physiologic measurement. Further, since the non-congruent backscatter-mode transducers investigated departed from the congruent optical geometry successfully used in the whole-blood studies, these experiments furnished the first approximation of the transfer functions of the non-congruent transducers for comparison with the transfer functions obtained during the whole-blood backscatter studies.

Study of the d.c. photomultiplier apparatus with the ALT transducers performed upon the STBS-II cuvette produced discrete transfer functions when dye concentrations were used corresponding to the optical densities of blood in the range of oxygen saturations of interest.

An evaluation of these same three annular lucite transducers (ALT) was conducted using the STBS-II with whole blood. The results of these experiments are presented in Figure FR-44, along with the transducers' working surface dimensions. A trend of increasing slope or sensitivity with increasing annular dimension was observed over the range of 80 to 100% oxygen saturation. Results at low oxygen saturation did not vary in any systematic manner with annular dimension.

---

\* Sensitivity is defined as the variation in transducer output for a given change in percent oxygen saturation.

Figure FR-44. Experimental External Biosensor System Studies on Skin-Tissue-Blood Simulator Cuvette Systems. Annular lucite transducer (ALT)/photomultiplier biosensor system transfer functions obtained on STBS-II using ALT transducers of various dimensions.

Backscattered Light Intensity Ratio  $I_{660}/I_{805}$  (System operating points set-up at beginning of each experiment to make  $I_{660}$  backscatter reading =  $I_{805}$  backscatter reading at known 100% Oxygen Saturation. Thereafter system operating points not altered and  $I_{805}/I_{660}$  of light source held constant.)

- ALT transducer # 2  
Annulus .500" OD, .375" ID
- ◐ ALT transducer # 3  
Annulus .625" OD, .500" ID
- ALT transducer # 5  
Annulus .875" OD, .750" ID

.125" D fiber optics input.  
S-1 response phototube.

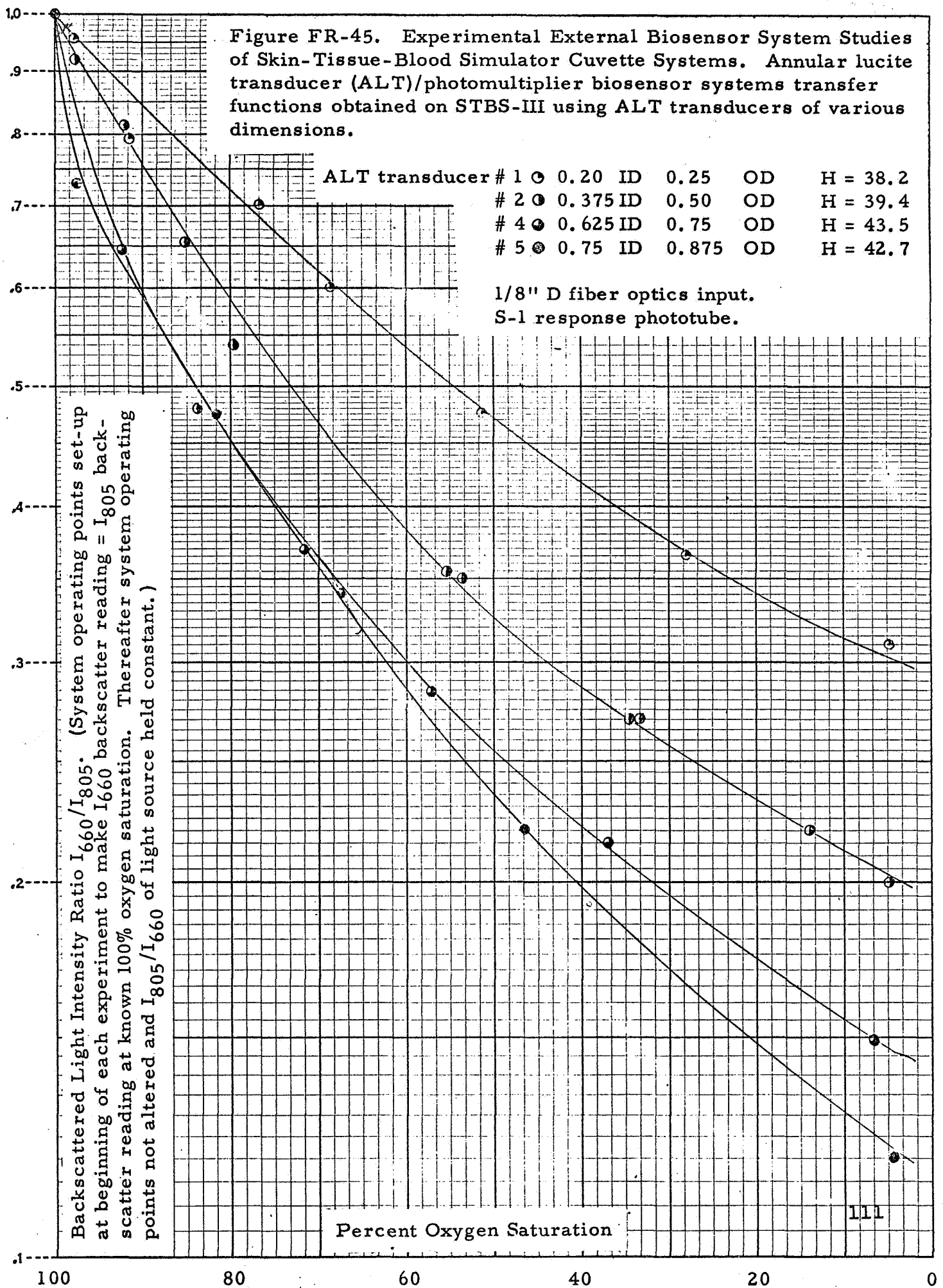
Percent Oxygen Saturation

Figure FR-45 displays additional results obtained with the ALT/Photomultiplier system on the model STBS-III cuvette. Blood hematocrit (the H numbers) varied over only a narrow range. In this study, the transducer sensitivity, or slope, was found to increase as annular dimension increased up to an inner diameter of 0.625" and an outer diameter of 0.75".

Figure FR-46 shows the effect of varying hematocrit at any one annular dimension on transducer sensitivity. The slope increased with increasing hematocrit. This behavior resembles that observed with whole-blood transmission systems, as demonstrated in Section III and confirmed in the literature.<sup>14,15</sup> Figures FR-45 and FR-46 demonstrate consistency of the data in the STBS; in this instance at a hematocrit of 39.4 for two different filter systems on two different runs. This hematocrit-dependence of the transfer functions suggested that the annular lucite transducer (ALT) was sensing a transmitted-light component.

In Figure FR-47, the results obtained on the same STBS-III cuvette with the CFT transducer/CLA biosensor system demonstrate increased sensitivity over the ALT/Photomultiplier system, an evaluation confirmed by subsequent animal data. (The data at a hematocrit of 37.3 was taken with a lower amplifier gain which, in this operation, corresponded to a lower sensitivity.) The data taken with the CFT/CLA system also shows much less hematocrit dependence than that taken with the ALT/Photomultiplier system over a similar range of hematocrits, indicating a closer approximation by the CFT transducer to the transfer functions implemented by a congruent optical geometry upon whole blood. Throughout the experiments with the CFT/CLA system, the eight-filter wheel was utilized, turning at 3,000 rpm or 400 cps light-chopping frequency.

Figure FR-45. Experimental External Biosensor System Studies of Skin-Tissue-Blood Simulator Cuvette Systems. Annular lucite transducer (ALT)/photomultiplier biosensor systems transfer functions obtained on STBS-III using ALT transducers of various dimensions.





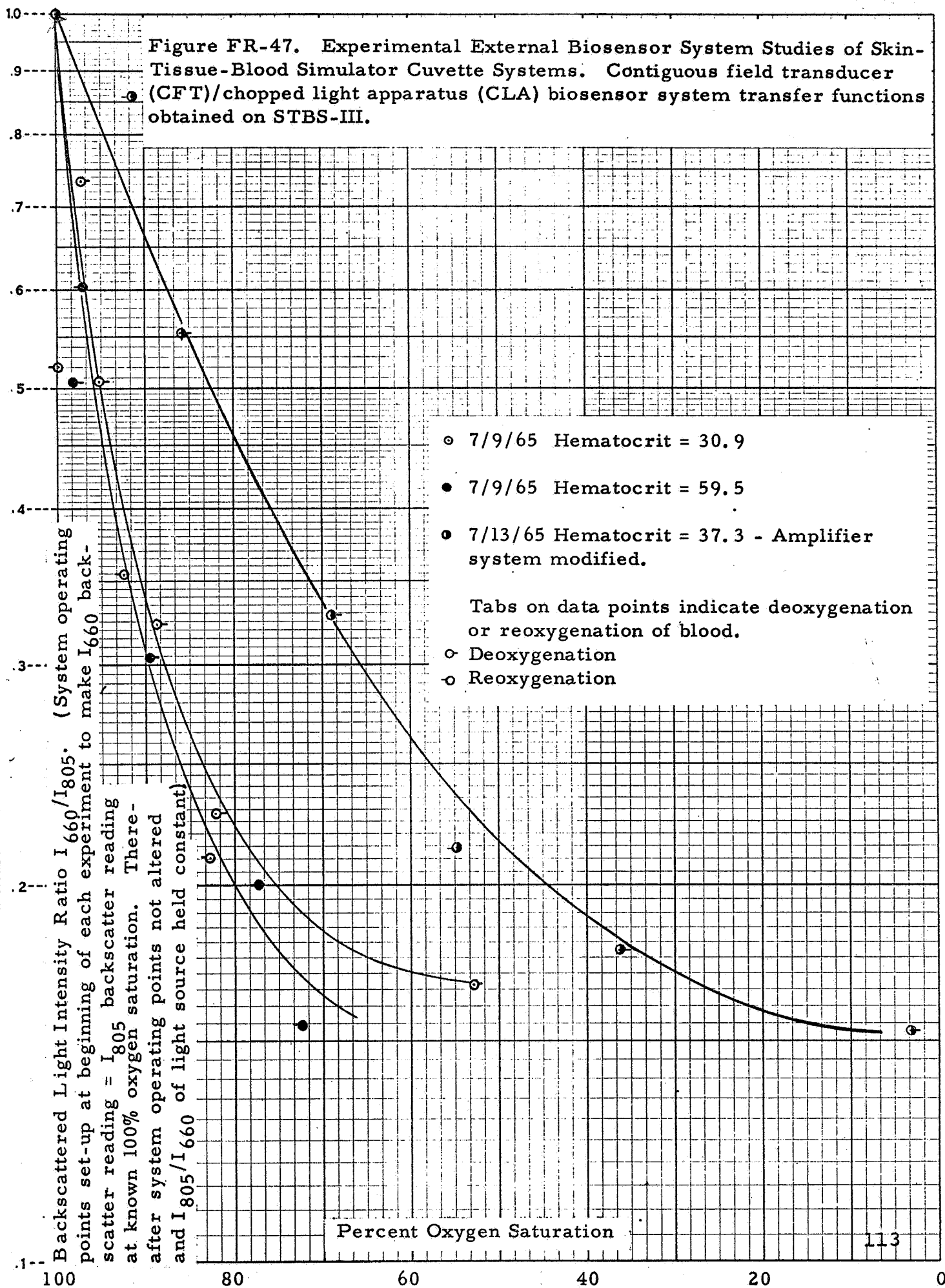
Backscattered Light Intensity Ratio  $I_{660}/I_{805}$ . (System operating points set-up at beginning of each experiment to make  $I_{660}$  backscatter reading =  $I_{805}$  backscatter reading at known 100% Oxygen Saturation. Thereafter system operating points not altered and  $I_{805}/I_{660}$  of light source held constant.)

Figure FR-46. Experimental External Biosensor System Studies of Skin-Tissue-Blood Simulator Cuvette Systems. Effect of hematocrit on transfer functions obtained on STBS-III using annular lucite transducer ALT # 2 (Figure FR-45)/photomultiplier biosensor system.

- 6/23/65 H = 39.4  
1% half-bandwidth interference filters, round.
- ⊖ Same blood, 3-4 % half-bandwidth interference filters, rectangular
- △ 6/24/65 H = 30.0  
Round filters
- ▲ 6/24/65 H = 46.4  
Round filters

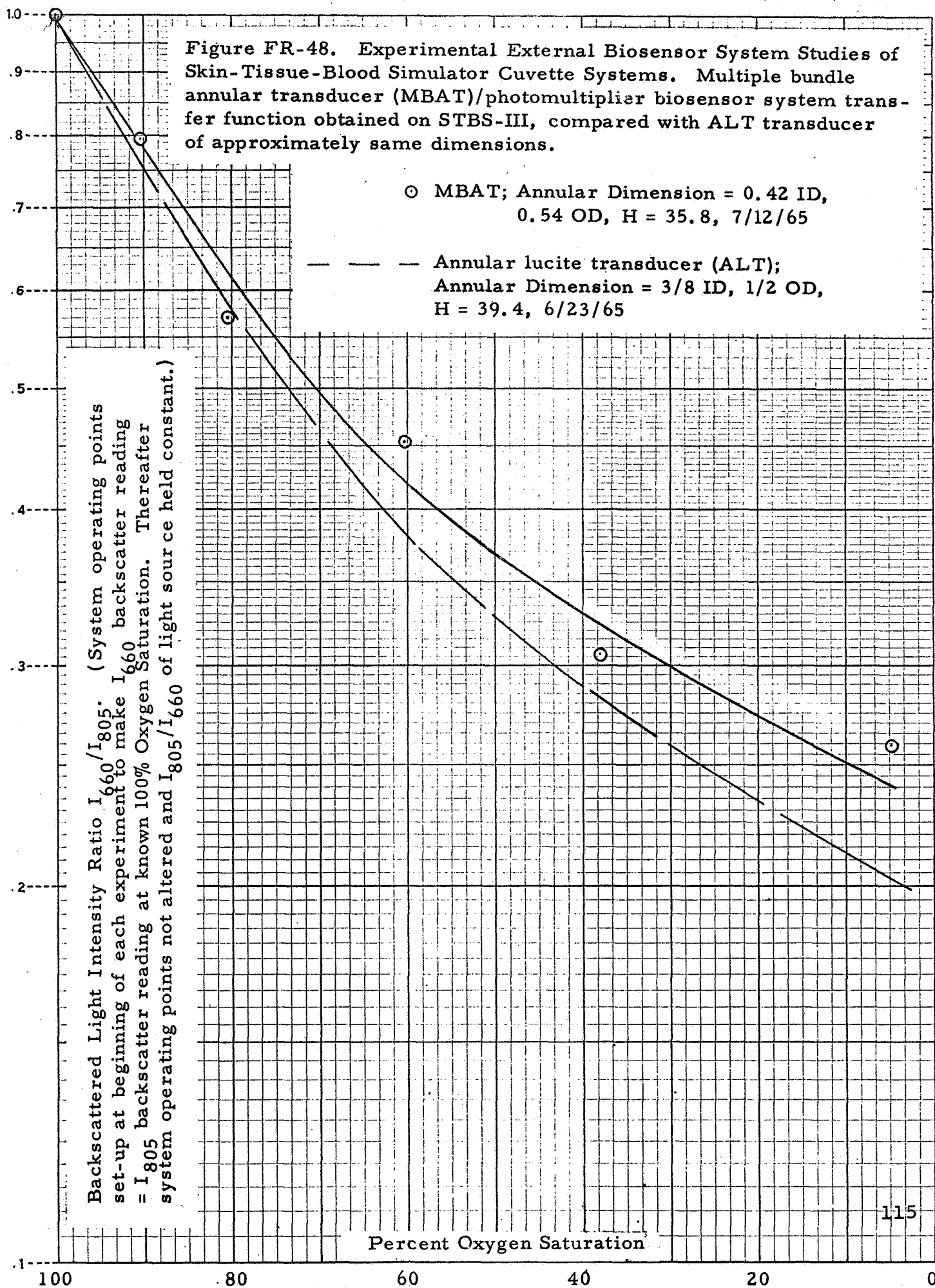
Percent Oxygen Saturation

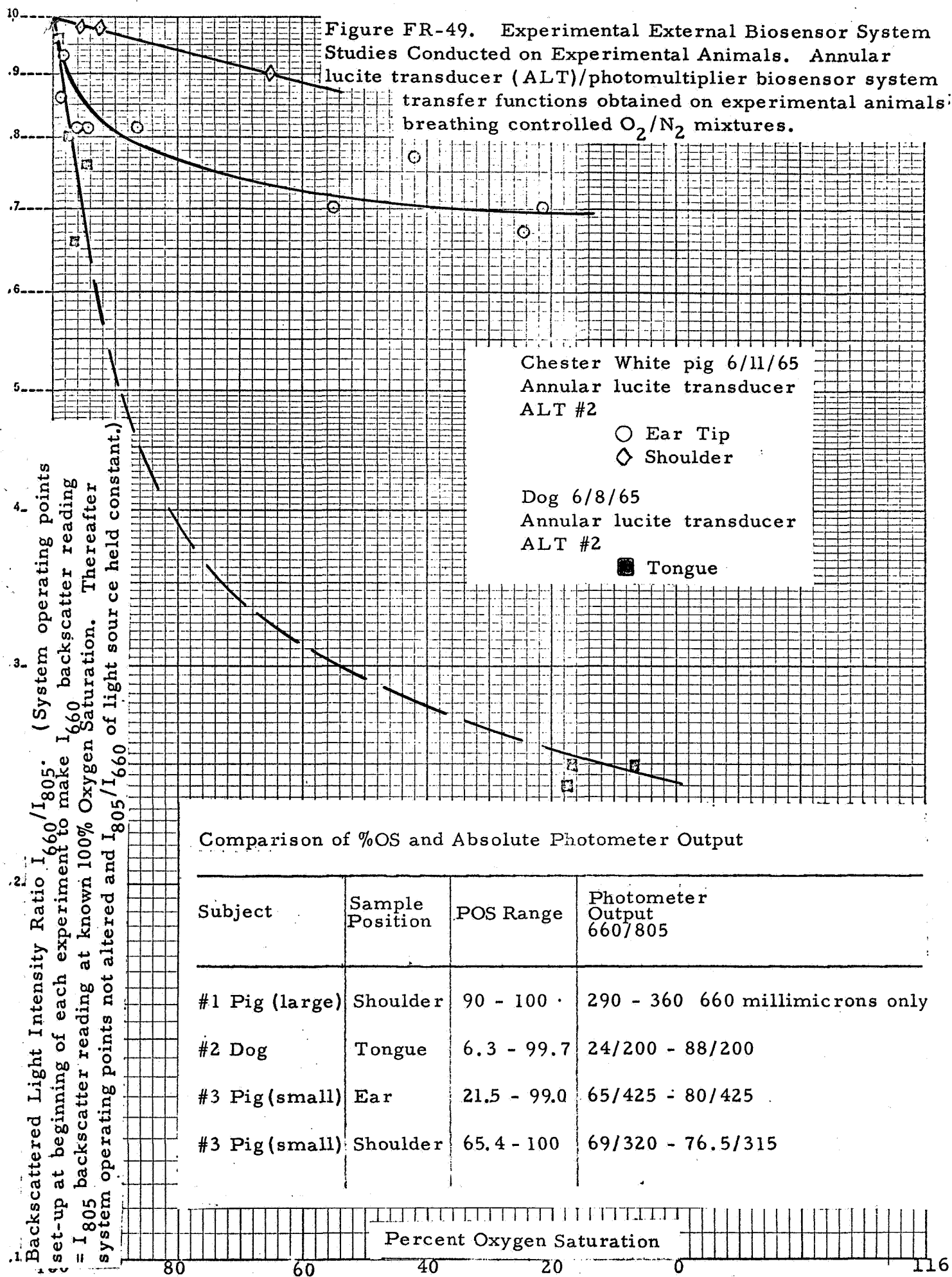
Figure FR-47. Experimental External Biosensor System Studies of Skin-Tissue-Blood Simulator Cuvette Systems. Contiguous field transducer (CFT)/chopped light apparatus (CLA) biosensor system transfer functions obtained on STBS-III.



The performance of the multiple-bundle light-guide annular transducer (MBAT) described above was compared on the standard STBS-III cuvette with the performance of the annular lucite transducer (ALT) of comparable dimensions. The results presented in Figure FR-48 indicate that the MBAT annular sector design was functionally the same as a complete annulus.

In general, the CFT/CLA biosensor system performance exhibited increased sensitivity over the ALT/Photomultiplier system when used on simulator cuvettes and, as reported below, on experimental animals. Almost linear transfer functions were generated relating the CFT/CLA biosensor output to oxygen saturation on a semilogarithmic plot over the range of 75% to 100% oxygen saturation with the STBS cuvettes.





F. Experimental External Biosensor System Studies  
Performed Upon Experimental Animals

In-vivo physiologic work with the experimental external biosensor systems was performed upon experimental animals because of the ease with which a wide range of variations in arterial oxygen saturation could be induced and arterial blood samples for the measurement of reference oxygen saturation could be drawn. With the exception of one set of measurements made on a dog, the experimental animals used were Chester White pigs, a breed used in radiation studies and chosen for these biosensor studies because of the humanoid character of the optical properties of their skin.<sup>16</sup>

Prior to the inception of the subject biosensor program, this laboratory had extensive experience in working with experimental animals. The laboratory, of course, strictly adheres to humane practices governing their care and use as set forth by the Council of the American Physiological Society.

In these experiments, the animals were anesthetized with Diabutal or with Fluothane, intubated, and ventilated with controlled mixtures of oxygen and nitrogen. Catheterization of the aorta through a peripheral artery was performed to obtain blood samples for standard-of-reference spectrophotometric oxygen saturation measurements performed as described in Section II. The animals received professional post-operative care, and in most instances survived the experiments with no ill effects.

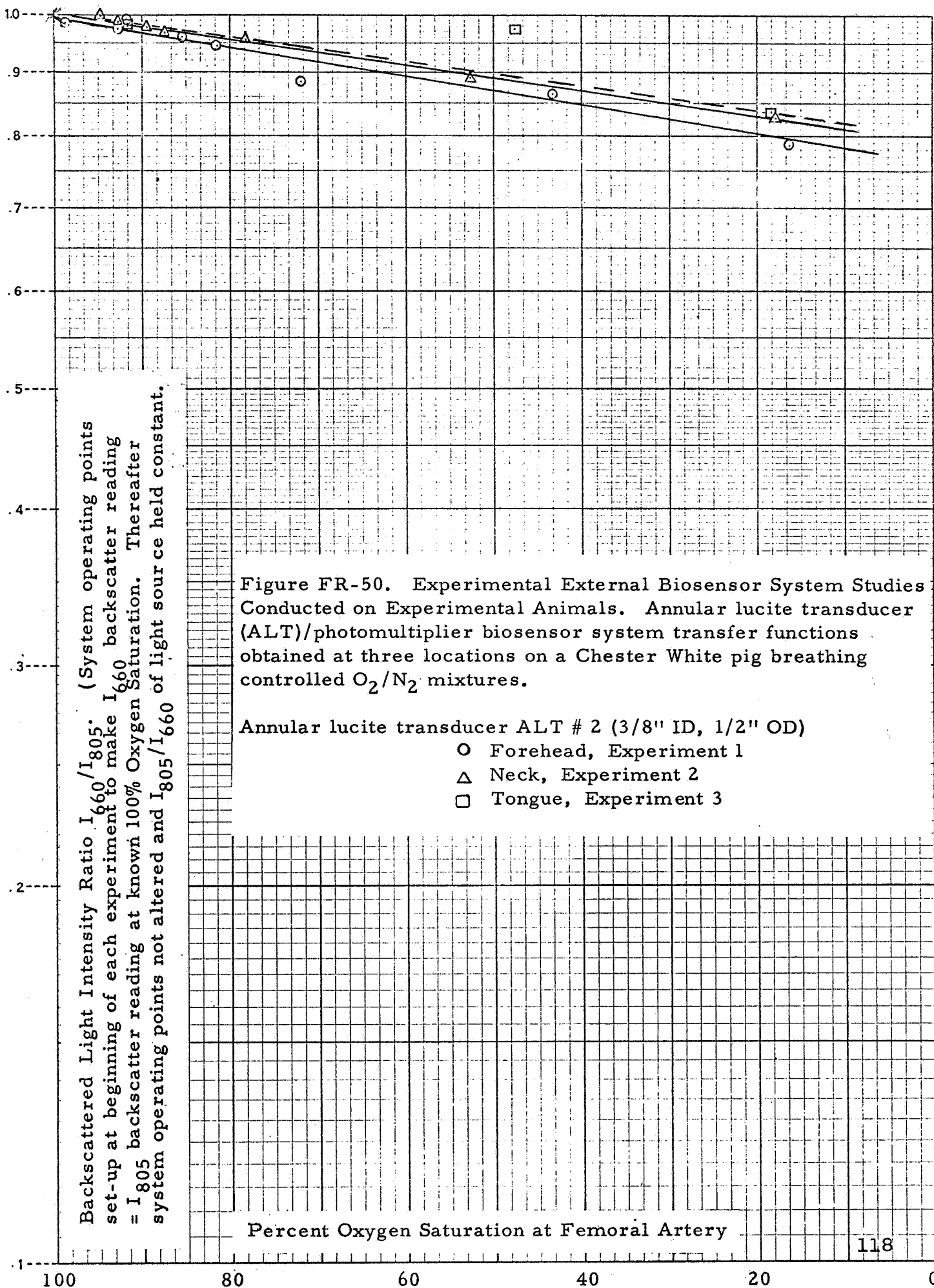
Representative results of the in-vivo external biosensor measurements performed upon the experimental animals are shown in Figures FR-49 through FR-53. Initial qualitative measurements on pigs with the ALT/Photomultiplier system in-

Backscattered Light Intensity Ratio  $I_{660}/I_{805}$  (System operating points set-up at beginning of each experiment to make  $I_{660}$  backscatter reading =  $I_{805}$  backscatter reading at known 100% Oxygen Saturation. Thereafter system operating points not altered and  $I_{805}/I_{660}$  of light source held constant.

Figure FR-50. Experimental External Biosensor System Studies Conducted on Experimental Animals. Annular lucite transducer (ALT)/photomultiplier biosensor system transfer functions obtained at three locations on a Chester White pig breathing controlled  $O_2/N_2$  mixtures.

Annular lucite transducer ALT # 2 (3/8" ID, 1/2" OD)

- Forehead, Experiment 1
- △ Neck, Experiment 2
- Tongue, Experiment 3





Backscattered Light Intensity Ratio  $I_{660}/I_{805}$ . (System operating points set-up at beginning of each experiment to make  $I_{660}$  backscatter reading =  $I_{805}$  backscatter reading at known 100% Oxygen Saturation. Thereafter system operating points not altered and  $I_{805}/I_{660}$  of light source held constant.)

Figure FR-51. Experimental External Biosensor System Studies Conducted on Experimental Animals. Comparison of contiguous field transducer (CFT)/chopped light apparatus (CLA) and annular lucite transducer (ALT)/photomultiplier biosensor systems. Transfer functions obtained on a Chester White pig breathing controlled  $O_2/N_2$  mixtures.

- Annular lucite transducer ALT on forehead
- Same after infrared heating of skin, (2nd Run)
- ▲ Contiguous field transducer, CFT

— — — Initial slope of Figure FR-50 data ALT

Percent Oxygen Saturation at Femoral Artery



Figure FR-52. Experimental External Biosensor System Studies Conducted on Experimental Animals. Multiple bundle annular transducer (MBAT)/photomultiplier biosensor system transfer functions obtained on 8/10/65 on the forehead of a Chester White pig breathing controlled  $O_2/N_2$  mixtures. (Additional data on the same pig weeks apart is shown in Figure FR-53).

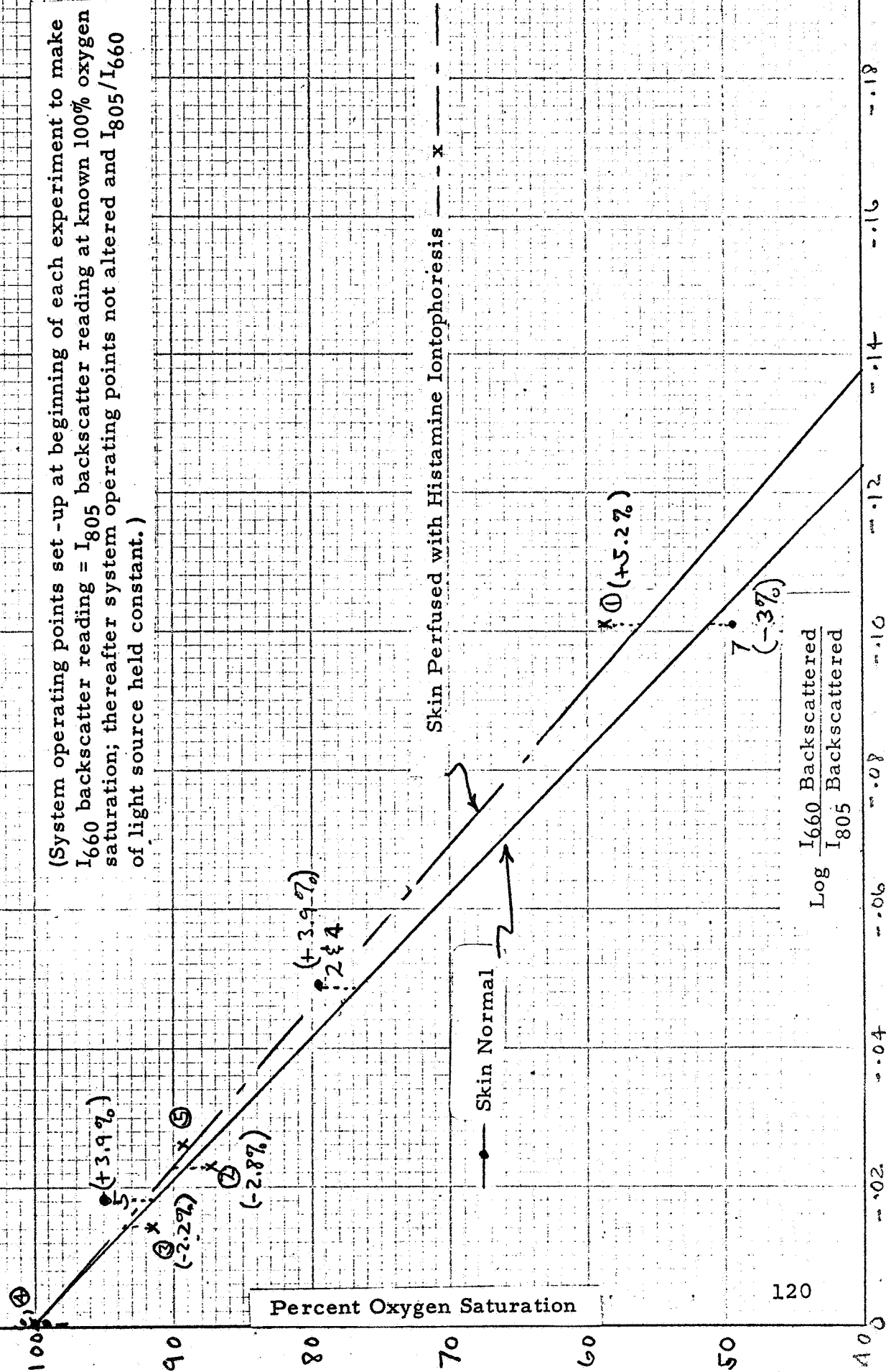
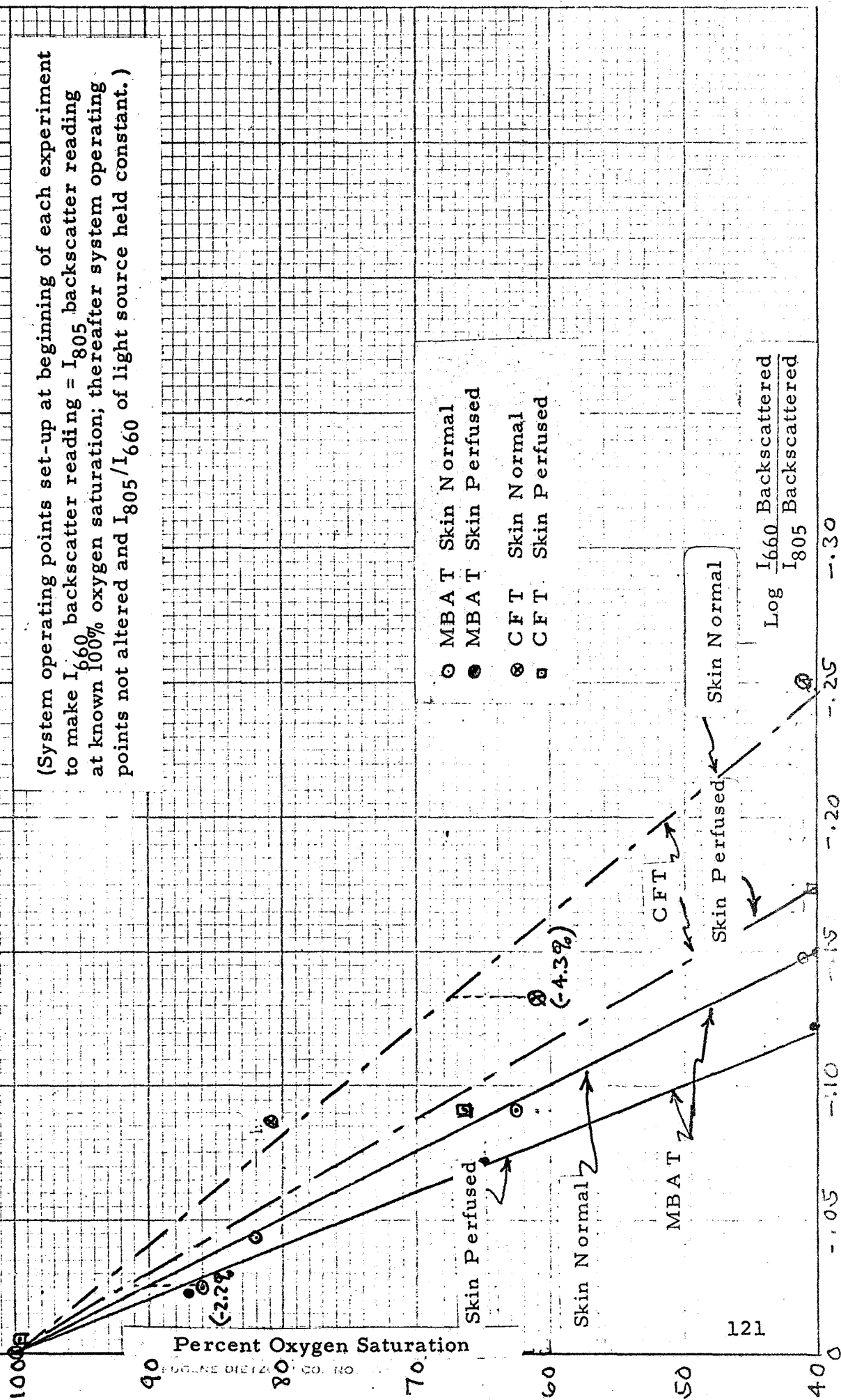


Figure FR-53. Experimental External Biosensor System Studies Conducted on Experimental Animals. Multiple bundle annular transducer (MBAT)/photomultiplier and contiguous field transducer (CFT)/chopped light apparatus (CLA) biosensor systems' transfer functions obtained several weeks after data presented in Figure FR-52 on a Chester White pig under normal and erythemized skin conditions breathing controlled O<sub>2</sub>/N<sub>2</sub> mixtures.



indicated that the best skin surface measurement site was the forehead and indicated that optical noise and spurious signal due to transient physiologic phenomena was not a significant problem. In Figure FR-49, the data on a black mongrel dog was taken using the tongue as a measurement site because of light attenuation by its black skin at other sites tested. All experimental studies performed with annular transducers utilized either ALT transducer #2 (I.D. .38", O.D. .50") or an MBAT transducer of the same general dimensions (I.D. .42", O.D. .54").

Figure FR-49 demonstrates greater system sensitivity on the pig forehead than on the pig shoulder. More extensive data from several body sites in the pig presented in Figure FR-49 for the shoulder, shows little scatter of data taken from various anatomic sites and suggests an essentially straight line relationship between the arterial oxygen saturation and

$$\text{Log } \frac{I_{660}}{I_{805}},$$

$$\text{O.S.} = K_1 \cdot \text{Log } \frac{I_{660} \text{ backscattered}}{I_{805} \text{ backscattered}} + K_2 \quad \text{Eq. 17 (= Eq. 3)}$$

where the ratio  $\frac{I_{805}}{I_{660}}$  of the light source is held constant,

a transfer function between the transmission (Eq. 1) and backscatter (Eq. 2) functions previously presented.

Figure FR-51 presents a more careful examination of the pig forehead utilizing a more sensitive amplifier configuration. An infrared lamp irradiated the skin in a specified dosage before the second series of measurements and provided uniform skin flushing for the duration of the experiment. The data for the "flushed" skin indicated that the increased blood content of the skin, i.e. increased "tissue hematocrit", caused some increased sensitivity in the performance of the experimental biosensor. Also evident in Figure FR-51 is the higher sensitivity of the

CFT transducer.

Figure FR-52 illustrates data taken on the forehead of a pig using the MBAT/Photomultiplier system both before and after flushing of the skin with histamine iontophoresis. Figure FR-52 (as does Figures FR-50 and FR-51) demonstrates linear functions between the  $\text{Log } \frac{I_{660}}{I_{805}}$  and oxygen saturation and a modest increase in biosensor system sensitivity after skin flushing. This increase in sensitivity due to active flushing of the skin to vary tissue hematocrit results in a maximum spread of  $\pm 1\%$  oxygen saturation at an oxygen saturation of 90% and a  $\pm 3\%$  spread at an oxygen saturation of 60% in these studies.

Data obtained from the same animal some weeks apart is presented in Figure FR-53. In this experiment the MBAT transducer was applied to normal skin and to skin "flushed" by means of IR irradiation. In this study, the normal and flushed skin had a range of slopes between 100% OS and 60% O.S., from -500 and -405, resulting in a deviation in oxygen saturation of  $\pm 1\%$  at 90% OS and  $\pm 4\%$  at 60% OS. The average calibration lines for the MBAT transducer in experiments presented in Figures FR-52 and FR-53 are very close, each having slopes of approximately -448  $\pm 1\%$ .

Data taken a month earlier from the same animal is shown in Figure FR-52. This data, however, was taken with a different transducer of lower sensitivity (the ALT #2). The data shows approximately the same change in slope when normal skin is subjected to IR irradiation flushing (slope change from -632 to -545). This data also approximates the straight line function

$$\text{POS} = K_1 \text{Log } \frac{I_{660}}{I_{805}} + K_2 \quad \text{Eq. 18 (= Eq. 3)}$$

where the ratio  $\frac{I_{805}}{I_{660}}$  of the light source is held constant over the range from 60% oxygen saturation to 100% oxygen saturation.

Data collected on two occasions weeks apart with the CFT transducer and presented in Figures FR-51 and FR-53 also generate a similar linear semilogarithmic transfer function over the range of oxygen saturation from 100% to 40%. Comparing the slopes for normal skin in these two experiments provides values of -247 in Figure FR-53 and -260 in Figure FR-51. This represents less than  $\pm 2\%$  deviation in oxygen saturation measurement from 100% to 40% oxygen saturation.

The increased sensitivity of the CFT apparatus over the MBAT apparatus demonstrated in the experimental animal studies is consistent with sensitivity findings for the CFT and MBAT transducers on the simulator cuvettes, as illustrated in Figures FR-47 and FR-48, respectively.

This in-vivo data obtained from the pig was most encouraging. Adequate sensitivity of the systems was demonstrated. The reproducibility of the data was quite good, although there was a large variation in slope when tissue hematocrit was artificially varied by inducing "flushed" skin. The fact that the straight line transfer function was of the form  $\text{Log } \frac{I_{660}}{I_{805}}$  suggested that the apparatus was sensing phenomena somewhat between previously studied backscatter and transmission modes of operation.

#### G. Experimental External Biosensor System Studies Performed Upon Human Patients

Following early experimental external biosensor systems studies performed upon Chester White pigs, the experimental systems were adapted for use in the Cardiac Catheterization Laboratory of the Presbyterian Hospital in San Francisco. Studies were performed with the MBAT/Photomultiplier system positioned upon the forehead of patients undergoing cardiac catheterization. Oxygen Saturation of arterial blood samples removed from the brachial artery was determined by the standard-of-reference method presented in Section II, and these oxygen saturation values were compared with the output of the experimental biosensor systems.

The range of oxygen saturation exhibited by patients during cardiac catheterization was too restricted (from 94% to 100% OS) to describe satisfactory transfer functions for the experimental systems. This data did demonstrate that the systems had sufficient sensitivity to detect changes of the order of 1% oxygen saturation and that the readings were in the proper direction.

The experimental systems were further refined for use in the surgical operating room. In adapting them for data acquisition during open-heart surgery, various mechanical and optical modifications were required. In particular, special optical and electrical coupling components had to be fabricated to prevent interference by the equipment and research personnel with the surgical team and procedure. Various automated calibration procedures were developed for this purpose.

Data acquisition was scheduled for 25 patients undergoing open-heart operations. Following the induction of

anesthesia with tracheal intubation, the transducer of the experimental biosensor system studied was placed in the desired position upon the patient. Following placement of the transducer, femoral artery catheterization was performed in order to monitor arterial blood pressure and obtain arterial samples prior to the institution of cardio-pulmonary bypass with the heart-lung machine. Patients were positioned in a right lateral position when mitral valve procedures were performed or atrial septal defects corrected; other patients were in a supine position upon the operating table.

Following thoracotomy, the superior and inferior vena cavae were cannulated and attached to the venous lines of the heart-lung machine and an iliac artery was cannulated for attachment to the arterial line of the heart-lung machine. Usually only a few scattered data points were taken during this phase of the procedure in which patient arterial oxygen saturation was usually quite constant.

With the institution of cardio-pulmonary bypass on the Osborn-Bramson-Gerbode heart-lung machine, backscattered-light signals from the experimental biosensor system output were continuously recorded either on a special multiple channel Offner Recorder (Figure FR-54) or on a Varian Recorder. Several times during the course of cardio-pulmonary bypass, the performance of the artificial lung would be gradually altered to produce arterial oxygen saturation variations through the range from 100% to 60% oxygen saturation. Intermittently, during these periods of changing arterial oxygen saturation, blood samples would be withdrawn from the arterial line leading from the artificial lung to the patient's aorta into heparinized and siliconized glass syringes for standard-of-reference measurements performed by the method described in Section II. Signal markers recorded the time of withdrawal

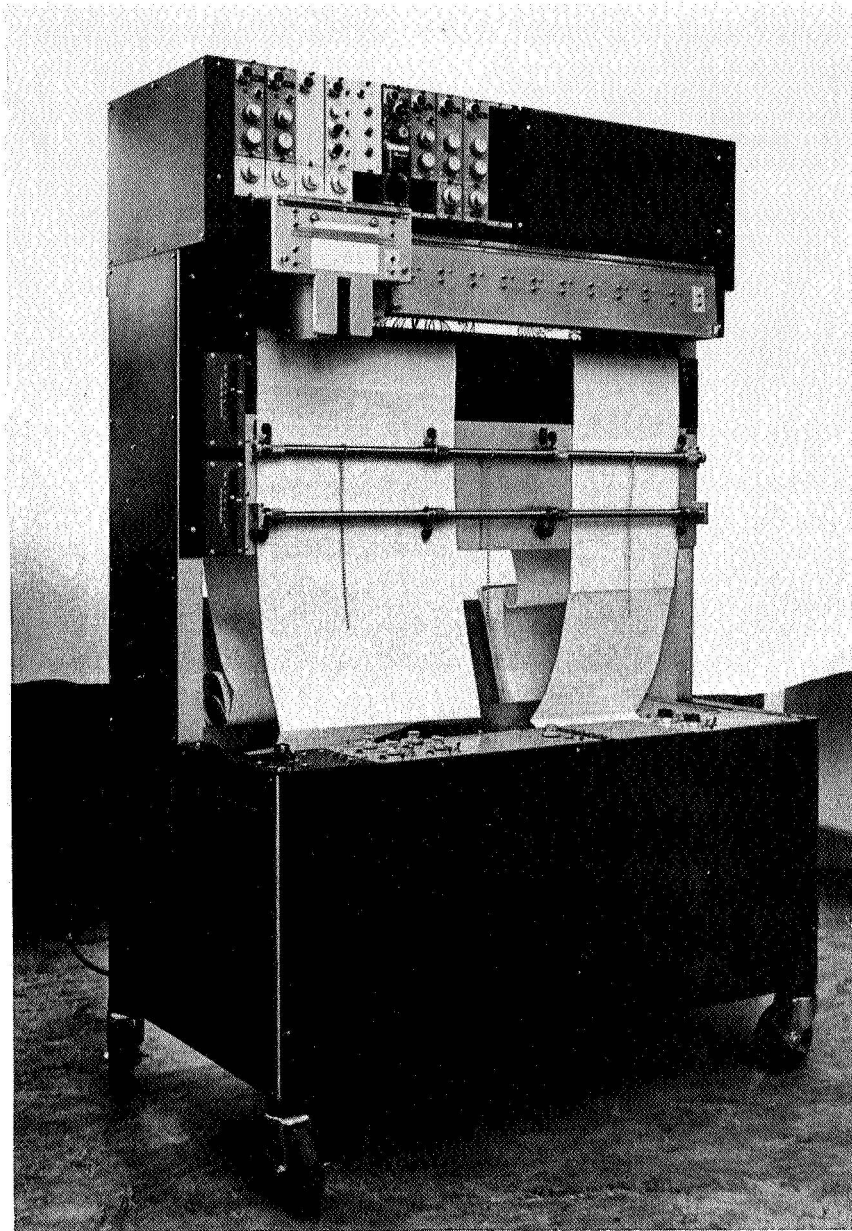


Figure FR-54. Experimental External Biosensor System Studies Performed on a Multi-Channel Recorder for Data Acquisition in Human and Animal Studies.



of these samples for data processing purposes.

In addition, the patient's total systemic blood flow, systemic blood pressure and systemic temperatures were recorded. Skin temperature and skin blood flow were widely varied during this phase of the procedure.

Following each experimental study, the light intensity data was manually converted from the graphic records into digital form at data points for which independent standard-of-reference oxygen saturation measurements were available. The external biosensor system light intensity data was processed utilizing a wide assortment of computational programs.

As in the experimental animal studies, the experimental external biosensor system data was found to conform most closely to a transfer function relating oxygen saturation to the logarithm of the ratio of intensities of light backscattered at the signal and isosbestic wavelength, i.e.,

$$\text{O.S.} = K_1 \cdot \text{Log} \frac{I_{660} \text{ backscattered}}{I_{805} \text{ backscattered}} + K_2 \quad \text{Eq. 19 (= Eq. 3)}$$

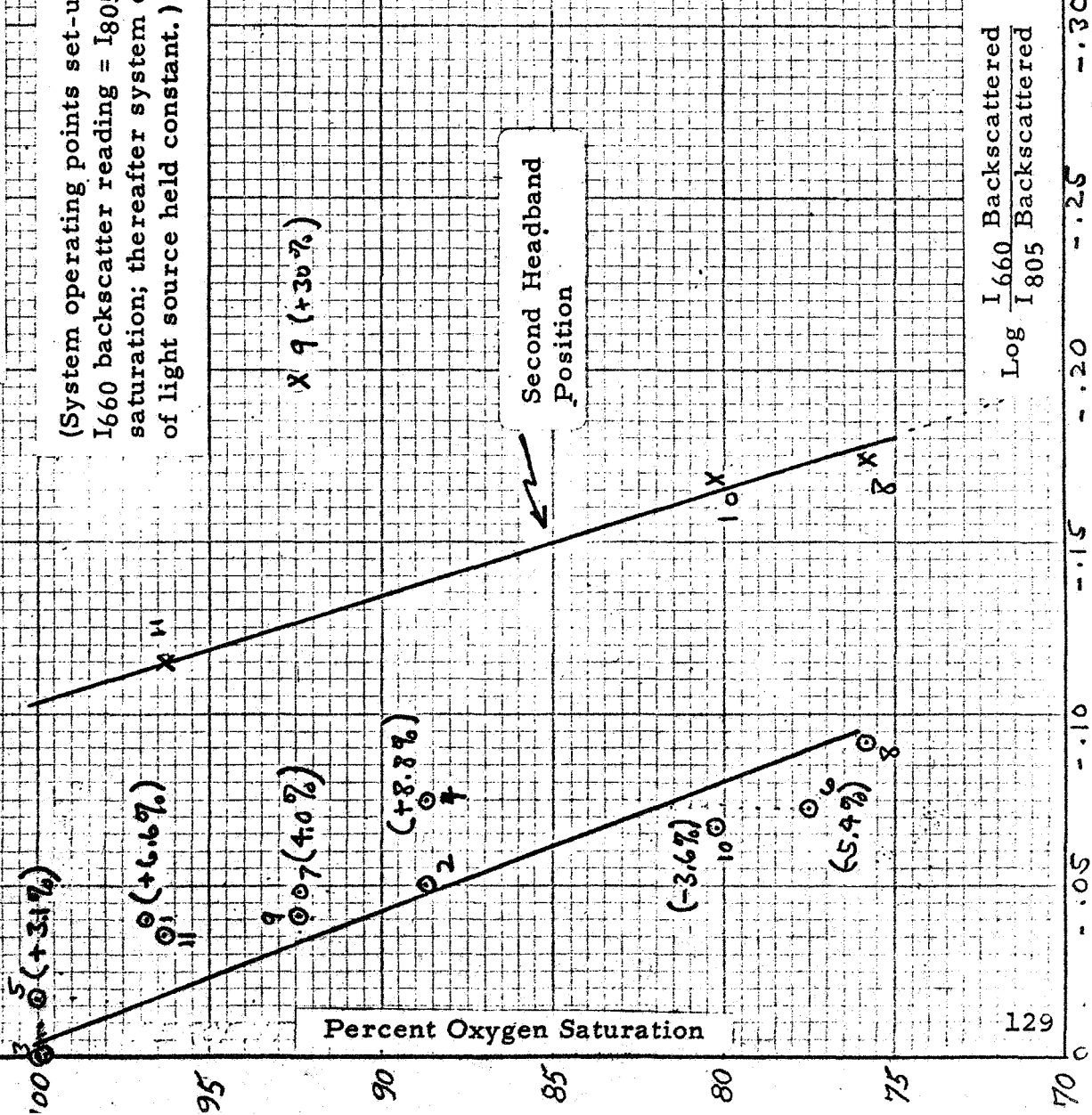
where the ratio  $\frac{I_{805}}{I_{660}}$  of the light source was held constant.

Figure FR-55 illustrates a typical plot of the log of the ratio of backscattered light intensities obtained with the CFT/CLA biosensor system vs. arterial oxygen saturation of a 63 year old white female patient, G. M. Two distinct positions of the transducer upon the forehead resulted in a marked offset of the data points and two distinct linear best fit curves.

The average slope of the above curves was -250, which falls midway between the slopes of the two examples of CFT/CLA transfer functions obtained on pigs presented in Figures FR-51

Figure FR-55. Experimental External Biosensor Studies  
 Conducted on Patients during Open-Heart Surgery. Contiguous  
 field transducer (CFT)/chopped light apparatus (CLA) biosensor  
 system transfer function obtained on G.M., white, Female,  
 Age 63, during open-heart surgery.

(System operating points set-up at beginning of each experiment to make  
 I<sub>660</sub> backscatter reading = I<sub>805</sub> backscatter reading at known 100% oxygen  
 saturation; thereafter system operating points not altered and I<sub>805</sub>/I<sub>660</sub>  
 of light source held constant.)



and FR-53 (slopes of -260 and -247 respectively). Thus, the average slopes of the transfer function of this human data and the pig data previously illustrated was essentially the same for the CFT/CLA systems, with deviations of less than 2% O.S. in the best fit line over the entire range of O.S. from 100% to 40%.

In this illustrative human study (Figure FR-55), the scatter of experimentally determined data points about the best fit linear curves for the CFT/CLA is equivalent to  $\pm 4\%$  oxygen saturation. (In retrospect, this scatter was found to be most likely due to lesser perturbations in positioning of the transducer upon the subject's forehead than the distinct positional change that produced the two separate curves in Figure FR-55; during five hours of chest surgery, considerable movement of the patient inevitably occurs.)

Comparable data acquired with the MBAT/Photomultiplier system upon this same patient and two other patients studied at roughly the same time are presented in Figure FR-56. For these three patients the MBAT/Photomultiplier system slopes were -408 (GM), -476 (HR) and -536 (NV), compared with a slope of -405 obtained with this same system upon a pig and presented in Figure FR-54.

The variation in slope demonstrated for three patients in Figure FR-56 is more fully seen in the data from eight patients presented in Figure FR-57. In Figure FR-57, the best fit lines for points of  $\text{Log } \frac{I_{660}}{I_{805}}$  is plotted against percent oxygen saturation for each of the eight patients.

Figure FR-56. Experimental External Biosensor System Studies Conducted on Patients during Open-Heart Surgery. Multiple bundle annular transducer (MBAT)/photomultiplier biosensor system transfer functions obtained on three patients.

(System operating points set-up at beginning of each experiment to make I660 backscatter reading = I805 backscatter reading at known 100% oxygen saturation; thereafter system operating points not altered and I805/I660 of light source held constant.)

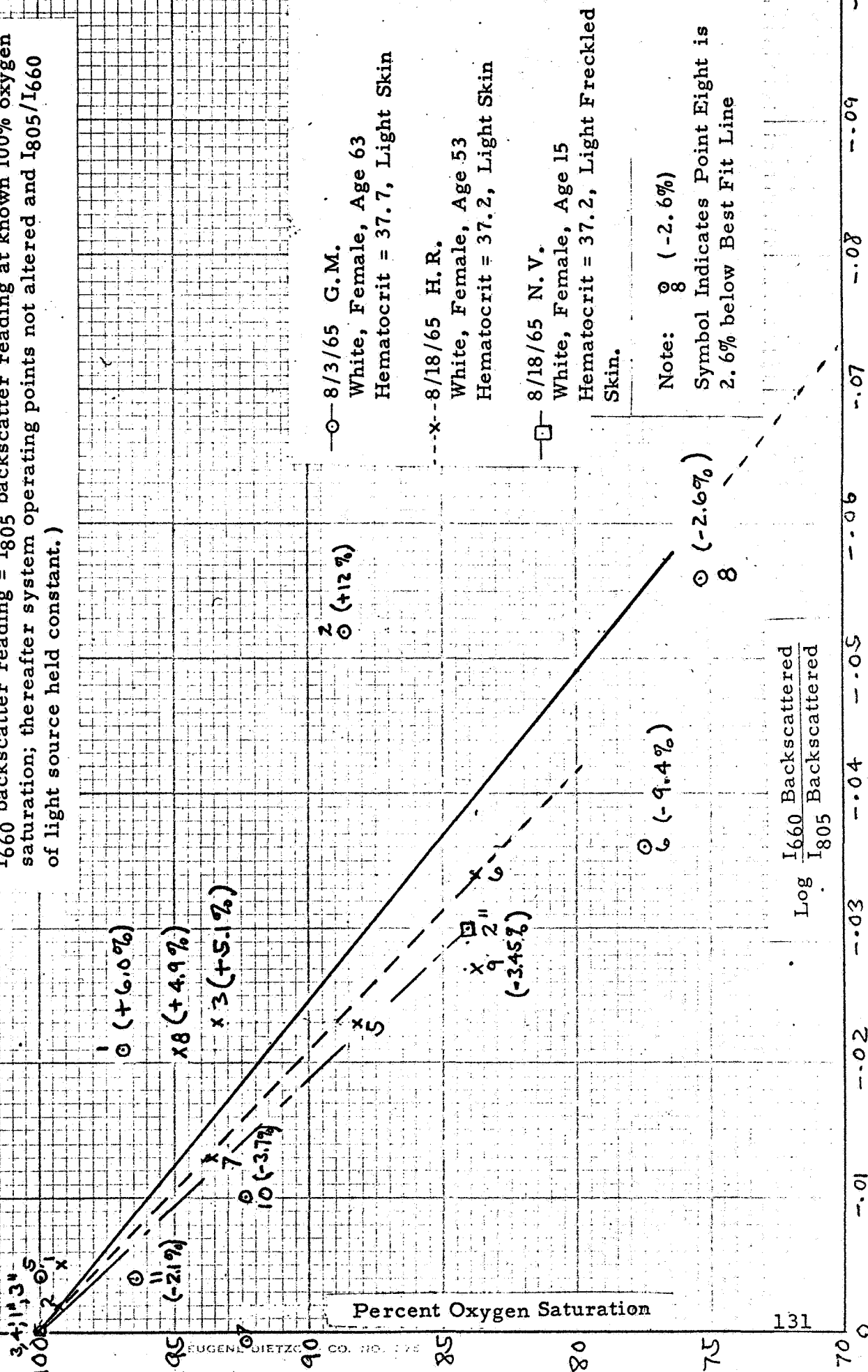
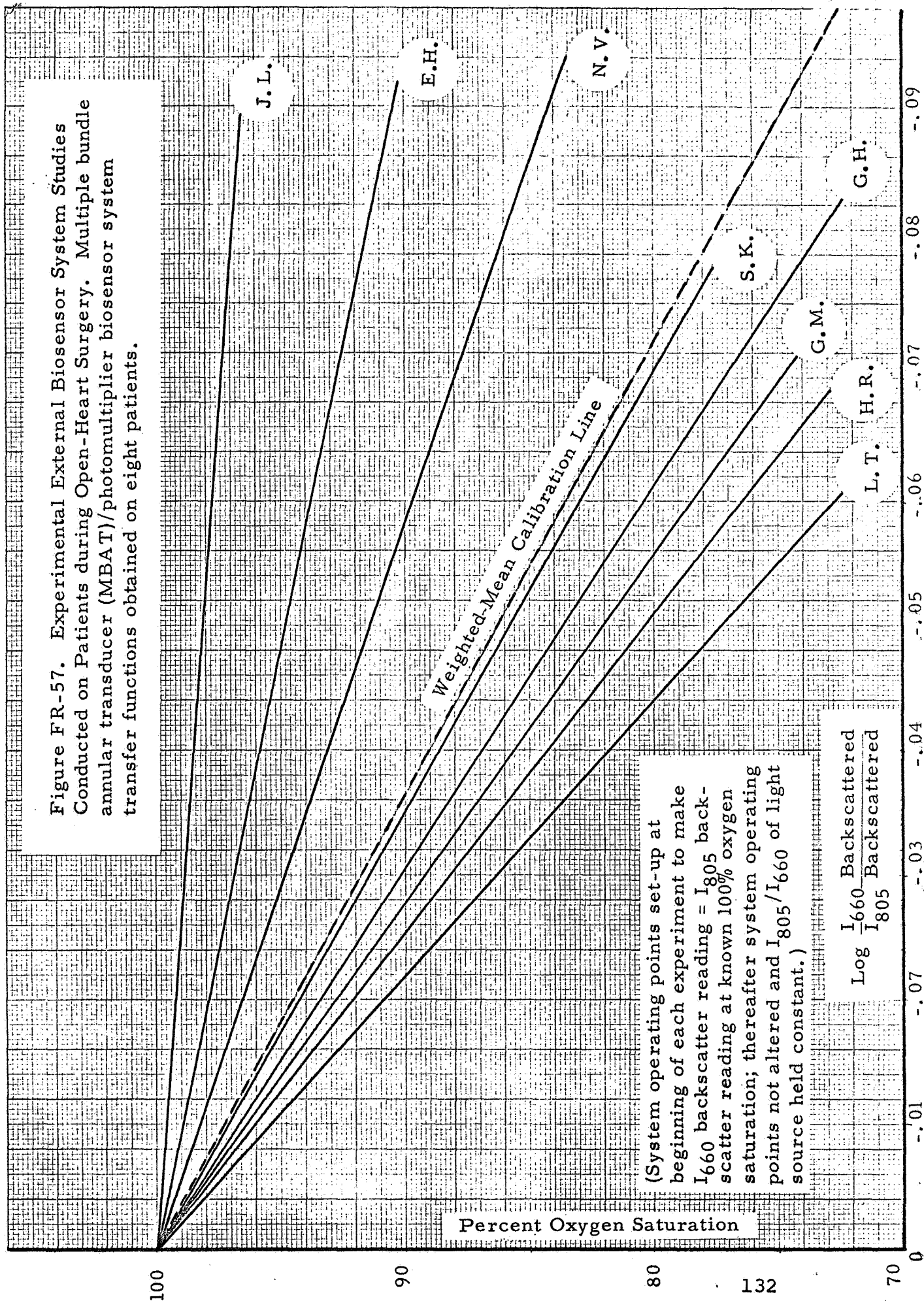
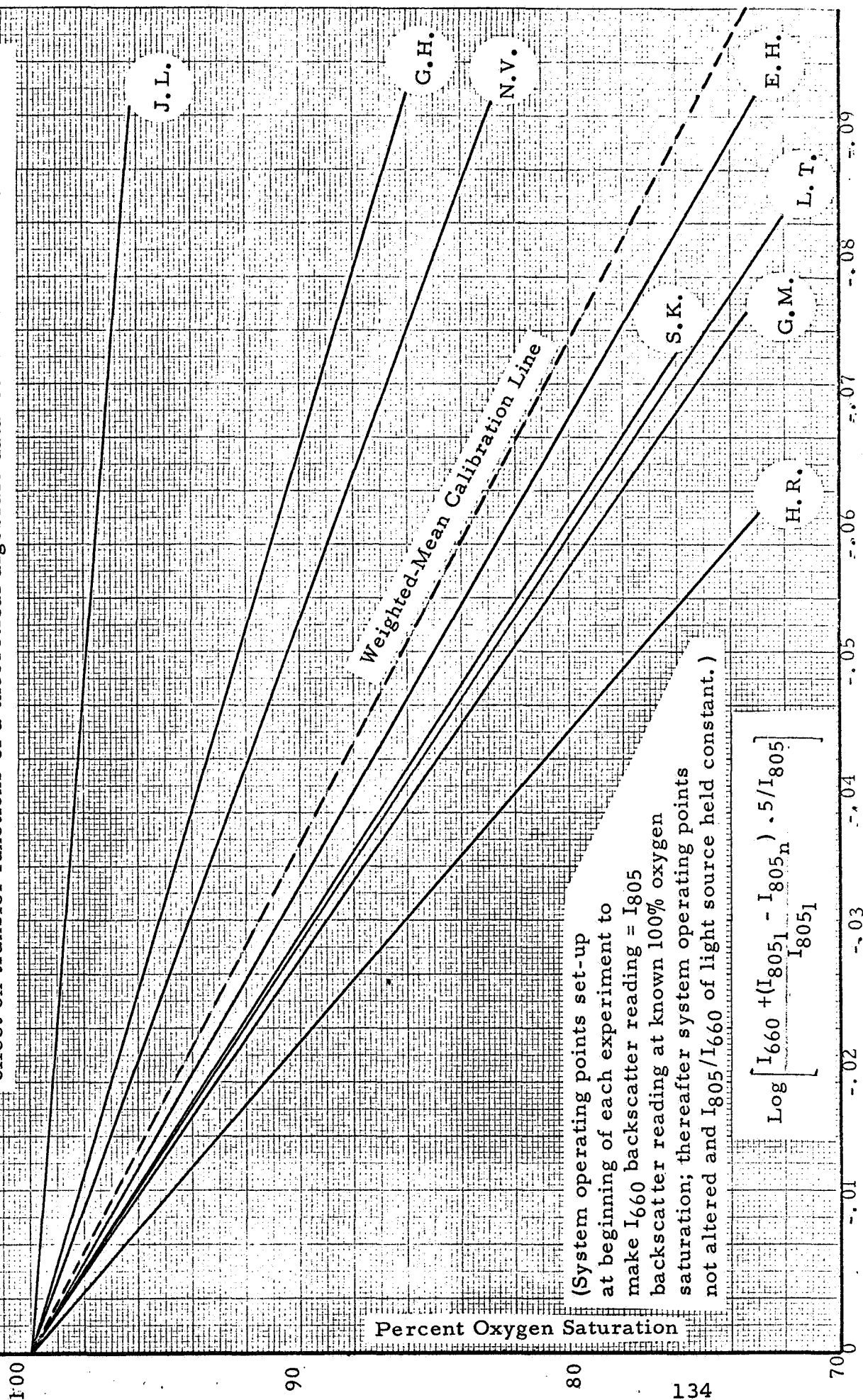


Figure FR-57. Experimental External Biosensor System Studies Conducted on Patients during Open-Heart Surgery. Multiple bundle annular transducer (MBAT)/photomultiplier biosensor system transfer functions obtained on eight patients.



Since the instrumentation operating points were set up at the beginning of each experiment to equalize the backscattered light reading at 660 and 805 m $\mu$  at known 100% oxygen saturation and were thereafter not altered, all calibration curves are identical at 100% oxygen saturation. However, as can be seen, the spread in best fit lines at progressively lower percent oxygen saturation is intolerable. No alternative computational program nor algebraic manipulation of this raw data (an example of which is presented in Figure FR-58) was found to make this data satisfactorily coherent.

Figure FR-58. Experimental External Biosensor System Studies Conducted on Patients during Open-Heart Surgery. Multiple bundle annular transducer (MBAT)/photomultiplier biosensor system transfer functions for eight patients shown in Figure FR-57, showing effect on transfer functions of a theoretical algebraic data-correlation factor.





#### H. Experimental External Biosensor System Studies Performed Upon Human Volunteers

A final series of experiments was performed with the experimental biosensor systems upon volunteers in the laboratory. These studies were directed toward systematically exploring the influence of variations in pressure, position and motion of the biosensor transducers upon the subjects by observing biosensor systems output during periods of known and constant oxygen saturation, while the pressure, position and motion of the biosensor transducers were systematically varied. In these studies, all subjects were healthy, young, adults who were maintained at 100% oxygen saturation by breathing oxygen at a pressure of 760 millimeters of mercury.

Initial studies in this series demonstrated that minor shifts in the position or pressure of the biosensor transducers upon the volunteers could result in marked perturbation of biosensor system output. Subsequently, several different kinds of auxiliary apparatus which furnished progressively greater stability of the physical relation of the biosensor to the subject were designed and fabricated. A monotonic relationship was found between reproducibility of the physical relation of the biosensor to the subject and stability of biosensor system output for a given biosensor system applied to the same subject on different days.



## VI CONCLUSIONS

Spectrophotometric studies of whole blood indicated that the principle of optical backscatter can be utilized for measuring oxygen saturation of whole-blood samples with a high degree of accuracy and reliability through the implementation of a congruent optical geometry in which the blood volume illuminated by the light source and the blood volume viewed by the photometric sensor are congruent. This apparatus followed the transfer function,

$$\text{O.S.} = K_1 \cdot \frac{I_{660} \text{ backscattered}}{I_{805} \text{ backscattered}} + K_2, \quad \text{Eq. 20 (= Eq. 2)}$$

where the ratio  $\frac{I_{805}}{I_{660}}$  of the light source was kept constant.

A congruent mode of backscatter operation, however, proved to be unsatisfactory in application upon the in-vivo skin-tissue-blood systems of human subjects and experimental animals because the excessive levels of non-information-bearing photic energy returned from the skin surface and tissues proved to be time-varying and inseparable from the signal-bearing photic energy returned from the blood contained within the skin, i.e. proved to be noise. Quantitative studies of the relative levels of signal and "noise" in the congruent geometry showed the signal-to-noise ratio to be approximately 1:7.

The likelihood of an unsatisfactory signal-to-noise ratio for congruent backscatter-mode transducers had been

anticipated in the original proposal and transducer configurations in which the area illuminated by the light source and the area observed by the photometric sensor were offset from each other rather than congruent were developed and investigated. It was hoped that these non-congruent transducers would eliminate the major source of system "noise" while performing in a manner sufficiently resembling the transfer functions of a congruent optical geometry to retain the operational advantages confirmed for the congruent optical geometry upon whole blood.

Experimental external biosensor systems utilizing a variety of non-congruent transducers were designed and fabricated. The operation of experimental systems utilizing such transducers were extensively studied upon skin-tissue-blood-simulator cuvettes, experimental animals, human patients and human volunteers.

Data from these studies demonstrated a significant transmissive component in the spectrophotometric behaviour of non-congruent backscatter-mode transducers. This transmissive component was manifest by both (a) system performance which related oxygen saturation to measured light intensities by a transfer function somewhat between the transfer functions of a congruent backscatter system (linear function of light intensities) and a transmission system (ratio of logs of light intensities), i.e.,

$$O.S. = K_1 \cdot \text{Log} \frac{I_{660} \text{ backscattered}}{I_{805} \text{ backscattered}} + K_2 \quad \text{Eq. 21 (= Eq. 3)}$$

where the ratio  $\frac{I_{805}}{I_{660}}$  of the light source is kept constant.

a log of ratios of light intensities and (b) a pronounced sensitivity to variations in pressure, position or motion between the transducer and the skin.

While characteristic (a) above is only an inconvenience, characteristic (b) above is of major practical import. With the demonstration of sensitivity to position, pressure and motion variation of the backscatter-mode of operation, the principal hoped-for advantage of external backscatter biosensors over classical external transmission-mode biosensors for use in active personnel disappeared.

In summary, non-congruent external backscatter-mode transducers have been demonstrated to manifest sufficient sensitivity and satisfactory signal-to-noise characteristics for instrument implementation. External backscatter-mode biosensors retain their obvious advantages in terms of flexibility of positioning and relative comfort of application over classical transmission-mode devices. However, the prominent transmissive component exhibited by realizable external backscatter biosensors makes these devices subject to the same perturbations in output caused by variations in pressure, position and motion as classical external transmission biosensors. In this critical respect, external backscatter biosensors have been demonstrated to hold no advantage over the classical transmission-mode devices.

This study has demonstrated that variations in physical and optical coupling of the transducers to the subjects is the chief problem for both backscatter and transmissive external biosensor systems. If a truly operational external biosensor for use upon active personnel is to be developed, it will be necessary to evolve techniques for either stabilizing the physical coupling of the transducers to the subject or for

continuously compensating for the resultant variations in optical coupling.

Attention to this now well-defined and remaining problem area is recommended to other experimenters in the field.

## REFERENCES

1. Investigation and Development of an External Biosensor, The Laboratory of Technical Development, The Institute of Medical Sciences, Presbyterian Medical Center, San Francisco, Progress Report P-5/167, Contract NAS 9-2937 November 30, 1965.
2. Verel, D., Saynor, R., and Kesteven, A. B., "A Spectrophotometric Method of Estimating Blood Oxygen Using the Unicam SP 600", J. Clin. Path., 13:361, 1960.
3. Op. Cit., The Laboratory of Technical Development, (Ref. 1).
4. Op. Cit., L.T.D., (Ref. 1).
5. Op. Cit., L.T.D., (Ref. 1).
6. Kramer, K., Elam, J. O., Saxton, G. A., and Elam, W. N., Jr., USAF School of Aviation Medicine, Randolph Field, Texas, Proj. No. 21-52-002, Report No. 1, 1950.
7. Kramer, K., Elam, J. O., Saxton, G. A., and Elam, W. N., Jr., "Influence of Oxygen Saturation, Erythrocyte Concentration and Optical Depth Upon the Red and Near-Infrared Light Transmittance of Whole Blood", Am. J. Physiol., 165:229, 1951.
8. Rodrigo, F. A., "The Determination of the Oxygenation of Blood In Vitro by Using Reflected Light", Am. H. J., 45:809, 1953.
9. Polyani, M. L. and Hehir, R. M., "New Reflection Oximeter", Rev. Sci. Instr., 31:401, 1960.
10. Polanyi, M. L. and Hehir, R. M., "In Vivo Oximeter with Fast Dynamic Response", Rev. Sci. Instr., 33:1050, 1962.

(continued)

11. Anderson, N. M. and Sekelj, P., "Studies on the Light Transmission of Nonhemolyzed Whole Blood. Determination of Oxygen Saturation", J. Lab. & Clin. Med., 65:153, 1965
12. Edwards, E. A. and Duntley, S. Q., "The Pigments and Color of Living Human Skin", Am. J. Anat., 64:1, 1939.
13. Zijlstra, W. G. and Mook, G. A., Medical Reflection Photometry, Vangorcum Ltd, Assen, The Netherlands, 1962.
14. Op. Cit., Kramer, K., et al, (Ref. 6).
15. Op. Cit., Kramer, K., et al, (Ref. 7).
16. Kuppenheim, H. F., Dimitroff, J. M., Melotti, P. M., Graham, I. C. and Swanson, D. W., "Spectral Reflectance of the Skin of Chester White Pigs in the Ranges 235-700 m $\mu$  and 0.707-2.6 $\mu$ ", J. Appl. Physiol., 9:75, 1956